January / February 2022
Volume 51, Number 1

AppliedRadiology®

YEARS

The Journal of Practical Medical Imaging and Management

SA–CME
The Future of Magnetic Resonance Imaging Contrast Agents

Imaging Torus Lesions of Jaw Bones

Small Coil MRI of the Nipple-Areola Complex and Retroareolar Breast

Medulloblastoma

Alzheimer Disease: The Role of Imaging AI

www.appliedradiology.com

Dotarem®
(gadoterate meglumine) Injection

Guerbet

MR **Comparison of Dotarem® to Gadavist® for Overall Visualization and Characterization in the MRI Diagnosis of Primary Brain Tumors**

Despite the difference in relaxivity between these 2 GBCAs

There Is No Measurable Difference in Clinical Benefit Observed Between Dotarem® and Gadavist®[2]

as demonstrated by the REMIND Study, a multicenter, double-blind, randomized, controlled intraindividual crossover study.[2]

This study "demonstrates the non-inferiority of gadoterate meglumine [Dotarem®] versus gadobutrol [Gadavist®] for overall visualization and characterization of primary brain tumors despite quantitative mean lesion percentage enhancement being higher with gadobutrol".[2]

- For all readers in the REMIND Study, more than 90% of patient images were scored with good or excellent overall lesion visualization and characterization with either Dotarem® or Gadavist®.[2]
- The REMIND Study also confirmed low incidence of immediate reported AEs with Dotarem® and with Gadavist®, as shown in multiple previous studies.[2,3,4]
- Dotarem® is an imaging contrast with macrocyclic and ionic structure for high thermodynamic and kinetic stability.[5,6]
- Dotarem® is not only trusted for high molecular stability[5,6]; the REMIND Study demonstrates that it is as effective as Gadavist® for MRI diagnosis of primary brain tumors.[2]

Please see Important Safety information on opposite page. For more information on Dotarem®, please see Full Prescribing Information including Boxed Warning and Medication Guide.

Scan the code to learn more or visit www.Dotarem-us.com/Remind-Study

DOTAREM® (GADOTERATE MEGLUMINE) INJECTION IMPORTANT SAFETY INFORMATION

WARNING: NEPHROGENIC SYSTEMIC FIBROSIS (NSF)

Gadolinium-based contrast agents (GBCAs) increase the risk for NSF among patients with impaired elimination of the drugs. Avoid use of GBCAs in these patients unless the diagnostic information is essential and not available with non-contrasted MRI or other modalities. NSF may result in fatal or debilitating fibrosis affecting the skin, muscle and internal organs.

- The risk for NSF appears highest among patients with:
  - Chronic, severe kidney disease (GFR < 30 mL/min/1.73m2), or
  - Acute kidney injury.
- Screen patients for acute kidney injury and other conditions that may reduce renal function. For patients at risk for chronically reduced renal function (e.g. age > 60 years, hypertension, diabetes), estimate the glomerular filtration rate (GFR) through laboratory testing.
- For patients at highest risk for NSF, do not exceed the recommended DOTAREM dose and allow a sufficient period of time for elimination of the drug from the body prior to any re-administration.

INDICATIONS AND USAGE

DOTAREM® (gadoterate meglumine) injection is a prescription gadolinium-based contrast agent indicated for intravenous use with magnetic resonance imaging (MRI) in brain (intracranial), spine and associated tissues in adult and pediatric patients (including term neonates) to detect and visualize areas with disruption of the blood brain barrier (BBB) and/or abnormal vascularity.

CONTRAINDICATIONS

History of clinically important hypersensitivity reactions to DOTAREM.

WARNINGS AND PRECAUTIONS

- Hypersensitivity Reactions: Anaphylactic and anaphylactoid reactions have been reported with DOTAREM, involving cardiovascular, respiratory, and/or cutaneous manifestations. Some patients experienced circulatory collapse and died. In most cases, initial symptoms occurred within minutes of DOTAREM administration and resolved with prompt emergency treatment.
- Before DOTAREM administration, assess all patients for any history of a reaction to contrast media, bronchial asthma and/or allergic disorders. These patients may have an increased risk for a hypersensitivity reaction to DOTAREM.
- Administer DOTAREM only in situations where trained personnel and therapies are promptly available for the treatment of hypersensitivity reactions, including personnel trained in resuscitation.
- Gadolinium Retention: Gadolinium is retained for months or years in several organs. The highest concentrations have been identified in the bone, followed by brain, skin, kidney, liver and spleen. The duration of retention also varies by tissue, and is longest in bone. Linear GBCAs cause more retention than macrocyclic GBCAs.
- Consequences of gadolinium retention in the brain have not been established. Adverse events involving multiple organ systems have been reported in patients with normal renal function without an established causal link to gadolinium retention.
- Acute Kidney Injury: In patients with chronically reduced renal function, acute kidney injury requiring dialysis has occurred with the use of GBCAs. The risk of acute kidney injury may increase with increasing dose of the contrast agent; administer the lowest dose necessary for adequate imaging.
- Extravasation and Injection Site Reactions: Ensure catheter and venous patency before the injection of DOTAREM. Extravasation into tissues during DOTAREM administration may result in tissue irritation.

ADVERSE REACTIONS

- The most common adverse reactions associated with DOTAREM in clinical trials were nausea, headache, injection site pain, injection site coldness and rash.
- Serious adverse reactions in the Postmarketing experience have been reported with DOTAREM. These serious adverse reactions include but are not limited to: arrhythmia, cardiac arrest, respiratory arrest, pharyngeal edema, laryngospasm," bronchospasm, coma and convulsion.

USE IN SPECIFIC POPULATIONS

- **Pregnancy:** GBCAs cross the human placenta and result in fetal exposure and gadolinium retention. Use only if imaging is essential during pregnancy and cannot be delayed.
- **Lactation:** There are no data on the presence of gadoterate in human milk, the effects on the breastfed infant, or the effects on milk production. However, published lactation data on other GBCAs indicate that 0.01 to 0.04% of the maternal gadolinium dose is present in breast milk.
- **Pediatric Use:** The safety and efficacy of DOTAREM at a single dose of 0.1 mmol/kg has been established in pediatric patients from birth (term neonates ≥ 37 weeks gestational age) to 17 years of age based on clinical data. The safety of DOTAREM has not been established in preterm neonates. No cases of NSF associated with DOTAREM or any other GBCA have been identified in pediatric patients age 6 years and younger.

You are encouraged to report negative side effects of prescription drugs to the FDA. Visit www.fda.gov/medwatch or call 1-800-FDA-1088.
Please see the full Prescribing Information, including Boxed Warning and the patient Medication Guide, for additional important safety information.

References: 1. Dotarem [package insert]. Princeton, NJ: Guerbet LLC; Oct 2019. **2.** Maravilla K et al. Comparison of Gadoterate Meglumine and Gadobutrol in the Diagnosis of Primary Brain Tumors: A Double-Blind Randomized Controlled Intraindividual Crossover Study (the REMIND Study). 2017 June 29. doi: 10:3174/ajnr.A5316. [Epub ahead of print]. **3.** de Kerviler E et al. Adverse reactions to gadoterate meglumine: review of ov¬oer 25 years of clinical use and more than 50 million doses. Invest Radiol 2016;51:544–51 CrossRef Medline. **4.** Endrikat J et al. Safety of gadobutrol: results from 42 clinical phase II to IV studies and postmarketing surveillance after 29 million applications. Invest Radiol 2016;51: 537–43 CrossRef Medline. **5.** Port M et al. Efficiency, thermodynamic and kinetic stability of marketed gadolinium chelates and their possible clinical consequences: a critical review. Biometals. 2008;21: 469-90. **6.** Frenzel T et al. Stability of gadolinium-based magnetic resonance imaging contrast agents in human serum at 37°C. Invest Radiol. 2008;43:817-828.

DOTAREM® is a registered trademark of Guerbet and is available by prescription only.

Gadavist® is a registered trademark of the Bayer group of companies, and is available by prescription only.

GU05210090

AppliedRadiology® 50 YEARS
The Journal of Practical Medical Imaging and Management

Anderson Publishing, Ltd
180 Glenside Avenue,
Scotch Plains, NJ 07076
Tel: 908-301-1995
Fax: 908-301-1997
info@appliedradiology.com

PRESIDENT & CEO
Oliver Anderson

GROUP PUBLISHER
Kieran N Anderson

ASSOCIATE PUBLISHER
Cristine Funke, RT(R)

EXECUTIVE EDITOR
Joseph F Jalkiewicz

PRODUCTION
Barbara A Shopiro

CIRCULATION DIRECTOR
Cindy Cardinal

EDITORS EMERITI
Theodore E Keats, MD
Stuart E Mirvis, MD, FACR

Editorial Advisory Board

EDITOR-IN-CHIEF

Erin Simon Schwartz, MD, FACR
Perelman School of Medicine, University of Pennsylvania, The Children's Hospital of Philadelphia, Philadelphia, PA

ASSOCIATE EDITOR FOR RADIOLOGICAL CASES

Kristin K Porter, MD, PhD
The Kirklin Clinic of UAB Hospital, Birmingham, AL

ADVOCACY/GOVERNMENTAL AFFAIRS

Associate Editor
David Youmans, MD, FACR
Princeton Radiology Associates, Princeton, NJ

Seth Hardy, MD, MBA, FACR
Penn State Health, Milton S Hershey Medical Center, Hershey, PA

Ryan K Lee, MD, MBA
Einstein Healthcare Network, Philadelphia, PA

Pradnya Y Mhatre, MD, MRMD(MRSC)
Emory University School of Medicine Atlanta, GA

ARTIFICIAL INTELLIGENCE

Associate Editor
Lawrence N Tanenbaum, MD, FACR
RadNet, Inc, New York, NY

Suzie Bash, MD
San Fernando Interventional Radiology, RadNet, Inc, Los Angeles, CA

Amine Korchi, MD, FMH
Imaging Center Onex–Groupe 3R, Singularity Consulting & Ventures, Geneva, Switzerland

BODY IMAGING

Elliot K Fishman, MD
Johns Hopkins Hospital, Baltimore, MD

BREAST IMAGING

Phan T Huynh, MD Baylor
St Luke's Medical Center, Houston, TX

Nina S Vincoff, MD
Donald and Barbara Zucker School of Medicine at Hofstra/Northwell, Hofstra University, Hempstead, NY

CARDIOPULMONARY IMAGING

Associate Editor
Charles S White, MD
University of Maryland School of Medicine, Baltimore, MD

Jeanne B Ackman, MD
Massachusetts General Hospital, Boston, MA

Saurabh Jha, MBBS, MRCS, MS
Perelman School of Medicine, University of Pennsylvania, Philadelphia, PA

EMERGENCY RADIOLOGY

Associate Editor
Melissa Davis, MD, MBA
Emory University School of Medicine, Atlanta, GA

Vahe M Zohrabian, MD
Donald and Barbara Zucker School of Medicine at Hofstra/Northwell, Hofstra University, Hempstead, NY

ENTERPRISE IMAGING

Christine Harris, RT(R)(MR), MRSO
Jefferson University Hospitals, Philadelphia, PA

Rasu Shrestha, MD, MBA
Atrium Health, Charlotte, NC

Eliot Siegel, MD
VA Maryland Healthcare System, University of Maryland School of Medicine, Baltimore, MD

INTERVENTIONAL RADIOLOGY

Associate Editor
Jeffrey C Hellinger, MD, MBA
Lenox Hill Radiology, New York, NY

Minhaj S Khaja, MD, MBA
University of Virginia Health System, Charlottesville, VA

MEDICAL INDUSTRY

Sonia Gupta, MD
University of South Florida, Tampa, FL

Ronald B Schilling, PhD
RBS Consulting Group, Los Altos Hills, CA

MEDICAL PHYSICS

David W Jordan, PhD, FAAPM
Case Western Reserve University, Cleveland, OH

Rebecca M Marsh, PhD
University of Colorado School of Medicine, Boulder, CO

William Sensakovic, PhD
Mayo Clinic, Phoenix, Arizona

MEDICOLEGAL

Michael M Raskin, MD, MPH, JD
University Medical Center, Tamarac, FL

MUSCULOSKELETAL IMAGING

Thomas Lee Pope, Jr, MD, FACR
Envision Healthcare, Denver, CO

Jamshid Tehranzadeh, MD
University of California Medical Center, Orange, CA

NEURORADIOLOGY

Associate Editor
Wende N Gibbs, MD
Mayo Clinic, Phoenix, AZ

Blake A Johnson, MD, FACR
Center for Diagnostic Imaging, Minneapolis, MN

C Douglas Phillips, MD, FACR
Weill Cornell Medical College/ New York-Presbyterian Hospital, New York, NY

NUCLEAR MEDICINE

Wengen Chen, MD, PhD
University of Maryland Medical Center, Baltimore, MD

K Elizabeth Hawk, MS, MD, PhD
Stanford University School of Medicine, Radiology Partners, Los Angeles, CA

PEDIATRIC RADIOLOGY

Associate Editor
Alexander Towbin, MD
Cincinnati Children's Hospital Medical Center, Cincinnati, OH

Michael L Francavilla, MD
Perelman School of Medicine, University of Pennsylvania, The Children's Hospital of Philadelphia, Philadelphia, PA

Marilyn J Siegel, MD, FACR
Washington University School of Medicine, Mallinckrodt Institute of Radiology, St. Louis, MO

ULTRASOUND

John P McGahan, MD
University of California, Davis, CA

©2022 Anderson Publishing, Ltd. All rights reserved. Reproduction in whole or part without written permission is strictly prohibited. USPS: 0943-180

Applied Radiology®

The Journal of Practical Medical Imaging and Management

January / February 2022
Vol 51 No 1

7 **The Future of Magnetic Resonance Imaging Contrast Agents**
Laura E Minton; Renu Pandit; WR Willoughby, PhD; Kristin K Porter, MD, PhD

Gadolinium (Gd)-based contrast agents dominate the current contrast-enhanced magnetic resonance imaging market. However, a personalized combination of contrast enhancement and image processing techniques is likely to be used in the future to optimize diagnosis and treatment planning while minimizing risk and cost.

SA-CME

12 **Imaging Torus Lesions of Jaw Bones**
Gary G Ghahremani, MD, FACR; David R Naimi, DO; Zohreh K Ghahremani, DDS

Torus is a common, benign exostosis of the jaw bones that develops in 5-30% of the world population, with considerable variation in prevalence among different genders and racial or ethnic groups. Radiologists should be aware of the numerous potential manifestations and complications related to tori.

16 **Small Coil MRI of the Nipple-Areola Complex and Retroareolar Breast**
Maria Soledad Munoz, MD; Maria Laura Alvares, MD; Daniela Munoz Tisera, MD; Marcelo Elias Munoz MD

Imaging assessment of the nipple-areola complex and the retroareolar breast includes diagnostic mammography and targeted ultrasound as first-line imaging techniques, with magnetic resonance imaging serving as a complementary alternative that nonetheless often leads to inconclusive results. This article presents a practical application of focused, magnified, high-resolution MRI with contrast using commercially available small coils.

EDITORIAL

4 2020, Too?
Erin Simon Schwartz, MD, FACR

EYE ON AI

25 Treatment Brings Hope in Alzheimer Disease: Role of Imaging AI
Suzie Bash, MD, and Lawrence N Tanenbaum, MD, FACR

RADIOLOGY MATTERS

31 Coping with COVID: Resilience in Radiology
Kerri Reeves

GLOBAL HEALTH IMAGING

34 Training Radiologists for Global Service
Farouk Dako, MD, MPH; Abass Noor, MD; Luis Goity, MD; Mary Scanlon, MD

RADIOLOGICAL CASES

37 Stress Fracture
Norman Holl, PhD; Kolja M Thierfelder, MD; Martin Ellenrieder, MD; Wolfram Mittelmeier, MD; Marc-André Weber, MD

40 Mazabraud Syndrome
Aynur Turan, MD; Tuba Dilay Unal, MD; Azad Hekimoglu, MD; Meltem Ozdemir, MD; Huseyin Coşkun, MD; Guldem Sagra, MD

43 Medulloblastoma
Jeff Wellard; John Sfondouris, MD; Scott A Jorgensen, MD; David Aria, MD, Carrie Schaefer, MD, Richard Towbin, MD, Alexander Towbin, MD

46 Hydranencephaly
Thane H Rosette; Richard B Towbin, MD; Carrie M Schaefer, MD; Alexander J Towbin, MD; David J Aria, MD

WET READ

48 A Modest Proposal
C Douglas Phillips, MD, FACR

Applied Radiology (ISSN 0160-9963, USPS 943180) is published in print 6 times a year, January, March, May, July, September, and November, by Anderson Publishing Ltd at 180 Glenside Ave., Scotch Plains NJ 07076. Periodicals postage paid at Scotch Plains, NJ and additional mailing offices. Free subscriptions for US-based qualified radiology professionals. Subscriptions for the US and its territories and possessions: $115 per year, $225 for two years. Foreign and Canadian subscriptions $215 for one year payable in US funds, international money orders, or by credit card only. Postmaster: Please send address changes to Applied Radiology, PO Box 317, Lincolnshire, IL 60069-0317 (847-564-5942) or email AppliedRadiology@Omeda.com.

Dr Schwartz is the Editor-in-Chief of *Applied Radiology*. She is the Chief of the Division of Neuroradiology and holds the Robert A Zimmerman Chair in Pediatric Neuroradiology in the Department of Radiology at The Children's Hospital of Philadelphia. She is also an Associate Professor of Radiology, Perelman School of Medicine, University of Pennsylvania. She can be reached at *erin@appliedradiology.com.*

2020, Too?

Erin Simon Schwartz, MD, FACR

With apologies to Whitesnake, here I go again. The first issue of the first volume of the second half of the first century for *Applied Radiology*. I should be energized and enthusiastic, brimming with ideas for articles and columns and new features and new board members. But nearly two years of this global pandemic have taken their toll.

Now we are surging again. What is this, the fifth? It feels almost worse this time. Our family, probably like so many of yours, was waiting with bated breath for when our kids could finally be vaccinated and life could resume again. It feels especially cruel to be facing another surge as we head into winter here in the United States. I hope that by the time this reaches your mailbox—digital or otherwise—we are not suffering the aftermath of holiday gatherings.

Enough doom and gloom.

For me, RSNA 2021 was a glimmer of the old normal and a much-needed breath of fresh air. As I walked from my hotel into the adjacent McCormick Place, I am not ashamed to admit that I welled up a little. I felt like my old self again, for the first time in far too long. After being grounded since February 2020, getting back to a meeting in person was joyful, especially seeing old friends and colleagues, even if they were much more difficult to recognize behind their masks. Either I need new glasses or the font on those nametags needs to be *a lot* bigger when everyone is masked. Probably both are true.

In Chicago, we celebrated our 50th anniversary with an amazing party, organized by our publisher, Kieran Anderson. If you were not able to attend, or did not get to stop by the booth, I encourage you to watch the video Kieran put together to commemorate this milestone. It's up on our website (appliedradiology.com/Videos/RSNA21) and well worth your time.

Our editorial board got to meet in person at RSNA. Seeing so many engaged, passionate members of our board was inspiring. You will see the fruits of our robust discussions in our print and online content, in our webinars, and in our social media postings. The different perspectives that each person brought to that table will help carry us through our next 50 years.

But our immediate focus is on 2022 and bringing you six terrific issues. As we transition to a new editorial management system and software that can meet our needs for on-demand publishing, we are looking forward to lifting our moratorium on radiological case submissions and adding more expert reviewers to our ranks, hopefully in the first half of the year. I find myself reluctant to affix a firm date to most anything anymore. As with so many other things, to paraphrase the old Yiddish, we make plans and COVID laughs.

Laugh all you want, COVID. We were here long before you and we will be here long after you. We are radiologists, technologists, administrators, nurses, assistants, and students. We are strong, we are resilient, and we are vaccinated.

You may tough, but we are tougher.

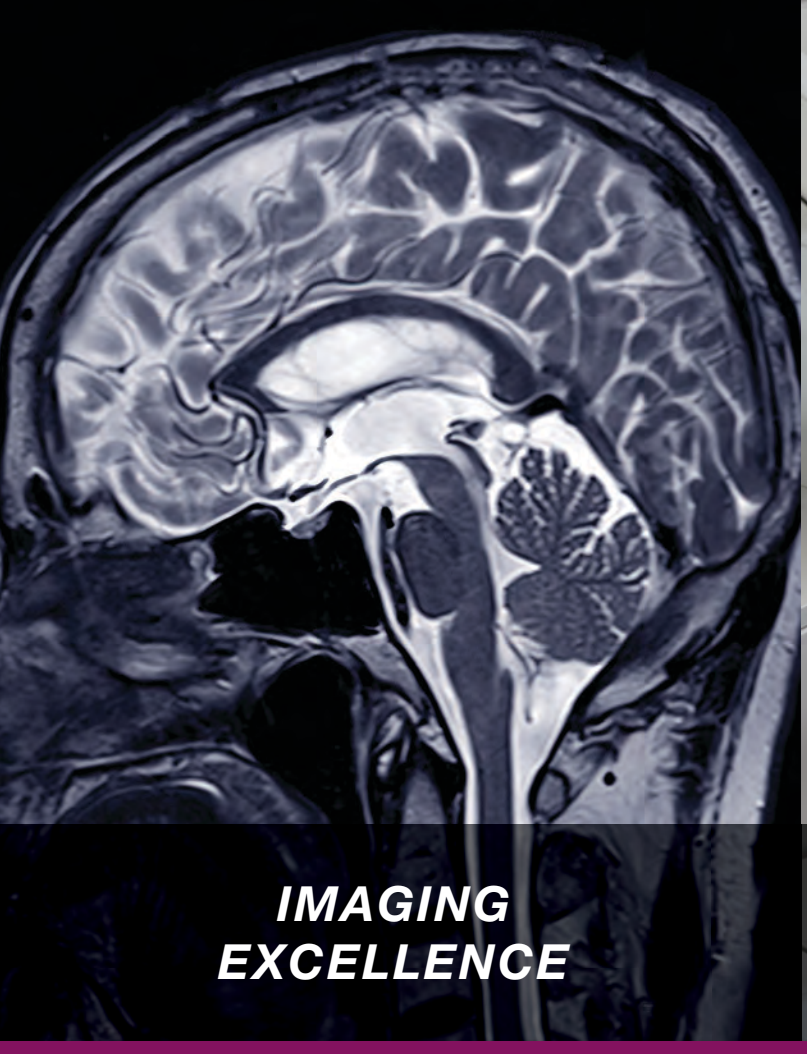

IMAGING EXCELLENCE

ACCELERATED WORKFLOW

THE GROUNDBREAKING

VELOCITY

TRUE OPEN MRI

Forget tradeoffs.

Velocity does it all. Fast exams. High quality images. Seamless and smooth workflow. All from a True Open MRI that patients prefer.

Discover all the advantages at
SeeTheWholeStory.com

© 2021 FUJIFILM Healthcare Americas Corporation

Transforming healthcare for the future

FUJIFILM
Value from Innovation

The Future of Magnetic Resonance Imaging Contrast Agents

Description

Gadolinium (Gd)-based contrast agents (GBCAs) dominate the current contrast-enhanced magnetic resonance imaging (CE-MRI) market and are proven to increase the efficacy of diagnostic magnetic resonance imaging (MRI) scans. However, in the future it is likely that a personalized combination of contrast enhancement and image processing techniques will be used to optimize diagnosis and treatment planning while minimizing risk and cost. This activity is designed to educate radiologists about the future of MRI contrasts agents, including high relaxivity macrocyclic GBCAs, alternatives to GBCAs, and imaging processing techniques.

Learning Objectives

Upon completing this activity, the reader should be able to:

- Identify potential limitations of current gadolinium contrast agents;
- Recognize possible advantages and disadvantages of alternative metal-based paramagnetic contrast agents and metal-free contrast agents; and,
- Explain how image analysis methods may provide radiologists the information they need to make accurate clinical assessments without contrast agents.

Accreditation/ Designation Statement

The Institute for Advanced Medical Education is accredited by the Accreditation Council for Continuing Medical Education (ACCME) to provide continuing medical education for physicians.

The Institute for Advanced Medical Education designates this journal-based CME activity for a maximum of 1 AMA PRA Category 1 Credit™. Physicians should only claim credit commensurate with the extent of their participation in the activity.

These credits qualify as SA-CME credits.

Authors

Laura E Minton; Renu Pandit; WR Willoughby, PhD; Kristin K Porter, MD, PhD.

Affiliation: University of Alabama at Birmingham School of Medicine, Birmingham, Alabama (all authors).

Target Audience

- Radiologists
- Related Imaging Professionals

System Requirements

In order to complete this program, you must have a computer with a recently updated browser and a printer. For assistance accessing this course online or printing a certificate, email *CustomerService@AppliedRadiology.org.*

Instructions

This activity is designed to be completed within the designated time period. To successfully earn credit, participants must complete the activity during the valid credit period. To receive SA–CME credit, you must:

1. Review this article in its entirety.
2. Visit *www.appliedradiology.org/SAM2*.
3. Log into your account or create an account (new users).
4. Complete the post-test and review the discussion and references.
5. Complete the evaluation.
6. Print your certificate.

Estimated time for completion: 1 hour

Date of release and review: January 1, 2022
Expiration date: December 31, 2023

Disclosures

Disclosures: Laura E Minton; Renu Pandit; and WR Willoughby, PhD, authors, report no relevant financial relationships with ineligible companies. Dr Porter, author, is a member of the Bracco Diagnostics Inc. COVID-19 Healthcare Professional Advisory Board and a stockholder of Pfizer. Dr Erin Schwartz, content reviewer, discloses no relevant financial relationships with ineligible companies.

No one at IAME who was in control of the content of this activity has relevant relationships with ineligible companies.

All relevant financial relationships with ineligible companies have been mitigated.

The Future of Magnetic Resonance Imaging Contrast Agents

Laura E Minton; Renu Pandit; WR Willoughby, PhD; Kristin K Porter, MD, PhD

Editor's note: This is the second part of a two-part series. The first part appeared in the November–December 2021 issue of Applied Radiology.

Gadolinium (Gd)-based contrast agents (GBCAs) dominate the current contrast-enhanced magnetic resonance imaging (CE-MRI) market and are proven to increase the efficacy of diagnostic magnetic resonance (MR) scans.[1] Adverse side effects of GBCAs are uncommon,[2] and the reported GBCA-associated incidence of nephrogenic systemic fibrosis (NSF) has declined due to pre-MR patient screening and replacement of linear GBCAs with macrocyclic compounds.[3] Recently, however, there has been concern about Gd de-chelation from GBCAs and possible effects of bioaccumulation in the central nervous system.[4-7]

The future of MR contrast may see a replacement of Gd with alternative metals, such as manganese (Mn) or iron-based agents. Metal-based paramagnetic contrast agents are limited by the intrinsic toxicity of many metal ions, their persistence in tissue, and their ability to provide only one type of contrast.[8] This has led researchers to pursue contrast mechanisms that do not require metals. A promising example is chemical exchange dependent saturation transfer (CEST) MRI, which can generate clinically useful contrasts using diamagnetic molecules with exchangeable protons in amine, amide and hydroxyl groups.[9-15]

Recent work has also been done to improve the relaxivity and in vivo lifetime of metal-free, nitroxide-based contrast agents.[16] Alternatively, the development of sequences, arrays of coils, k-space strategies, stochastic imaging, and machine learning-based image analysis procedures[17] have provided numerous opportunities to improve image contrast in MRI.[18] MRI sequences and post-processing techniques may be developed to replace or decrease the use of contrast agents (for example 4D MRI instead of MRA and CEST imaging) or hybrid technologies such as PET/MR may rely on radiotracers in lieu of MR contrast agents.[19]

Affiliation: University of Alabama at Birmingham School of Medicine, Birmingham, Alabama. Disclosure: Dr Porter is a member of the Bracco Diagnostics Inc. COVID-19 Healthcare Professional Advisory Board (2020) and a stockholder of Pfizer Inc.

Higher-relaxivity Gadolinium agents

Given the history of NSF and Gd retention in the brain and other organs, the lowest GBCA dose should be used that provides enough enhancement for diagnosis in routine practice.[20] Thus, the development of next-generation high-relaxivity GBCAs meets a real medical need. By revisiting the GBCA dose-response relationship, such agents would allow reduction of the injected Gd dose with the same efficacy or improvement in the rate of lesion detection and characterization with the usual dose.

An example of a high-relaxivity GBCA is the blood pool agent gadofosveset trisodium, which noncovalently binds to human serum albumin at the proportion of 80% to 90%.[21] Gadofosveset trisodium was indicated for MRA; however, after poor sales, production was discontinued in 2017. Another high-relaxivity macrocyclic agent, Gadopiclenol, is currently in phase III clinical trials.[22] With its higher relaxivity, Gadopiclenol may only require half of a standard Gd dose to reach the same efficacy compared to agents already available.[23]

Manganese-based agents

Manganese (Mn)-based products have been identified as a potential alternative to GBCAs.[24] Two Mn-based agents, commercially sold as Teslascan (Mangafodipir) and LumenHance, have been available in the past,[25] but were withdrawn from the US market due to toxicity concerns and poor

Table 1. Next-generation MR contrast imaging enhancement mechanisms

CLASS	PROS	CONS	EXAMPLES
Gd-based, high relaxivity	▪ Lower dosages for relaxivity comparable to GBCAs ▪ Improved lesion detection	▪ Possible Gd accumulation	▪ Gadofosveset trisodium (discontinued) ▪ Gadopiclenol (phase III trials)
Mn-based	▪ Comparable relaxivity, CE-MRA to GBCAs	▪ Possible neurotoxicity ▪ Not commercially available	▪ Mn-DPDP (discontinued) ▪ Mn-PyC3A (preclinical trials)
Fe-based	▪ Favorable for imaging metastatic disease ▪ Long intravascular half-life ▪ Superior CE-MRA	▪ Possible hypersensitivity reactions	▪ Ferrotran (approved in Netherlands) ▪ Ferumoxytol (not FDA approved for CE-MRI)
CEST	▪ Metal-free ▪ Can be non-invasive ▪ Molecular imaging applications	▪ Longer imaging times ▪ Specialized, high-SAR sequences ▪ Under active development	▪ Iopamidol, iopromide (pHe) ▪ Endogenous lactate (phenotype tumors) ▪ Dextrans + PSMA ligands (prostate cancer)
ORCAs	▪ Metal-free ▪ ROS imaging	▪ Limited lifetime ▪ Limited relaxivity ▪ In preclinical trials	▪ BASP-nitroxide ▪ TMV nitroxyls
Image processing	▪ Metal-free ▪ Non-invasive	▪ Reproducibility under investigation	▪ Generative adversarial networks (segmentation)

sales. As of 2021, no Mn-based contrast agent is currently commercially available, and it is unknown whether Mn products will become a safer alternative to GBCAs as approved MR contrast agents.

Manganese dipyridoxildiphosphate (Mn-DPDP), marketed as Teslascan (Mangafodipir), was first used in humans as an intravenous, paramagnetic, hepatobiliary MR contrast agent for the detection and characterization of liver lesions.[25] This water-soluble molecule was taken up selectively by hepatocytes; it dissociated in vivo into the metal and chelate. The Mn was absorbed intra-cellularly and excreted in bile, while the chelate was eliminated via renal filtration.[25] More recently, Mn-PyC3A was shown in studies with baboons and mice to provide comparable relaxivity and contrast enhanced MR angiography to GBCAs.[26,27] The PyC3A component serves as a chelator, which helps to prevent hepatic uptake and optimizes elimination.[26]

These studies demonstrate that Mn-PyC3A is excreted both renally and partially by the hepatobiliary system, with near complete elimination (>99.5% after 24 hours).[28] This partial hepatobiliary elimination allows for delayed phase visualization of liver metastases in mouse models.[28] PET-MRI studies in rat models with renal impairment showed that Mn-PyC3A was eliminated more completely from nephrectomy rats than gadoterate meglumine was, and that this was the result of increased hepatobiliary excretion.[29] Although more studies are needed, these studies indicate that Mn-PyC3A has potential as a contrast agent in humans.

Studies of industrial workers exposed to Mn-containing fumes, suggest that Mn may induce neurotoxicity in human brains with behavioral consequences and cognitive deficits because of decreased globus pallidus and cerebellar volume.[30] This is an important consideration, given that the Gd retention in the brain has, as of yet, not shown neurotoxicity. As such, it is uncertain whether the benefit-risk balance of Mn-based agents will ultimately reach or exceed that of GBCAs.

Iron-based agents

The identification of iron-based agents as a potential alternative to GBCAs has led to extensive preclinical and clinical research, although the only MR contrast agent commercially available is Ferrotran (formerly Combidex, ferumoxtran-10), an iron oxide nanoparticle approved in the Netherlands for detection of metastatic disease in lymph nodes.[31] Iron oxide is a super-paramagnetic agent that leads to a disproportionate shortening of the T2 time, resulting in a strong decrease in the MR signal and thus producing a negative contrast in vivo. Additionally, when iron oxide particles are present at low concentration in the blood stream, they can also produce a signal enhancement on T1 sequences with very short echo times and produce positive contrast. After intravenous administration, the ultra-small formulations of superparamagnetic particles of iron oxide are removed from the blood by the reticuloendothelial system in the liver, spleen, and lymph nodes, a helpful distribution when considering imaging metastatic

disease. These agents also have an extremely long intravascular half-life, making iron-based agents an attractive choice for MRA.[32]

Feraheme (ferumoxytol) has been approved for iron supplementation in patients with end-stage renal disease. While it has been used to visualize the vasculature in children and adults with MR, it is not FDA approved as an MRI contrast agent. Moreover, its labeling includes a boxed warning concerning the risk of fatal and serious hypersensitivity reactions as well as a contraindication for patients who have had an allergic reaction to any intravenous iron replacement product.[33] In a 2015 study with 15 renal transplant participants, ferumoxytol was shown to deliver superior vessel sharpness with high-resolution steady state MRA and equivalent signal to noise ratio when compared to standard first-pass MRA. Because it is not Gd based, ferumoxytol can be used without concern for NSF or Gd retention.[34]

Chemical exchange saturation transfer (CEST) imaging

A relatively new class of contrast agents known as CEST agents have been studied and developed since 2000. In a process similar to magnetization transfer contrast (MTC), these agents provide contrast via selective radiofrequency (RF) saturation of the nuclear magnetization of protons on the agent molecules and subsequent chemical exchange of these saturated protons with water protons. After many successive saturation pulses and exchanges, a detectable decrease in the nearby water signal accumulates and generates contrast enhancement.

An appealing advantage of many of these contrast agents is the lack of paramagnetic metal that may lead to side effects or lasting health effects. Other promising features of the technique are its ability to provide molecularly specific information and its wide applicability. However, CEST imaging sequences are currently limited by long acquisition times, increased specific absorption of radiation (SAR), and strong dependence on experimental factors like field inhomogeneities.[35]

The CEST technique using contrast agents like iopamidol and iopromide has been successful in measuring extracellular pH (pHe) for the detection and characterization of tumors and even for the evaluation of tumor acidosis.[9,10,13] Since the only requirement for a compound to be utilized for CEST contrast is having a proton that is exchangeable with water, the CEST technique can be used for clinically relevant molecular imaging with MRI.[36] For example, extracellular lactate, a diamagnetic CEST (diaCEST) agent was successfully imaged using a paramagnetic shift reagent.[37] This technique could eventually be used to detect not only the presence of tumors, but also their specific phenotypes. Diamagnetic dextran, a glucose polymer that is already clinically indicated as a plasma volume expander, has been modified with prostate-specific membrane antigen (PSMA) targeting ligands to provide MRI contrast specifically for prostate cancer without metals or radiotracers.[38]

The CEST technique also opens the door to theranostic applications without the use of radiotracers. Many pharmaceuticals cannot be imaged directly with MRI but contain exchangeable protons. This provides the possibility of image-guided drug delivery and pharmacokinetic studies without the risks associated with ionizing radiation.[36] CEST contrast, however, requires specialized MR sequences that can increase SAR and prolong clinical examination times.

Organic radical contrast agents (ORCAs)

Another class of metal-free contrast agents uses the magnetic interaction of unpaired electrons on organic radical moieties and nearby water protons to modulate MR contrast. These organic radical contrast agents (ORCAs) provide another avenue to metal-free MR contrast enhancement, and since they are paramagnetic, do not require specialized pulse sequences with long, adiabatic RF pulses to provide contrast enhancement, like CEST agents. However, the stable organic radical nitroxide has only one unpaired electron, compared to the seven unpaired electrons on the Gd^{3+} ion or five unpaired electrons on the Fe^{3+} ion, which limits the relaxivity and contrast enhancement provided by the molecule.[39]

The appeal of metal-free organic contrast agents has led to broad interest in addressing the limitations of nitroxide-based MR contrast, which include the relatively low relaxivity and rapid metabolic reduction of nitroxide to molecules that do not enhance contrast.[39] Rajca, et al, demonstrated that nitroxide radicals on polymeric scaffolds can increase the lifetime of ORCAs in vivo and provide proton relaxivity r_1 close to that of GBCAs, about 5 mM^{-1} s^{-1}. Nguyen, et al, showed that synthesizing nitroxide radicals into brush-arm star polymeric (BASP) structures substantially increases both the relaxivity due to a larger concentration of paramagnetic species and the half-life of ORCAs in vivo. MR contrast enhancement with r_2 relaxivities greater than 1000 mM^{-1} s^{-1} in rodents was observed up to 24 hours post-injection of BASP-ORCAs.[40]

Nguyen, et al, also showed the usefulness of BASP-ORCAs as theranostic agents, where the relaxivity could be modulated with drug-activated triggers.[41] Dharmawardana, et al, synthesized nitroxyl groups onto rigid tobacco mosaic virus (TMV) protein coats to achieve r_1 relaxivity of 1.5 mM^{-1} s^{-1} and r_2 relaxivity of 4.5 mM^{-1} s^{-1} at 1.5 T, which is on the order of relaxivities of GBCAs.[42] TMV-based contrast agents could also be

used to image superoxide production in cases of deep tissue injury due to their unique structure that prevents the quenching of fluorophores by nearby free radicals.[42] None of these compounds have progressed further than preclinical testing, however, and further developments need to be made before ORCAs are approved for clinical use.

Contrast Without the Agents

Ongoing research makes contrast agents safer, more effective, and more biochemically specific for precision diagnoses. On the other hand, recent developments in the field of radiomics, machine learning, and image processing algorithms are taking steps toward lessening or even eliminating the need for intravenous injection of foreign materials into the body to improve the diagnostic efficacy of MRI. Advanced machine learning algorithms based on generative adversarial networks have been developed that, when trained, provide approximately the same segmentation information from non-CE MRI of liver lesions and cardiac cine imaging without the use of contrast agents compared to the gold-standard CE-MRI.[17,43] These image analysis methods can provide radiologists with the information they need to make accurate clinical assessments without expensive, potentially unsafe use of GBCAs. However, more work needs to be done to evaluate the reproducibility of radiomic data provided by such algorithms across a broader population.

Conclusion

Despite significant efforts in preclinical, translational, and clinical research to identify and develop alternative Gd-free diagnostic agents, it is most probable that the next generation of MRI contrast agents will still include Gd, suggesting that true high relaxivity macrocyclic GBCAs may be at least in the near future. Looking forward, a personalized combination of contrast enhancement and image processing techniques is likely to be used to optimize diagnosis and treatment planning while minimizing risk and cost.

References

1) Li H, Meade TJ. Molecular magnetic resonance imaging with Gd(III)-based contrast agents: challenges and key advances. *J Am Chem Soc.* 2019;141(43):17025-17041.

2) Bruder O, Schneider S, Pilz G, et al. 2015 Update on acute adverse reactions to gadolinium based contrast agents in cardiovascular MR. Large multi-national and multi-ethnical population experience with 37788 patients from the EuroCMR registry. *J Cardiovasc Magn Reson.* 2015;17:58.

3) Attari H, Cao Y, Elmholdt TR, Zhao Y, Prince MR. A systematic review of 639 patients with biopsy-confirmed nephrogenic systemic fibrosis. *Radiology.* 2019;292(2):376-386.

4) Ohashi T, Naganawa S, Iwata S, Kuno K. Age-related changes in the distribution of intravenously administered gadolinium-based contrast agents leaked into the cerebrospinal fluid in patients with suspected endolymphatic hydrops. *Jpn J Radiol.* 2021;39(5):433-441.

5) Rasschaert M, Weller RO, Schroeder JA, Brochhausen C, Idee JM. Retention of gadolinium in brain parenchyma: pathways for speciation, access, and distribution. A critical review. *J Magn Reson Imaging.* 2020;52(5):1293-1305.

6) Richter H, Bucker P, Martin LF, et al. Gadolinium tissue distribution in a large-animal model after a single dose of gadolinium-based contrast agents. *Radiology.* 2021:210553.

7) Runge VM. Critical Questions Regarding Gadolinium Deposition in the Brain and Body After Injections of the Gadolinium-Based Contrast Agents, Safety, and Clinical Recommendations in Consideration of the EMA's Pharmacovigilance and Risk Assessment Committee Recommendation for Suspension of the Marketing Authorizations for 4 Linear Agents. *Invest Radiol.* 2017;52(6):317-323.

8) Gu L, Cao X, Mukhtar A, Wu K. Fe/Mn multilayer nanowires as dual mode T1 -T2 magnetic resonance imaging contrast agents. *J Biomed Mater Res B Appl Biomater.* 2021;109(4):477-485.

9) Anemone A, Consolino L, Conti L, et al. Tumour acidosis evaluated in vivo by MRI-CEST pH imaging reveals breast cancer metastatic potential. *Br J Cancer.* 2021;124(1):207-216.

10) Chen LQ, Howison CM, Jeffery JJ, Robey IF, Kuo PH, Pagel MD. Evaluations of extracellular pH within in vivo tumors using acidoCEST MRI. *Magn Reson Med.* 2014;72(5):1408-1417.

11) Guivel-Scharen V, Sinnwell T, Wolff SD, Balaban RS. Detection of proton chemical exchange between metabolites and water in biological tissues. *J Magn Reson.* 1998;133(1):36-45.

12) Lindeman LR, Randtke EA, High RA, Jones KM, Howison CM, Pagel MD. A comparison of exogenous and endogenous CEST MRI methods for evaluating in vivo pH. *Magn Reson Med.* 2018;79(5):2766-2772.

13) Longo DL, Dastru W, Digilio G, et al. Iopamidol as a responsive MRI-chemical exchange saturation transfer contrast agent for pH mapping of kidneys: In vivo studies in mice at 7 T. *Magn Reson Med.* 2011;65(1):202-211.

14) Walker-Samuel S, Ramasawmy R, Torrealdea F, et al. In vivo imaging of glucose uptake and metabolism in tumors. *Nat Med.* 2013;19(8):1067-1072.

15) Ward KM, Aletras AH, Balaban RS. A new class of contrast agents for MRI based on proton chemical exchange dependent saturation transfer (CEST). *J Magn Reson.* 2000;143(1):79-87.

16) Guo S, Wang X, Dai Y, et al. Enhancing the efficacy of metal-free MRI contrast agents via conjugating nitroxides onto PEGylated cross-linked poly(carboxylate ester). *Adv Sci (Weinh).* 2020;7(14):2000467.

17) Xu C, Howey J, Ohorodnyk P, Roth M, Zhang H, Li S. Segmentation and quantification of infarction without contrast agents via spatiotemporal generative adversarial learning. *Med Image Anal.* 2020;59:101568.

18) de Figueiredo EH, Borgonovi AF, Doring TM. Basic concepts of MR imaging, diffusion MR imaging, and diffusion tensor imaging. *Magn Reson Imaging Clin N Am.* 2011;19(1):1-22.

19) Jadvar H, Colletti PM. Competitive advantage of PET/MRI. *Eur J Radiol.* 2014;83(1):84-94.

20) Davenport MS. Choosing the safest gadolinium-based contrast medium for MR imaging: not so simple after all. *Radiology.* 2018;286(2):483-485.

21) Bane O, Lee DC, Benefield B, Markl M, Carr J, Carroll TJ. A pilot study of leakage and compartmentalization of the contrast agent Ablavar. *Journal of Cardiovascular Magnetic Resonance.* 2013;15(1):E7.

22) Guerbet. Efficacy and Safety of Gadopiclenol for Body Magnetic Resonance Imaging (MRI) (PROMISE). clinicaltrials.gov. https://clinicaltrials.gov/ct2/show/NCT03986138. Published 2019. Accessed Jul 14 2021.

23) Robert P, Vives V, Grindel AL, et al. Contrast-to-dose relationship of gadopiclenol, an MRI macrocyclic gadolinium-based contrast

agent, compared with gadoterate, gadobenate, and gadobutrol in a rat brain tumor model. *Radiology.* 2020;294(1):117-126.

24) Lancelot E, Raynaud JS, Desche P. Current and future MR contrast agents: Seeking a better chemical stability and relaxivity for optimal safety and efficacy. *Invest Radiol.* 2020;55(9):578-588.

25) Pan D, Schmieder AH, Wickline SA, Lanza GM. Manganese-based MRI contrast agents: past, present and future. *Tetrahedron.* 2011;67(44):8431-8444.

26) Gale EM, Atanasova IP, Blasi F, Ay I, Caravan P. A manganese alternative to gadolinium for MRI contrast. *J Am Chem Soc.* 2015;137(49):15548-15557.

27) Gale EM, Wey HY, Ramsay I, Yen YF, Sosnovik DE, Caravan P. A manganese-based alternative to gadolinium: Contrast-enhanced MR angiography, excretion, pharmacokinetics, and metabolism. *Radiology.* 2018;286(3):865-872.

28) Erstad DJ, Ramsay IA, Jordan VC, et al. Tumor contrast enhancement and whole-body elimination of the manganese-based magnetic resonance imaging contrast agent Mn-PyC3A. *Invest Radiol.* 2019;54(11):697-703.

29) Zhou IY, Ramsay IA, Ay I, et al. Positron emission tomography-magnetic resonance imaging pharmacokinetics, In vivo biodistribution, and whole-body elimination of Mn-PyC3A. *Invest Radiol.* 2021;56(4):261-270.

30) Chang Y, Jin SU, Kim Y, et al. Decreased brain volumes in manganese-exposed welders. *Neurotoxicology.* 2013;37:182-189.

31) Fortuin AS, Brüggemann R, van der Linden J, et al. Ultra-small superparamagnetic iron oxides for metastatic lymph node detection: back on the block. *Wiley Interdiscip Rev Nanomed Nanobiotechnol.* 2018;10(1).

32) Finn JP, Nguyen KL, Han F, et al. Cardiovascular MRI with ferumoxytol. *Clin Radiol.* 2016;71(8):796-806.

33) Varallyay CG, Toth GB, Fu R, et al. What does the boxed warning Tell Us? Safe Practice of Using Ferumoxytol as an MRI Contrast Agent. *AJNR Am J Neuroradiol.* 2017;38(7):1297-1302.

34) Corwin MT, Fananapazir G, Chaudhari AJ. MR Angiography of Renal Transplant Vasculature with Ferumoxytol: Comparison of High-Resolution Steady-State and First-Pass Acquisitions. *Acad Radiol.* 2016;23(3):368-373.

35) Kim J, Wu Y, Guo Y, Zheng H, Sun PZ. A review of optimization and quantification techniques for chemical exchange saturation transfer MRI toward sensitive in vivo imaging. *Contrast Media Mol Imaging.* 2015;10(3):163-178.

36) Chen Z, Han Z, Liu G. Repurposing Clinical Agents for Chemical Exchange Saturation Transfer Magnetic Resonance Imaging: Current Status and Future Perspectives. *Pharmaceuticals (Basel).* 2020;14(1).

37) Zhang L, Martins AF, Mai Y, et al. Imaging Extracellular Lactate In Vitro and In Vivo Using CEST MRI and a Paramagnetic Shift Reagent. *Chemistry.* 2017;23(8):1752-1756.

38) Liu G, Banerjee SR, Yang X, et al. A dextran-based probe for the targeted magnetic resonance imaging of tumours expressing prostate-specific membrane antigen. *Nat Biomed Eng.* 2017;1:977-982.

39) Fu C, Yu Y, Xu X, et al. Functional polymers as metal-free magnetic resonance imaging contrast agents. *Progress in Polymer Science.* 2020;108:101286.

40) Nguyen HV, Chen Q, Paletta JT, et al. Nitroxide-Based Macromolecular Contrast Agents with Unprecedented Transverse Relaxivity and Stability for Magnetic Resonance Imaging of Tumors. *ACS Cent Sci.* 2017;3(7):800-811.

41) Nguyen HV, Detappe A, Harvey P, et al. Pro-organic radical contrast agents ("pro-ORCAs") for real-time MRI of pro-drug activation in biological systems. *Polym Chem.* 2020;11(29):4768-4779.

42) Dharmarwardana M, Martins AF, Chen Z, et al. Nitroxyl Modified Tobacco Mosaic Virus as a Metal-Free High-Relaxivity MRI and EPR Active Superoxide Sensor. *Mol Pharm.* 2018;15(8):2973-2983.

43) Xiao X, Qiang Y, Zhao J, Yang X, Yang X. Segmentation of Liver Lesions Without Contrast Agents With Radiomics-Guided Densely UNet-Nested GAN. *IEEE Access.* 2020;PP:1-1.

Imaging Torus Lesions of Jaw Bones

Gary G Ghahremani, MD, FACR; David R Naimi, DO; and Zohreh K Ghahremani, DDS

Torus is a common, benign exostosis of the jaw bones that develops in 5%-30% of the world population, with considerable variation in prevalence among different genders and racial or ethnic groups.[1-5] This pathologic process usually manifests around puberty and continues to grow during adulthood. These lesions will then appear as lobulated protuberances on the lingual side of the jaw bones or hard palate.

Small torus lesions are usually asymptomatic and first noticed by the patient or detected incidentally during dental examination. Patients with larger tori, however, may experience longstanding symptoms including interference with proper mastication and oral hygiene, impaired speech, recurrent traumatic ulceration and inflammation of the gingival mucosa over the prominent tori, and ill-fitting dental appliances. Larger tori can also cause a wide spectrum of other complications.

There have been reports of patients seeking advice from primary care physicians because of concern that an enlarging or ulcerated torus may represent a malignancy. Such cases can pose a diagnostic challenge to physicians who may not be well informed about the appearance and potential implications of this abnormality. Radiologists should be aware of the numerous potential manifestations and complications related to tori.

Figure 1. Radiographic appearance of torus mandibularis (TM) on lateral view of the maxillofacial bones presents as sclerotic areas projected over the roots of the lower teeth (arrows). Note correlation with photograph of the lesion (inset).

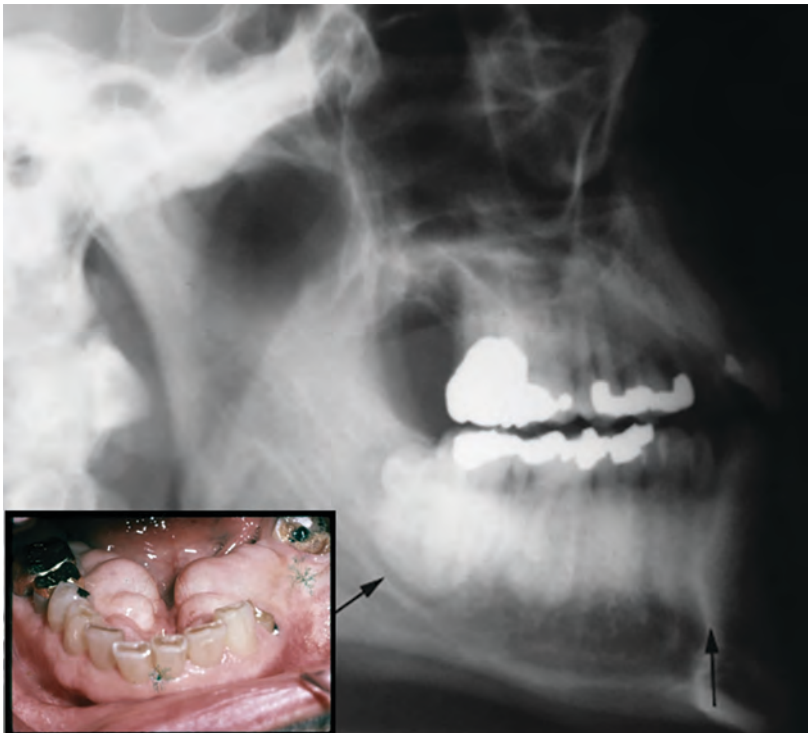

There are three major types of tori: torus mandibularis (TM), torus palatinus (TP), and torus maxillaris (TMAX).

Torus Mandibularis

On visual inspection, torus mandibularis (TM) appears as a multi-lobulated mass on the inner aspect of bicuspid and premolar regions, commonly with almost

Affiliations: University of California-San Diego Medical Center, San Diego, CA (Dr G Ghahremani), Naval Hospital Camp Pendleton, Oceanside, CA (Dr Naimi), Northwestern University Dental Clinic, Chicago, IL (Dr Z. Ghahremani).
Disclosures: None.

Figure 2. Axial CT section of the mandible in TM shows prominent bilateral exostoses (arrows). Intraoral photograph (inset) demonstrates lobulated subgingival masses on the inner aspect of premolar regions.

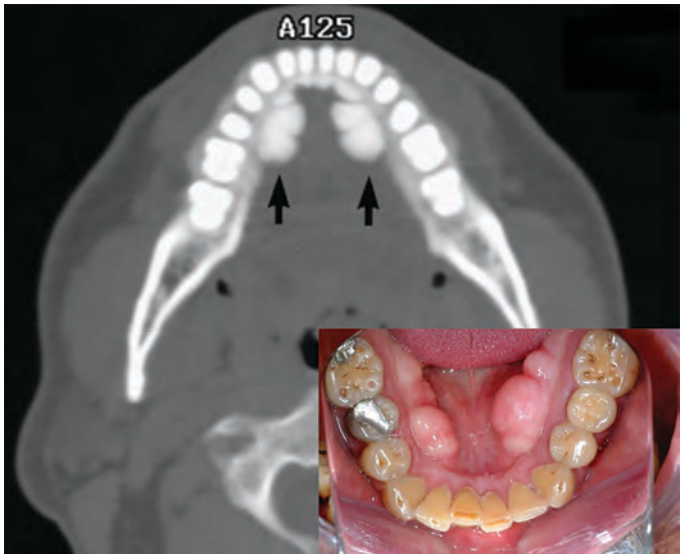

Figure 3. Torus mandibularis presenting as extensive osteomas on CT (arrows), and as lobulated masses protruding medially on intraoral view (inset). There was progressive impairment of speech and mastication owing to posterior displacement of the tongue, requiring surgical excision.

symmetrical extent on both sides. They typically measure 3-4 cm long, up to 1.5 cm thick, and are covered by intact gingival mucosa.

On lateral radiographs of the mandible, TM appears as a very dense sclerotic lesion or area of increased bone density superimposed on the roots of the lower teeth (Figure 1). Computed tomography (CT) demonstrates the TM as lobulated exophytic masses of cortical hyperostosis, located bilaterally above the mylohyoid line (Figures 2,3). The size and location of TM can cause posterior displacement of the tongue and interfere with speech.

Torus Palatinus

Torus palatinus (TP) manifests as a fungating mass of variable size and configuration that protrudes into the oral cavity from the center of the hard palate. The core of TP will appear as a dense and lobulated exostosis on radiographs and CT images (Figures 4,5). Intraoral inspection and photographs of larger lesions may reveal inflamed and ulcerated mucosa (Figure 6). Most patients will have experienced the same problem following repeated traumatic erosion by hard foods, such as candy. Therefore, surgical removal of a large TP by local osteotomy may be necessary to alleviate symptoms.

Torus Maxillaris

Torus maxillaris (TMAX) often appears bilaterally as prominent and lobulated masses arising from the medial aspects of the upper jaw. In contrast to TM, TMAX lesions are located more posteriorly along the molar regions. These tori are very firm and consist of marked cortical hyperostosis on CT sections (Figure 7).

On rare occasions a TMAX may be associated with a coexisting TP or other osseous abnormalities of the maxilla. We have anecdotally noticed that several patients with torus lesions had evidence of frontal hyperostosis on lateral radiographs of the skull. There are some similarities in the radiographic features of both conditions.

Etiological Considerations

Torus is a common benign exostosis that represents a developmental lesion, usually first appearing in puberty or early adulthood and becoming larger with advancing age. It has a hereditary etiology in about a third of cases. Curran, et al,[6] found TM and TP in three generations of women in one family. In the study by Eggen,[7] the genetic origin of TM was documented in 29.5% of patients. The remaining 70% were attributed to either environmental factors or mechanical issues caused by occlusal stress.[4,5] Torus mandibularis and TMAX both have a predilection for developing adjacent to the teeth receiving local stress because of excessive teeth grinding and jaw clenching, also known as bruxism.[4, 5, 8]

Torus Prevalence and Manifestation

The most common age range at onset of torus is 10-30 years, but its growth may continue until the seventh decade of life.[9, 10] Tori prevalence varies with ethnicity and gender. One study of 448 female residents of Washington, DC, found tori present in 35% of African Americans, 38% of Asians, 32% of Caucasians, 30% of Hispanics, and 20% of Native Americans.[2]

Another investigation involving patients from the southern US revealed

Figure 4. Panographic dental images (A,B) in two patients demonstrate torus palatinus (TP) as a small spindle-shaped lesion (A, arrow) and a large lobulated mass protruding from the center of the hard palate (B, arrows).

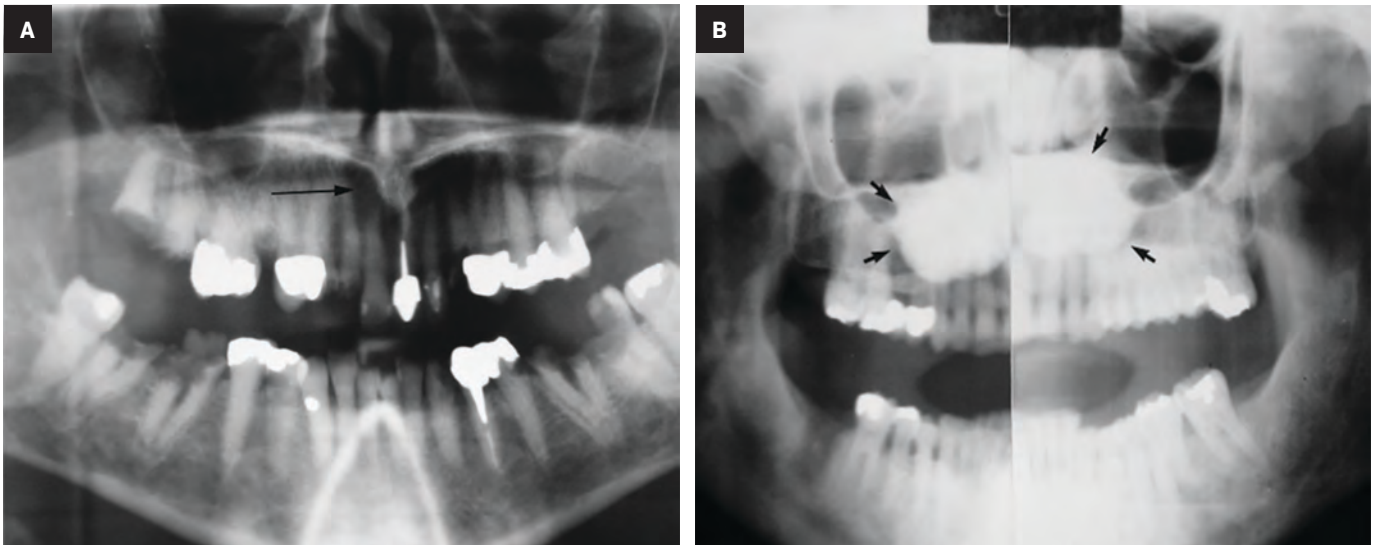

Figure 5. Axial CT image and intraoral photograph demonstrate TP as a prominent multi-lobulated mass protruding from center of the hard palate (arrow). This torus was removed surgically because of its large size and recurrent superficial ulceration of its gingival mucosa.

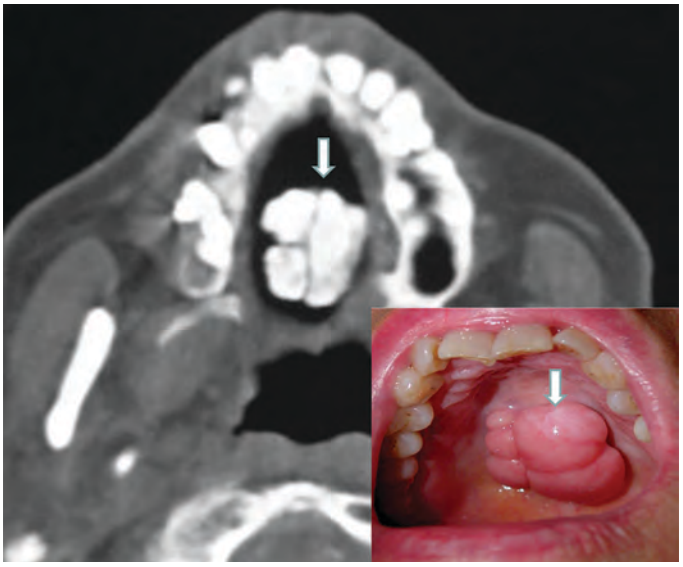

that 25% of Caucasian men and 24% of women had TM, whereas TMAX was present in 22% of men and 40% of women. In comparison, TM was present in 18% of African American men and 13% of African American women, while TMAX was present in 14% of African American men and 45% of African American women.[1]

A high incidence of tori has been reported among Asian populations. Morita and associates found TM in 58% of healthy students at Hiroshima University in Japan.[11] Another study involving 1,520 dental patients in Thailand showed prevalence rates of 60.5% for TP, 32.2% for TM, and concurrent tori in 23.2%.[12] Most published large series show female predominance for TP and a slight male predilection for TM.[10,13]

Clinical Presentation and Management

Most tori are asymptomatic and present as incidental findings during oral or dental examination. As they enlarge and become more prominent, however, tori may cause a wide spectrum of problems. These include interference with mastication and speech, compression and posterior displacement of the tongue, causing snoring or sleep apnea, and difficulty with placement and function of dental appliances, including dentures.[14] Additionally, tori can promote plaque formation and periodontal disease because of food retention.[3,8]

Patients with large tori often experience recurrent ulceration and inflammation of the covering gingival mucosa from trauma induced during chewing and ingestion of hard food items (Figure 5). Prominent TP lesions may also interfere with endotracheal intubation during general anesthesia.[15] There have been several reports concerning painful ulceration and osteonecrosis of torus in patients receiving bisphosphonate for treatment of osteoporosis.[16]

In some instances, larger, symptomatic tori may necessitate surgical removal.[3,17] This procedure was performed in two of the illustrated cases (Figures 2,4). Indications for resection included interference with

Figure 6. CT image shows TP lesion as an exostosis of the hard palate. Photograph reveals superficial erosions and inflammation of its mucosal surface (inset, arrows).

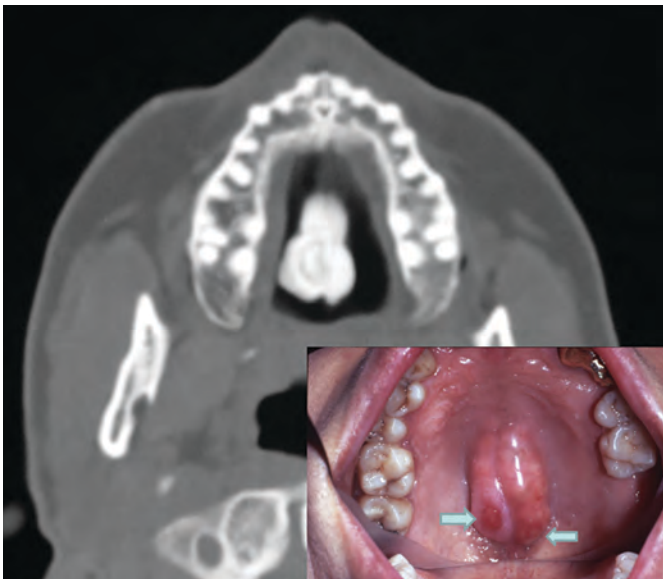

Figure 7. Torus Maxillaris (TMAX). CT shows very prominent bilateral exostoses of the molar regions (large black arrows), minimal cortical thickening anteriorly (small arrows), and a coexisting TP (white arrow). Intraoral photograph demonstrates the tori (inset).

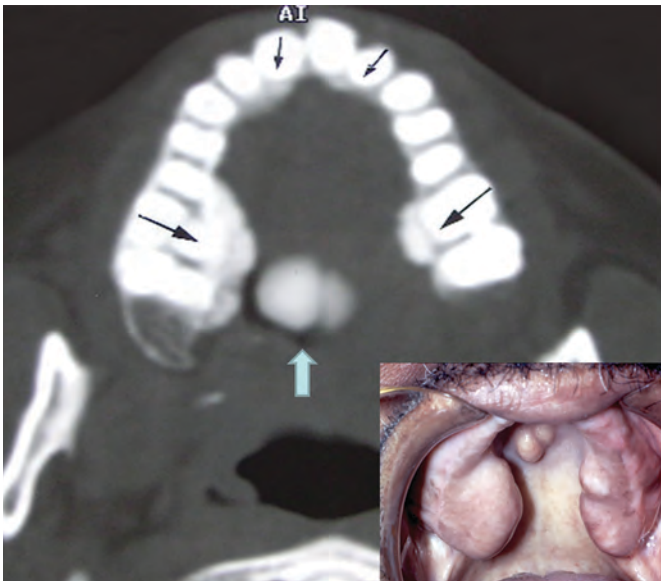

phonation or mastication, traumatic inflammation and ulceration, prosthetic instability, and in patients with disproportionate fear of malignancy.[10] A potential use of an excised torus is as an autogenous bone graft in periodontal surgery and as an implant elsewhere.[10, 18]

Although torus represents a common, well-recognized pathologic abnormality among dental professionals, the pathology has received scant mention in the medical literature. The lesion may be detected incidentally during routine radiological or physical examinations. Some patients may first seek medical advice because of concern for malignancy.

Although several causal factors have been postulated for the development of tori, their exact etiology in any individual patient may need further assessment. Radiologist familiarity with tori and their potential clinical complications can help assuage patient fears, improve diagnostic accuracy, and guide patient management.

References

1) King DR, King AC. Incidence of tori in three population groups. *J Oral Med.* 1981; 36(1): 21-23.

2) Chohayeb AA, Volpe AR. Occurrence of torus palatinus and mandibularis among women of different ethnic groups. *Am J Dent.* 2001; 14(5): 278-280.

3) Gonsalves WC, Chi AC, Neville BW. Common oral lesions: Part II. Masses and neoplasia. *Am Fam Physician* 2007; 75**:** 509-512.

4) Choi Y, Park H, Lee JS, et al. Prevalence and anatomic topography of mandibular tori: computed tomographic analysis. *J Oral Maxillofac Surg.* 2012; 70(6): 1286-1291.

5) Sonnier KE, Horning GM, Cohen ME. Palatal tubercles, palatal tori, and mandibular tori: prevalence and anatomical features in a U.S. population. *J Periodontol.* 1999; 70(3); 329-336.

6) Curran AE, Pfeffle RC, Miller E. Autosomal dominant osteosclerosis: report of a kindred. *Oral Surg Oral Med Oral Pathol Oral Radiol Endod.* 1999; 87: 600-604.

7) Eggen S. Torus mandibularis: an estimation of the degree of genetic determination. *Acta Odontol Scand.* 1989; 47: 409-415.

8) Morrison MD, Tamimi F. Oral tori associated with local mechanical and systemic factors: a case-control study. *J Oral Maxillofac Surg.* 2013; 71(1): 14-22.

9) Bruce I, Ndanu TA, Addo ME. Epidemiological aspects of oral tori in a Ghanaian community. *Int Dent J.* 2004; 54: 78-82.

10) Garcia-Garcia AS, Martinez-Gonzales JM, Gomez-Font R, etal. Current status of the torus palatinus and torus mandibularis. *Med Oral Patol Oral Cir Bucal.* 2010; 15(2): 353-360.

11) Morita K, Tsuka H, Shintani T, et al. Prevalence of torus mandibularis in young healthy dentate adults. *J Oral Maxillofac Surg.* 2017; 75(12): 2593-2598.

12) Jainkittivong A, Apinhasmit W, Swasdison S. Prevalence and clinical characteristics of oral tori in 1,520 chulalongkorn university dental school patients. *Surg Radiol Anat.* 2007; 29(2): 125-131.

13) Eggen S, Natvig B. Concurrence of torus mandibularis and torus palatinus. *Scand J Dent Res.* 1994; 102(1): 60-63.

14) Ahn SH, Ha JG, Kim JW, et al. Torus mandibularis affects the severity and position-dependent sleep apnoea in non-obese patients. *Clin Otolaryngol.* 2019; 44(3): 279-285.

15) Durrani MA, Barwise JA. Difficult endotracheal intubation associated with torus mandibularis. *Anesth Analg.* 2000; 90(3): 757-759.

16) Godinho M, Barbosa F, Andrade F, et al. Torus palatinus osteonecrosis related to bisphosphonate: a case report. *Case Rep Dermatol.* 2013; 5(1): 120-125.

17) Lee KH, Lee JH,Lee HJ. Concurrence of torus mandibularis with multiple buccal exostoses. *Arch Plast Surg.* 2013; 40(4):466-468.

18) Ganz SD. Mandibular tori as a source for onlay bone graft augmentation: a surgical procedure. *Pract Periodontics Aesthet Dent.* 1997; 9: 973-982.

Small Coil MRI of the Nipple-Areola Complex and Retroareolar Breast

Mariá Soledad Muñoz, MD; Maria Laura Alvares, MD; Daniela Muñoz Tisera, MD; Marcelo Elias Muñoz, MD

Imaging assessment of the nipple-areola complex and the retroareolar breast includes diagnostic mammography and targeted ultrasound as first-line imaging techniques, with magnetic resonance imaging (MRI) serving as a complementary alternative that nonetheless often leads to inconclusive results.[1-6]

In MRI, the sequences and coils, regardless of their brand or design, lack the necessary resolution for effective analysis of the ductal system, its contents, and the surrounding parenchyma.[7]

In this article, we present a practical application of focused, magnified, high-resolution MRI with contrast using commercially available small coils.[8] This approach is equivalent to the microfocus, spot magnification view traditionally used in diagnostic mammography. In this regard, we must discuss pioneering publications dealing with the efficacy of small coils in high-resolution analysis of different kinds of breast lesions.[9]

The small coil is used mainly to detect lesions not seen on standard imaging evaluation, to confirm positive findings with conventional techniques (mammography, ultrasound, MRI), and to present them in an accessible way for surgeons and the pathologists.[10]

Affiliation: Clinica Camara Gamma, Rosario, Argentina.
Disclosures: None

Breast MRI with Small Coil Technique

The exam is performed on a 1.5T MRI scanner with a small surface coil focused on the areola instead of a conventional bilateral coil.

Owing to its design and dimensions, the small coil allows for ventral and lateral decubitus explorations according to the patient's anatomical needs. The coil's high performance facilitates the study of the areola and the underlying parenchyma up to a depth of 6-7 cm from the nipple, including divisions of the ducts up to the fourth grade.[11]

The protocol consists of T2 3D TSE (3D turbo spin echo), T1 3D FFE (3D fast field echo) and T1 3D FFE EPI (3D fast field echo-echo planar), fat-saturated sequences with and without contrast and obtained only in the axial plane. The geometry and contrast of these sequences are shown in Table 1.

The first sequence (T2 SPAIR) demonstrates ducts with serous or serosanguinous content. The second (T1 SPIR) and the third sequence (T1 SPIR-EPI) mainly detect blood products and are used before contrast administration.

After contrast injection, the second and third sequences are repeated, with the fourth sequence concluding the imaging. The fourth sequence (T1 SPIR FOV 150 mm) is optional; it has a lower resolution but a larger FOV, and provides information regarding the topography, lesion extension, and any additional findings.

Only fat-saturation sequences are applied, not only because gadolinium is used but also because the resolution provided by the coil does not require the presence of fat to identify typical lesions in this breast segment. The only artifacts are those generated by patient movement that can occur.

This is predominately a high-resolution morphological study without dynamic curves because the small coil provides images with average acquisition times of two to three minutes. The enhancement hierarchy could be visually estimated.

Regarding FOV, the software adjusts the matrix, providing 0.49 × 0.49 mm pixels with 0.7 mm slices in T2 (TSE) and 0.23 × 0.23 mm pixels with 0.6 mm slices in T1 (FF3D), with a resolution eight times higher than that of a conventional breast coil. This software also builds nonisotropic voxels that allow reconstruction in MIP (maximum intensity projection) and 3D volume rendering in

Table 1. Contrast and geometry of sequences

SEQUENCE	(1) T2 SPAIR	(2) T1 SPIR	(3) T1 SPIR-EPI	(4) T1 SPIR FOV 150 MM
Parameter	3D TSE	3D FFE	3D FFE	3D FFE
TE (ms)	235	8.7	7	8.7
TR (ms)	2000	43	35	43
Flip angle (°)	90	50	50	50
Reconstructed voxel size (mm)	0.49 x 0.49 x 0.7	0.23 x 0.23 x 0.6	0.22 x 0.22 x 1	0.23 x 0.23 x 2
Scan Time (min)	3.50 (2 NEX)	3.15 (1 NEX)	1.12 (2 NEX)	2.41 (1 NEX)
FOV (mm)	70	80	80	150

Philips Multiva 1.5T with dStream Microscopy coil® - Philips 4.7 cm diameter

(1) T2 SPAIR, spectral attenuated inversion recovery (3D turbo spin echo)

(2) T1 SPIR, spectral pre-saturation with inversion recovery (3D fast field echo)

(3) T1 SPIR-EPI (3D fast field echo + echoplanar)

(4) T1 SPIR FOV 150 (3D fast field echo with 150 mm field of view)

the most representative planes (axial and sagittal) and video editing in three planes.[12]

Imaging Findings

The resolution provided by the small coil represents the anatomy of the central major ducts to detect its signal (serous, sanguineous, and mixed) and the presence of filling defects. This high resolution allows detailed analysis of enhancements of the paramagnetic contrast inside the ducts and on their walls, as well as of masses and non-masses in the surrounding parenchyma.

The protocol is primarily used to evaluate patients with clinically significant nipple discharge, palpable findings in an inverted or retracted nipple, and Paget disease.

Clinically Significant Nipple Discharge

Nipple discharge is the third-most common reason for clinical evaluation after mastodynia and palpable lump(s). The most common breast entities related to clinically significant nipple discharge are intraductal papilloma (40-70% of cases) and other benign causes.

Less frequent, but more relevant and concerning, is a malignant lesion (more commonly associated with bloody nipple discharge) that may be occult on mammography and ultrasound, such as in situ ductal carcinoma (DCIS).[13,14]

Papilloma

Papillomas are classified into central, peripheral, and intracystic types and categorized as single or multiple. Central papillomas originate outside the terminal ductal-lobular unit and are generally solitary, whereas peripheral types tend to occur in multiples, owing to their origin in the terminal duct-lobular units.[15]

On mammograms papillomas are usually < 10 mm, circular/oval masses, with or without associated calcifications, which can be either coarse or crushed stone-like.[15]

The ultrasound appearance of intraductal papilloma is a solid, vascularized nodule located within a single, dilated duct in the subareolar area. The presence of a circumscribed margin does not distinguish benign from malignant papillary lesions.[16]

With the small coil, central papillomas appear as measurable, solid, filling defects in a major central duct with or without gadolinium enhancement and with the most prominent ectasia in the proximal segment of the duct with varying MRI signal characteristics on T1 and T2, depending on the serous, proteinaceous, or hemorrhagic content (Figure 1, 2).[17]

Papillomas are characterized as single masses of different sizes and morphologies (node, bar-shaped, bifurcated, coral-like; Figure 3).

Multiple papillomas (10 percent of intraductal papillomas) are often deeper, more peripheral, and occur bilaterally; they are related to hyperplasia, atypia, adenosis, and sclerosing lesions. They appear on MRI as random enhancing small masses not always associated with ectatic ducts. Single papillomas are rarely associated with cancer (1.3%), but multiple papillomas confer a greater risk of cancer than a single papilloma.[18,19,20]

Intracystic papillomas (Figure 4) are rare (1%) and frequently occur in multiples. Differential diagnosis between intracystic papillomas and intracystic papillary carcinoma is difficult preoperatively.

Other Benign Entities

There are other more diffuse, nonspecific, benign entities that

Figure 1. Central single papilloma. (A) Axial MIP T2 showing an ectatic central duct with bright serous signal intensity and filling defect (arrow). (B) Axial MIP T1 with gadolinium, showing an enhancing mass. Central multiple papillomas: (C) Axial MIP T2 showing an ectatic and tortuous central duct with serous signal intensity with filling defects (arrows); (D) Volume rendering.

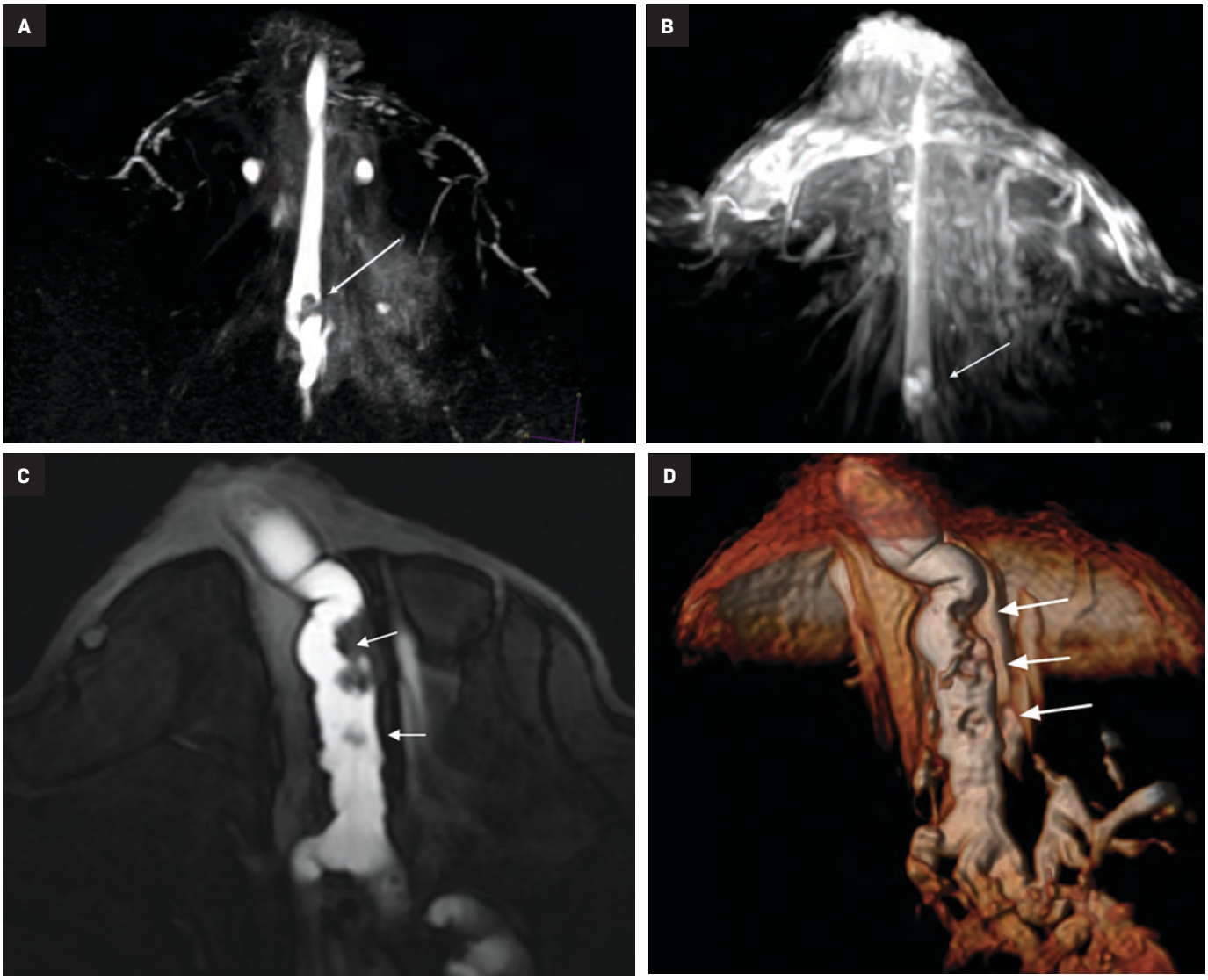

allow more expectant management, including simple ductal ectasia, galactoceles (Figure 5), and fibrocystic mastopathies (Figure 6).

Normal milk ducts have longitudinal folds that disappear when the duct is distended by accumulation of fluid, cells, tumor, and detritus.[21] Small coil MRI readily demonstrates distended major lactiferous ducts. Given this, the more appropriate descriptive term is "ductal ectasia" instead of "dilated duct," as the former refers to a measurement that originated and was used in ultrasound imaging, within a range 1.0-4.4 mm.[22]

Depending on degree of distention and their contents, ectatic ducts can appear as filiform structures, tubular formations, or coarse cystic conglomerates in their most chronic stages. Ductal ectasia is usually an asymptomatic and nonspecific finding, but it may present with nipple discharge and is a frequent finding on ultrasound. MRI in simple ductal ectasia reveals uniformly distended ducts with fluid or serosanguineous intensity signal with normal caliber, not distorted, with or without submillimeter filling defects and without wall enhancement. MRI with small coils also helps to precisely locate the compromised segment or quadrant if surgery is required.

Breast Cancer

Breast cancer may clinically manifest with nipple inversion or retraction, a size increase and/or asymmetry on areolar palpation, as in Paget disease, or with significant nipple discharge as the only finding.

Figure 2. Papilloma at the nipple base. (A) Axial MIP T2, ectatic tortuous central duct with serous signal intensity and filling defect. (B) Volume rendering. (C) MIP T1 with contrast enhancing mass. Note: The tortuous segment of the duct at the base of the ampullary segment is a normal anatomical finding (small arrow in A, B).

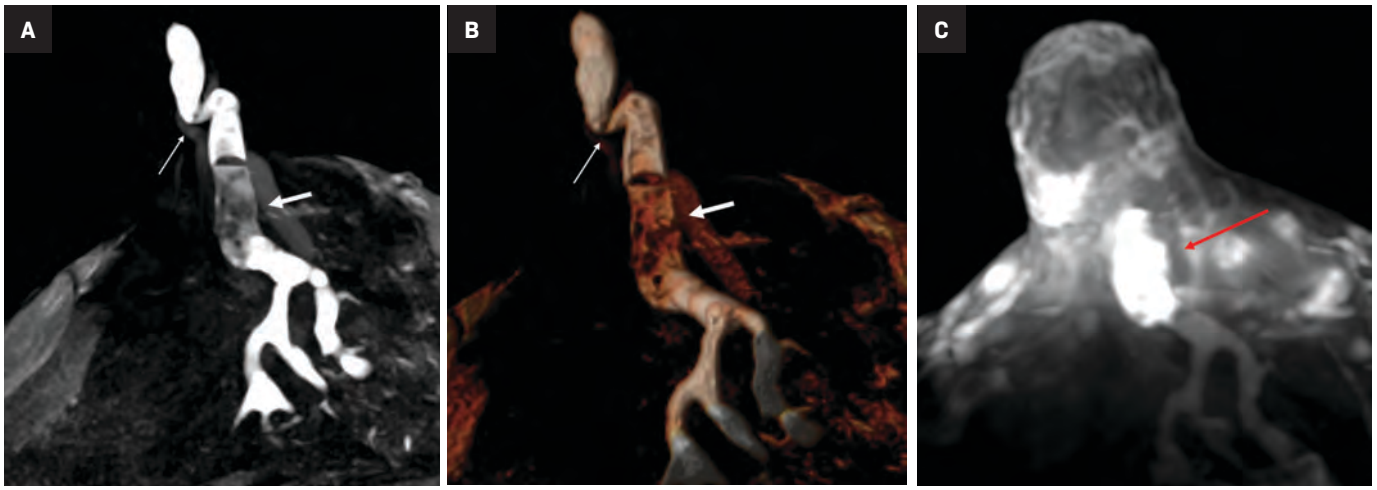

Figure 3. Coral-shaped papilloma enhancing on postcontrast T1 MIP. (A) Confluent multiple bars on MIP reconstruction and (B) volume-rendered reconstruction.

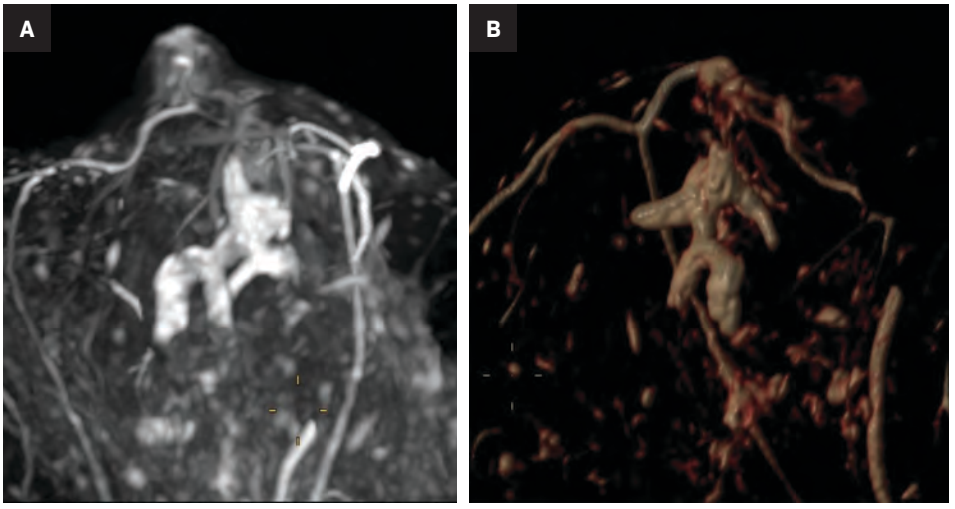

One subtype of breast cancer originating from the major lactiferous ducts presents with serous or bloody nipple discharge with a tumor growth pattern showing a mixture of papillary/micropapillary and/or cribriform growth without necrosis. No calcifications are expected on mammography in these cases, because, as Tabar indicates, "the nipple discharge prevents the long-term fluid stagnation within the duct". [23,24,25]

As an initial exam, breast ultrasound can be effective for the detection of invasive carcinomas and certain types of DCIS, including intraductal papilloma with DCIS or intraductal papillary carcinoma, which appear as masses. However, ultrasound may not be effective in detecting DCIS that manifests only with nipple discharge.

With small coil MRI, the micropapillary and cribriform growth patterns appear in discontinuous patches toward the nipple as non-mass-like regions of contrast enhancement, often in clustered rings, branching in an increasing number of abnormal ducts (neoductogenesis)[25,26], with little or no contrast washout for 5-10 minutes.

Detected by MRI, these features allow for more accurate determination of their extent and anatomic location better than ultrasound, which is known to underestimate the extent of DCIS.[27,28] MRI with small coils better represents segmental distribution; ie, triangular on maximum intensity projections and pyramidal on 3D volume rendering (Figures 7, 8). This finding supports previously published data that confirmed the high positive predictive value for a malignant lesion when encountering the clustered ring enhancement pattern and segmental disposition.[29,30]

Palpable Lesions with Inverted or Retracted Nipples

Small coil image findings may be conclusive in these clinical situations;

Figure 4. Giant intracystic papilloma presenting as a palpable mass. (A) Ultrasound of complex cystic mass with peripheral blood vessels along the solid component (arrows). (B) MIP T2 of cyst with filling defect from a frond-like mass (arrow). (C) Postcontrast T1 MIP shows the enhancing intracystic mass (black arrow) and small satellite masses. (D) Volume rendering of the same lesion with small satellite masses (white arrows).

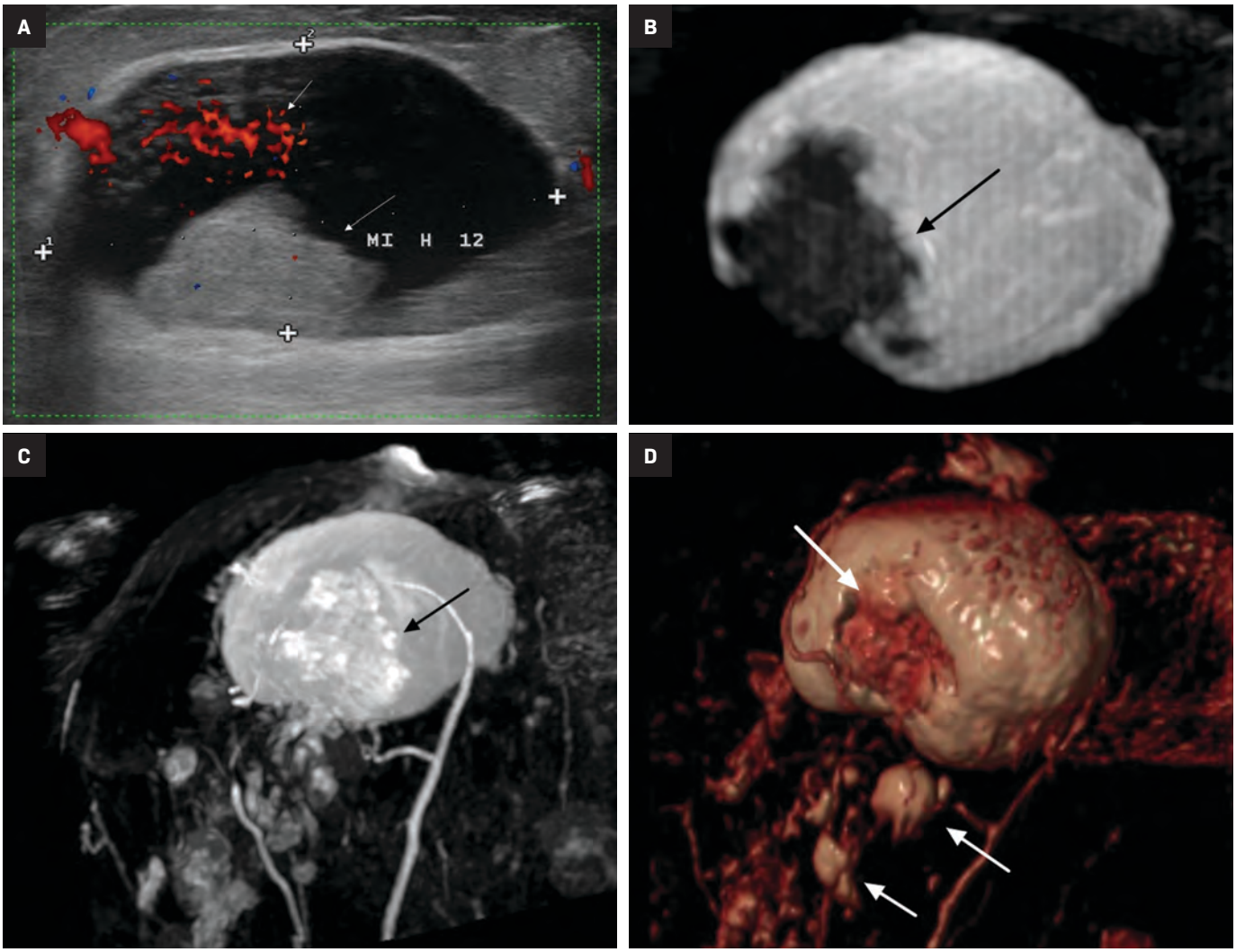

they are primarily used to detect and characterize masses, to associate the retracted nipple with chronically diseased ducts, or to assess the need for surgical exploration (Figures 9, 10).

Paget Disease

Once a lesion has been confirmed, either by mammography or ultrasound breast, MRI should also performed, as the modality offers a detailed exploration of the central cone of the breast (Figure 11) to search for an underlying cancer.[31]

Conclusion

MRI with small coils can provide a high-resolution targeted study (similar to diagnostic spot-magnified mammography) that can serve as an adjunct to standard techniques for evaluation of the nipple-areola complex and retroaleolar breast.

References

1) Bahl M, Gadd M, Lehman C. Diagnostic utility of MRI after negative or inconclusive mammography for the evaluation of pathologic nipple discharge. *AJR* 2017; 209:1404–1410.

2) Berger N, Luparia A, Di Leo G, et all. Diagnostic Performance of MRI versus galactography in women with pathologic nipple discharge: A systematic review and meta-analysis. *AJR* 2017; 209:465–471.

3) Sarica O, Ozturk E, Demirkurek H, Uluc F. Comparison of ductoscopy, galactography, and imaging modalities for the evaluation of intraductal lesions: A critical review. *Breast Care.* 2013; 8:348–354.

4) Srinivasan A, Nia E, Gupta M, Sun J, Leung J. Retrospective statistical analysis on the diagnostic value of ductography based on lesion pathology in patients presenting with nipple discharge. *The Breast Journal* 2019; 25:585–589.

5) Schedule K, Schnitzer A, Krammer J, Kaiser C, Schönberg S.O, Wasser K. Value of galactography for the diagnostic work-up of pathological nipple discharge in multimodal breast diagnostics. *Radiologe.* 2014. 54:160–166.

Figure 5. Galactocele. MIP T2 of ectatic ducts with large cystic dilatation (Inset: Volume-rendered reconstruction). (B) Ductal ectasia: MIP T2, ectatic ducts with serous signal intensity, no filling defects (Inset: volume-rendered reconstruction).

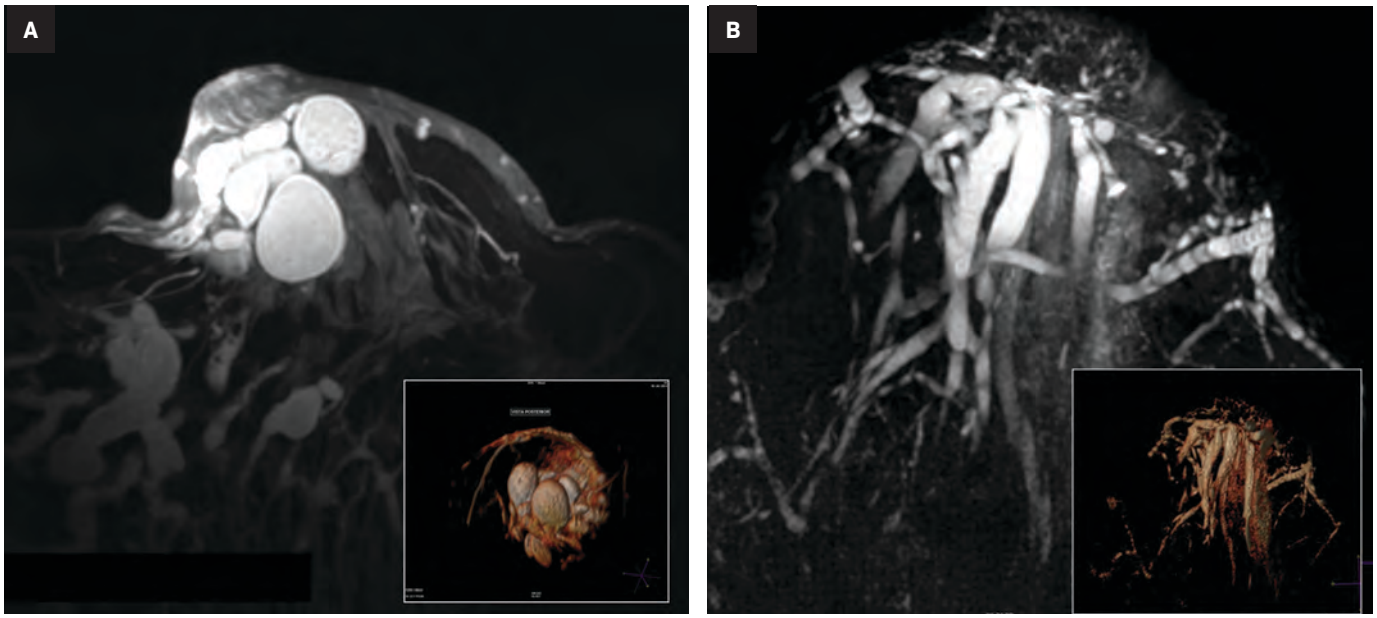

Figure 6. Fibrocystic mastopathy, mixed pattern with small nodules and cysts. (A) MIP T2 of cysts (white arrows) interposed with nodules (yellow arrows). (B) MIP T1 with gadolinium showing multiple small nodules (yellow arrows) along with central and peripheral ductal ectasia (white arrows).

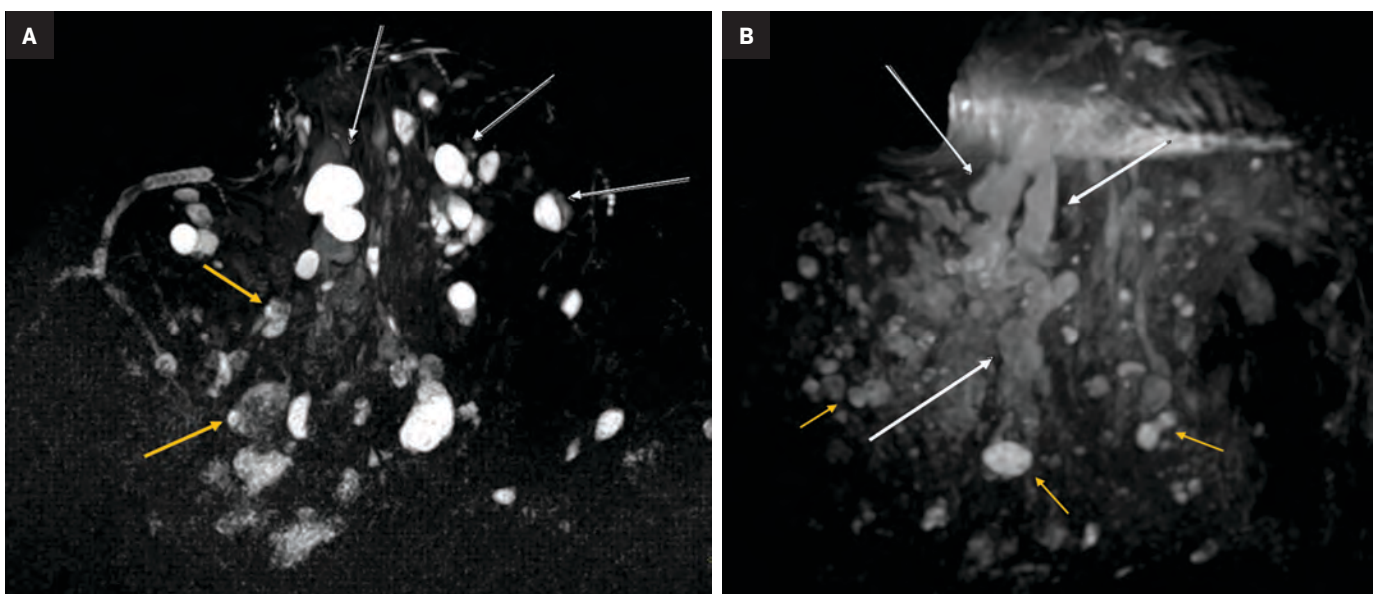

6) Morrogh M, Park A, Elkin E.B, King T.A. Lessons learned from 416 cases of nipple discharge of the breast. *Am J Surg.* 2010; 200:73–80.

7) Kurihara Y. Microscopy coils provide SNR to resolve smallest anatomy. *http://clinical.netforum.healthcare.philips.com/global/Explore/Best-Practices.*

8) Kanemaki Y, Kurihara Y, Okamoto K, Nakajima Y, Fukuda M, Maeda I, et al. MR mammary ductography using a microscopy coil for assessment of intraductal lesions. *AJR.* 2004; 182:1340–1342.

9) Kanemaki Y, Kurihara Y, et al. Ductal carcinoma in situ: correlations between high-resolution magnetic resonance imaging and histopathology. *Radiat Med.* 2007; 25:1–7.

10) Zacharioudakis K, Kontoulis T, Vella J. Can we see what is invisible? The role of MRI in the evaluation and management of patients with pathological nipple discharge. *Breast Canc Res Treatm.* 2019; 178(1):115-120.

11) Ohuchi N, Abe R, Takahashi T, Tezuka F. Origin and extension of intraductal papillomas of the breast: a three-dimensional reconstruction study. *Breast Cancer Res Treat.* 1984;4(2):117-28.

12) Simpfendörfer T, Li Z, Gasch C, et al. Three-dimensional reconstruction of preoperative imaging improves surgical success in laparoscopy. *J Laparoendo Adv Surg Techn.* 2017; 27(2):181-185.

13) Lippa N, Hurtevent–Labrot G, Ferron S, Boisserie-Lacroix M. Nipple discharge: The role of imaging. *Diagn Intervent Imag.* 2015; 96(10):1017-1032.

Figure 7. Carcinoma presenting with bloody nipple discharge, negative ultrasound. (A) T1 with gadolinium, lateral focal non-mass enhancement (yellow arrow) (Inset: T1 without contrast, with bright hemorrhagic signal intensity in ectatic central ducts, white arrow). (B) Volume rendering (Inset: histopathology of papillary and cribriform carcinoma).

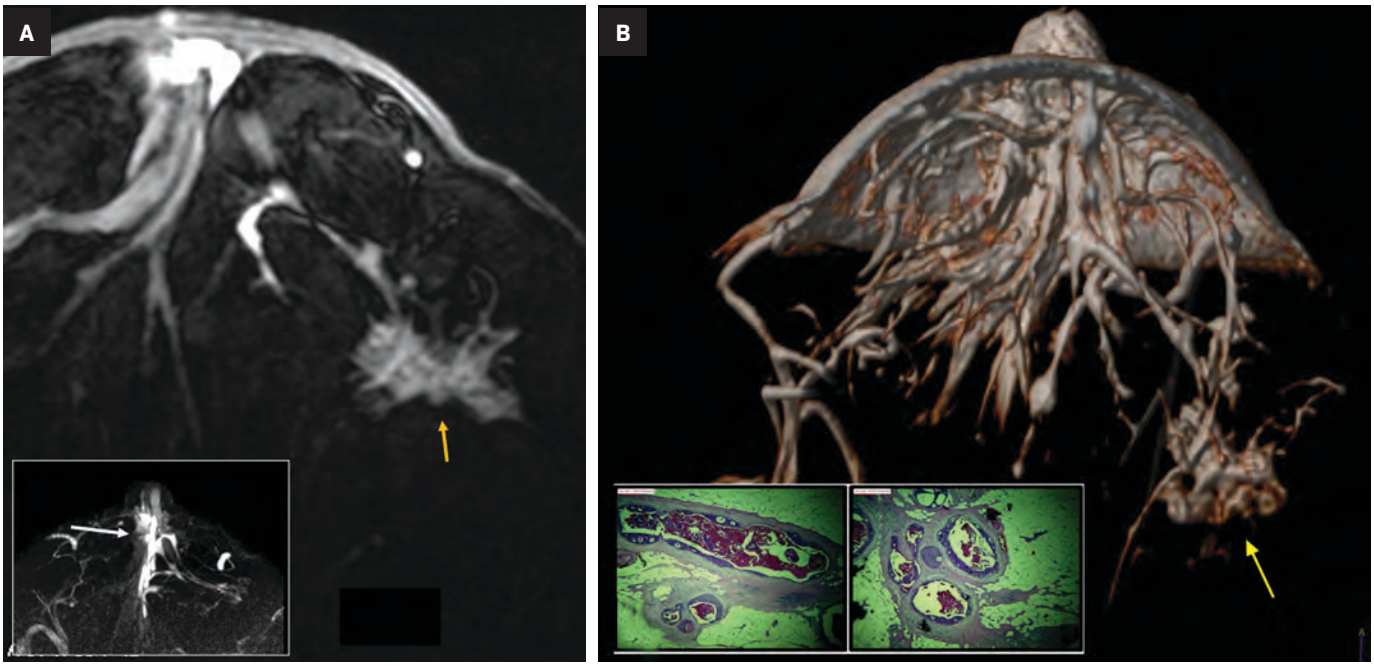

Figure 8. Carcinoma presenting with bloody nipple discharge. (A) MIP T1 with gadolinium, central duct with bright hemorrhagic signal intensity (yellow arrow) and non-mass enhancement in conglomerated rings (white arrows). (B) Volume rendering showing thickened walls in the central duct (yellow arrow) and conglomerated rings branching in ducts (white arrows). (C) Conglomerated rings: hypointense centers (yellow arrows) represent ducts filled by malignant proliferation and bright rings (red arrows) represent neo-angiogenesis in the stroma enhanced with gadolinium.

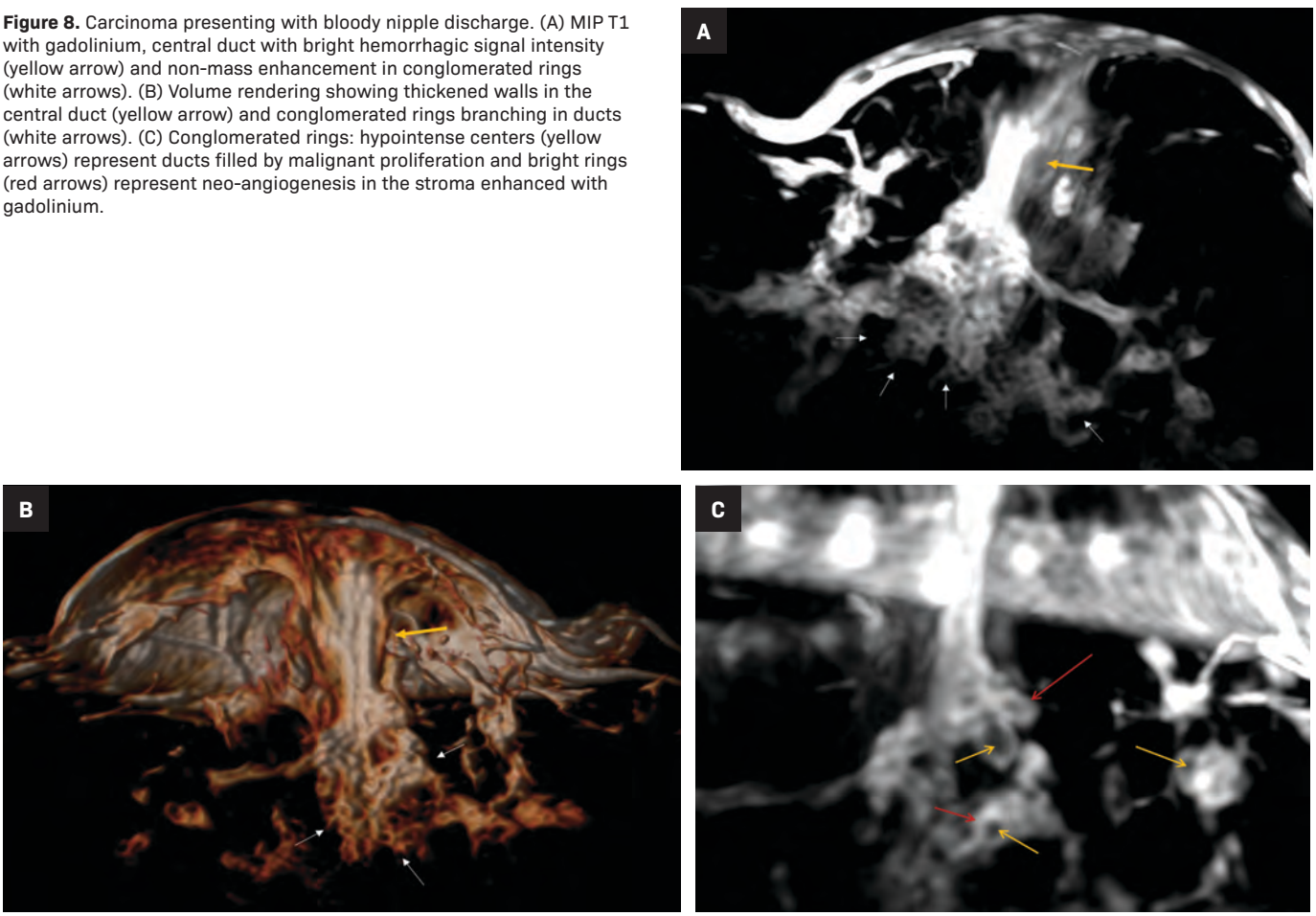

Figure 9. Palpable findings. (A) Ductal carcinoma: T1 with gadolinium, highly vascular, spiculated mass (inset: volume rendering). (B) Nipple adenoma: T1 with gadolinium, enhancing circumscribed lymph node (Inset: ultrasound showing nipple enlarged by a solid, vascular mass).

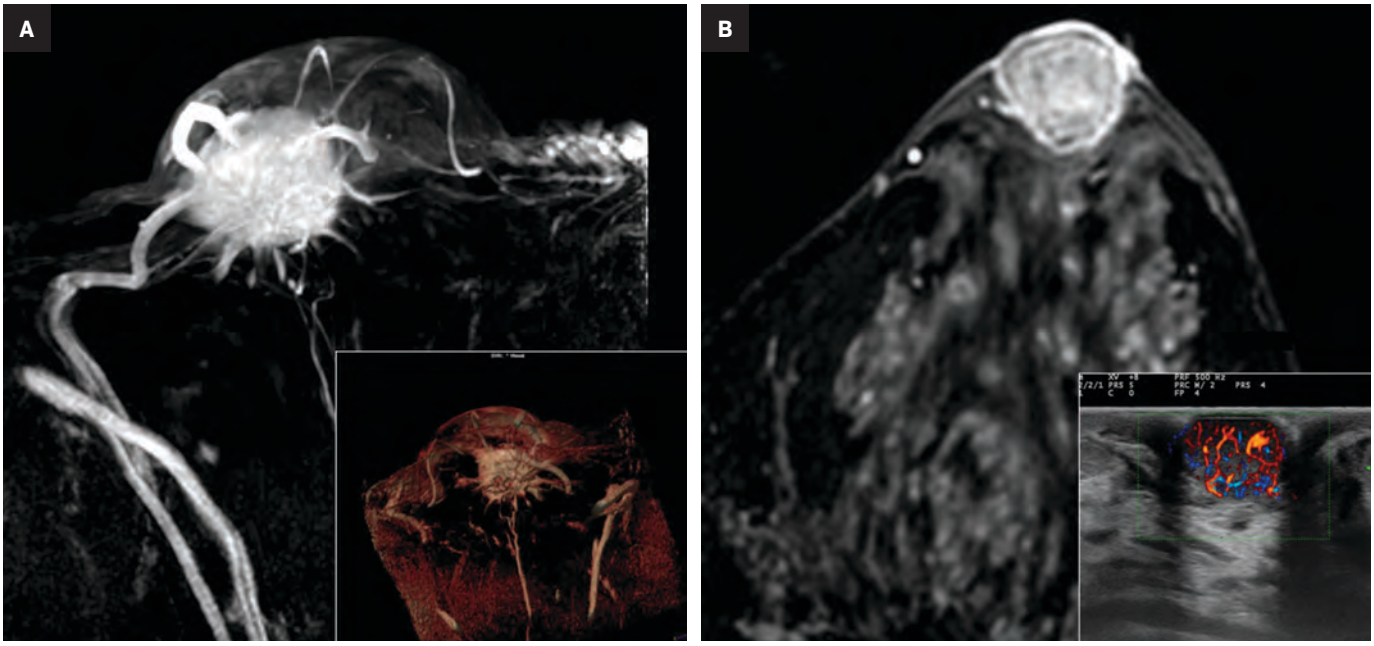

Figure 10. Retracted nipple. (A) Mammogram with subareolar distortion and retracted nipple (white arrow). (B) T1 with gadolinium, irregular spiculated mass (white arrow) with a thick retro-areolar band (yellow arrow). (C) Volume rendering of a classic lobular carcinoma.

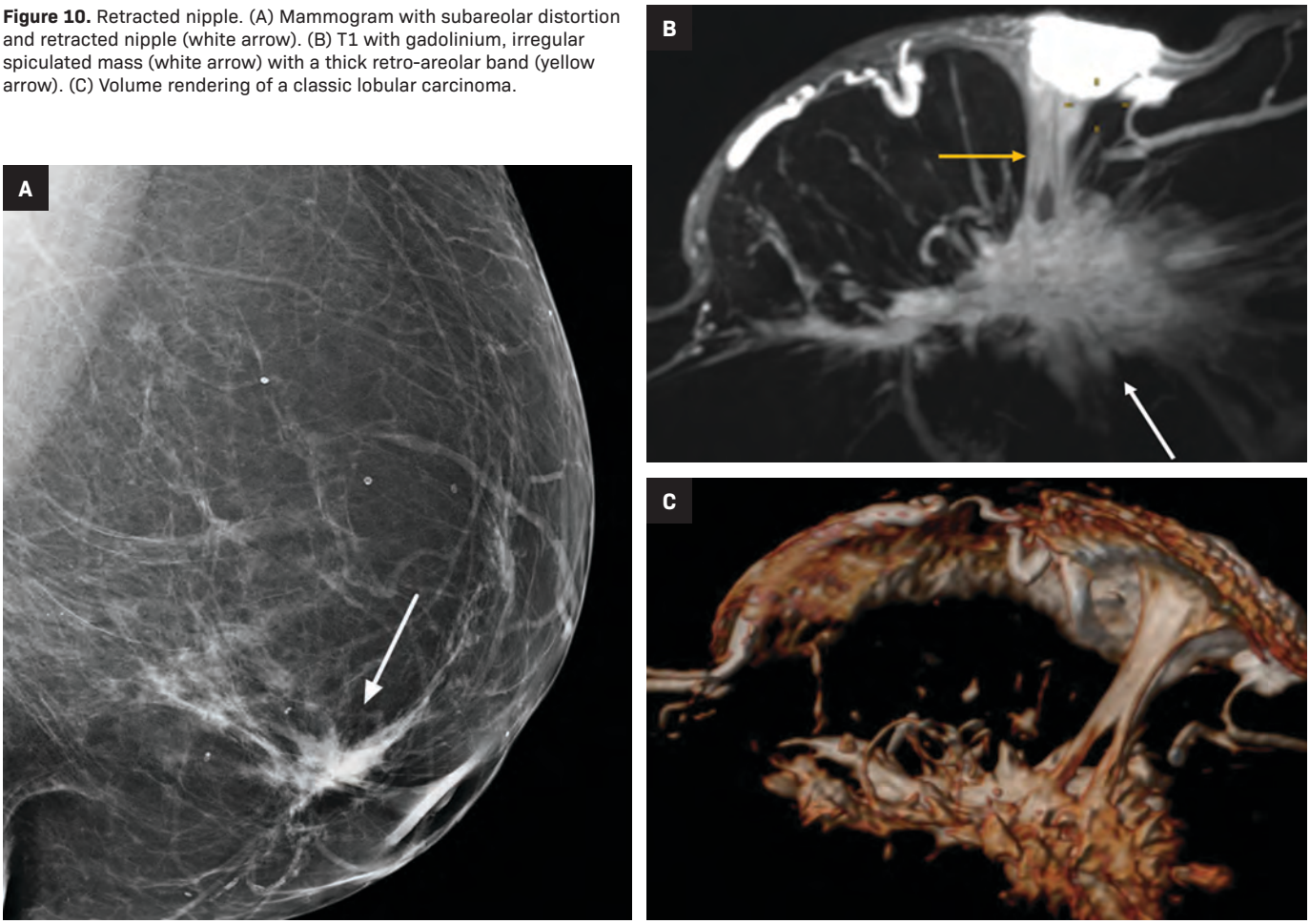

Figure 11. Two patients with Paget disease. Patient 1: eczema-like lesion on the nipple and serous discharge. (A) Axial T1 MIP with gadolinium and (B) volume rendering both showing segmental, non-mass enhancement (white arrow) confluent to a central duct facing the nipple (yellow arrow). Patient 2: (C) Axial T1 MIP with gadolinium and (D) volume rendering both showing an enlarged nipple and lateral segmental non-mass enhancement with nipple-oriented conglomerated rings (white arrows). (Inset: mammogram with punctate segmental macrocalcifications in a ductal adenocarcinoma [yellow arrows]).

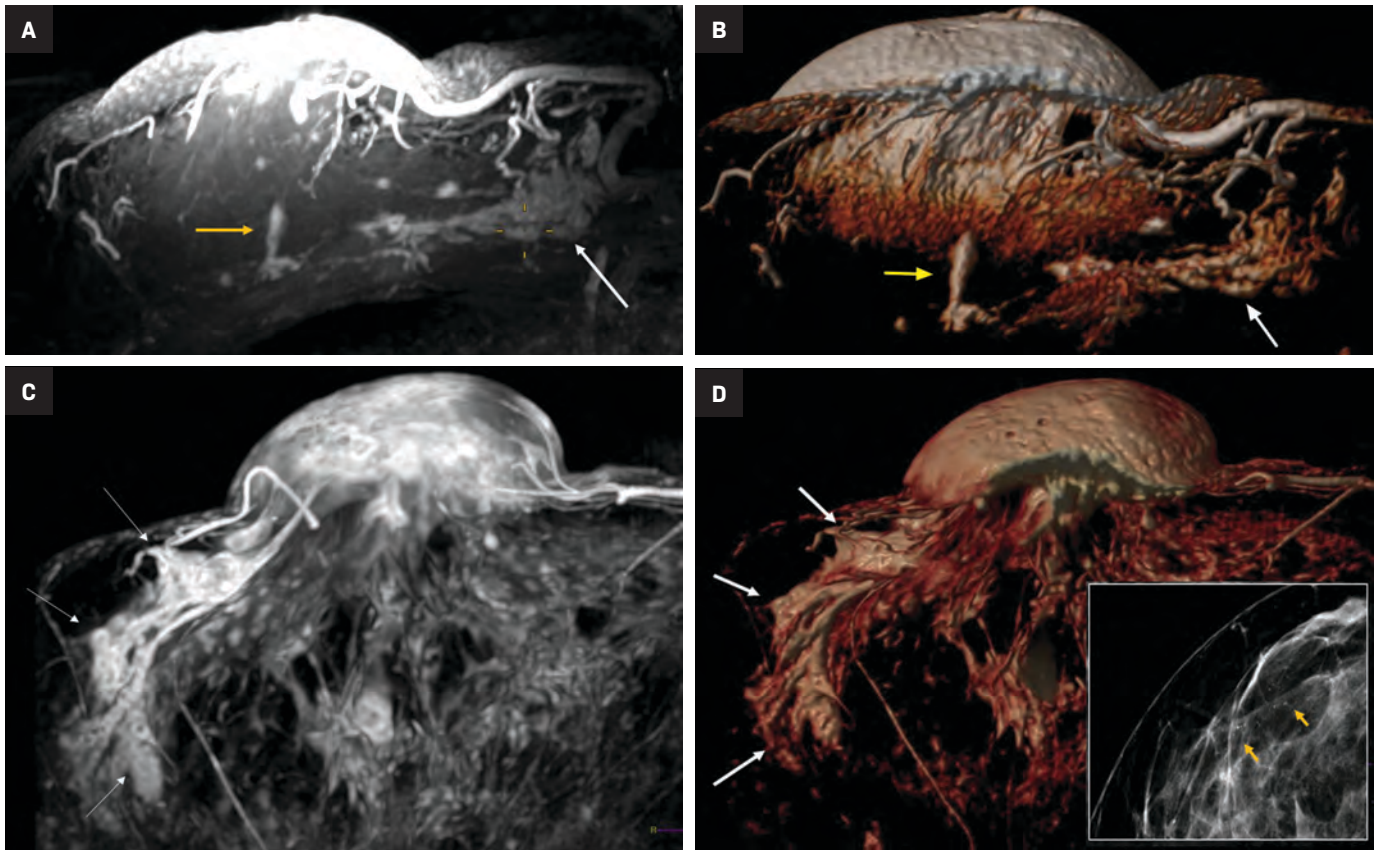

14) Chen L, Zhou WB, Zhao Y,et all. Bloody nipple discharge is a predictor of breast cancer risk: a meta-analysis. *Breast Cancer Res Treat*. 2012;132(1): 9-14.

15) Tot T, Tabar L, Dean, P, *Practical Breast Pathology 2014 2nd edition*. Thieme Verlag Gruppe, Stuttgart. Nueva York, 2014:86-93

16) Kim TH, Kang DK, Kim SY, Lee EJ, Jung YS y Yim H. Sonographic differentiation of benign and malignant papillary lesions of the breast. *J Ultrasound Med*. 2008; 27:75-82.

17) Son EJ, Kim EK, Kim JA, Kwak JY, Jeong J. Diagnostic value of 3D fast low-angle shot dynamic MRI of breast papillomas. *Yonsei Med J*. 2009; 50(6):838-44.

18) Ueng SH, Mezzetti T, Tavassoli FA. Papillary neoplasms of the breast: a review. *Arch Pathol Lab Med*. 2009; 133(6): 893-907.

19) Liberman L, Tornos C, Huzjan R, Bartella L, Morris EA, Dershaw DD. Is surgical excision warranted after benign, ¿concordant diagnosis of papilloma at percutaneous breast biopsy? *AJR Am J Roentgenol*. 2006; 186(5):1328-1334.

20) Li X, Aho M, Newell MS, et al. Papilloma diagnosed on core biopsies has a low upgrade rate. *Clin Imaging*. 2020; 60(1):67-74.

21) Tabár L, Tot T, Dean P. Understanding the breast in health and disease. Hong Kong. C & C Offset Printing Co. 2012; 7-9

22) Ramsay D, Kent J, Hartmann R, Hartmann P. Anatomy of the lactating human breast redefined with ultrasound imaging. *J Anat.*. 2005; 206(6): 525-534.

23) Tabár L, Tot T, Dean P. Multimodality Imaging in the Interdisciplinary Management of Breast Diseases. In: Jones G, *Bostwick's Plastic and Reconstructive Breast Surgery, 4th Ed, Vol 1: Thieme*; 2020:119-134.

24) Tabár L, Tot T, Dean P. *Understanding the breast in health and disease*. Hong Kong. C & C Offset Printing Co; 2012:7-9.

25) Tot T, Gere M. Radiological-pathological correlation in diagnosing breast carcinoma: The role of pathology in the multimodality era. *Pathol Oncol Res*. 2008; 14(2):173-178.

26) Tot T, Gere M, Pekar G, Tarjan M, Hofmeyer S, Hellberg D, et al. Breast cancer multifocality, disease extent, and survival. *Hum Path*. 2011; 42(11):1761-1769.

27) Nakahara H, Namba K, Watanabe R. A comparison of MR imaging, galactography and ultrasonography in patients with nipple discharge. *Breast Cancer.* 2003;(4):320-329.

28) Lee Su Ju, Sobel L, Shamis M, Mahoney M. Asymmetric ductal ectasia: An often-overlooked sign of malignancy. *Am J Radiol.*2019; 213(2):473-481.

29) Tozaki M, Igarashi T, Fukuda K. Breast MRI using the VIBE sequence: clustered ring enhancement in the differential diagnosis of lesions showing non-masslike enhancement. *Am J Radiol.* 2006; 187(2):313–321.

30) Tokuda Y, Kuriyama K, Nakamoto A, Choi S, Yutani K, KunitomiY, et al. Evaluation of suspicious nipple discharge by magnetic resonance mammography based on breast imaging reporting and data system magnetic resonance imaging descriptors. *J Comput Assist Tomogr*. 2009; 33:58-62

31) Sripathi S, Ayachit A, Kadavigere R, Kumar S, Eleti A, Sraj A. Spectrum of imaging findings in Paget's disease of the breast—a pictorial review. *Insights Imaging*. 2015; 6(4): 419–429.

Treatment Brings Hope in Alzheimer Disease: Role of Imaging AI

Suzie Bash, MD, and Lawrence N Tanenbaum, MD, FACR

Affiliations: Dr Bash is a neuroradiologist at RadNet, Inc, Los Angeles, CA. She is also a member of the Editorial Advisory Board of *Applied Radiology.* Disclosures: Dr Bash is a consultant to Cortechs.ai, icometrix, Subtle Medical, and Darmiyan. Dr Tanenbaum is VP and CTO at RadNet, Inc, New York, NY. He is also a member of the Editorial Advisory Board of *Applied Radiology.* Disclosures: Dr Tanenbaum is a consultant to icometrix, Subtle Medical, and Darmiyan.

Alzheimer disease (AD) is a devastating, lethal disease affecting 6 million in the US (and 20 million worldwide). The hallmarks of AD in the brain are beta-amyloid (Aβ) plaques, which are imaged with amyloid PET (Figure 1), and neurofibrillary tangles, which are imaged with tau PET.

AD is the most common form of dementia and death rates are rising. For example, while death from heart disease is down 7 percent since 2000, deaths from AD are up 145 percent. The incidence of AD doubles every five years after the age of 60. *APOE ε4* status is the strongest genetic risk factor for AD, with 25 percent of the US population carrying one *APOE ε4* allele (increasing the risk of AD threefold) and 2-3 percent of the US population carrying two *APOE ε4* alleles (increasing risk twelve-fold). One in three seniors will die of dementia, which kills more people than breast and prostate cancer combined.

Artificial intelligence (AI) plays an important role in diagnosis and follow-up of dementia, particularly in the realm of quantitative volumetric neuroimaging (QNI). Quantitative

Figure 1: Amyloid PET. Amyloid PET-CT fusion with color overlay (A) and amyloid PET-MR fusion (axial T2W) with color overlay (B). This is a positive amyloid PET study in a patient with Alzheimer disease, with diffuse binding of the amyloid tracer to the beta-amyloid (Aβ) plaque throughout the cortex.

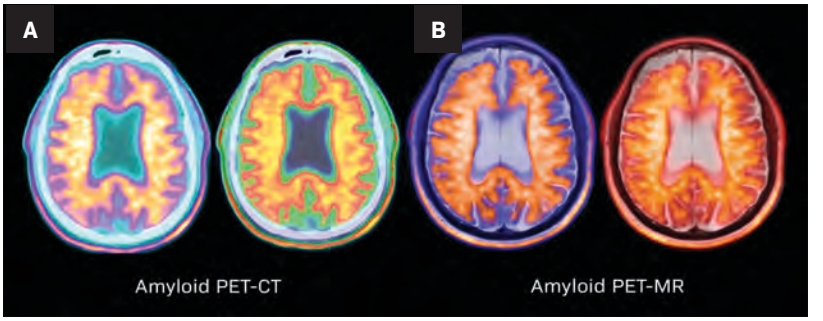

Figure 2. Quantitative volumetric MR segmentation with NeuroQuant™. Sagittal T1W with NeuroQuant™ (A) and sagittal T1W with icobrain™ (B)

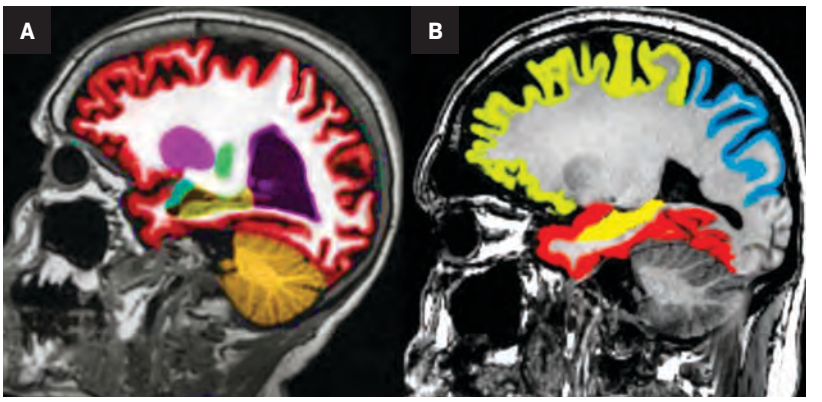

assessment reduces reader subjectivity, and improves inter- and intra-reader consistency, factors referrers value highly. Quantitative analysis includes color-coded segmentation and volumetric assessment of anatomic substructures pertinent to dementia, with comparison to a large normative age and gender-matched database (Figure 2). Values that fall more than two standard deviations from the mean are highlighted. For longitudinal studies, the rate of drop-off from the normative curve can be useful in differentiating mild cognitive impairment (MCI) from progression to AD, as 40 percent of patients with MCI will progress to AD. Assessment of the volumes of pertinent brain substructures can be useful in distinguishing between types of dementia. Some AI products also incorporate clinical information, *APOE ε4* status, and additional quantitative imaging features in an attempt to improve prediction of which patients may progress to AD.

Biogen's Aduhelm™, a monoclonal antibody which targets the epitope on Aβ plaque, and the first potentially disease-modifying therapy for AD, was approved by the FDA under its Accelerated Approval Program (AAP) in June 2021 — a decision seen by some as controversial due to concerns over cost and evidence of efficacy.

While both Biogen's Phase 3 clinical trials successfully met the surrogate endpoint (effective removal of Aβ plaque as shown on amyloid PET when compared to placebo), only one of the two trials met the primary endpoint of improved cognition. (The high-dose limb of one trial showed a 23 percent improvement.)

The financial impact of untreated AD is high, costing $355 billion in 2021 and rising to $1.1 trillion by 2050 in the US alone. Although Aduhelm remains expensive, Biogen has just slashed the price in half (now 28K/year). While nearly all US states will reimburse on a case-by-case basis, a federal CMS decision to approve payment has yet to be made but is expected no later than April 2022. A nationwide approval isessential to ensure consistent inclusion in hospital formularies and facilitate treatment. While the European Medicine Agency (EMA) recently recommended denying market authorization for Aduhelm, Biogen has formally requested a re-examination. Several other potential disease-modifying therapies are in the overall pharmaceutical pipeline, some of which have already been granted FDA Breakthrough Therapy designation.

Imaging enterprises will be significantly impacted by AD therapy, especially if CMS approves reimbursement. Although not label-required, confirmation of the presence of Aβ plaque is likely to be expected before patients will be treated with Aduhelm. This is accomplished through lumbar

Figure 3. ARIA-E (parenchymal edema) in left parietal lobe on axial FLAIR. Unsegmented (A) and quantitative volumetric MR segmentation with icobrain™ in green (B).

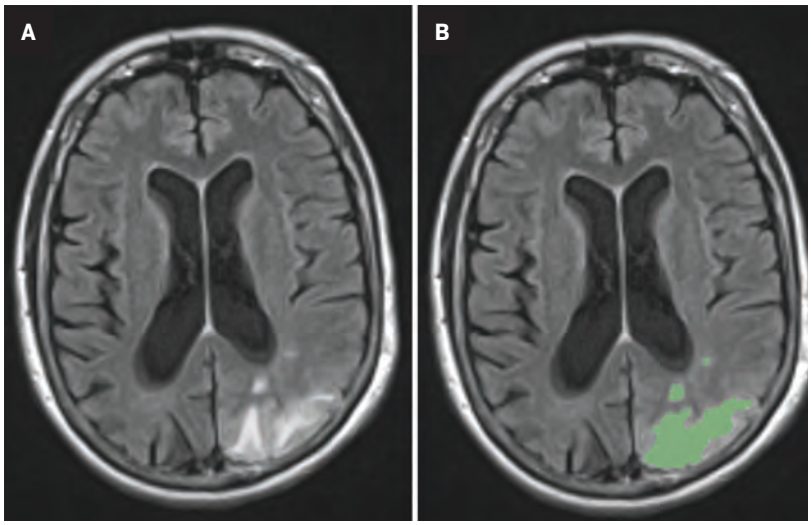

Figure 4. ARIA-E (sulcal effusion) in bilateral temporal and occipital regions on axial FLAIR. Unsegmented (A) and quantitative volumetric MR segmentation with icobrain™ in green (B).

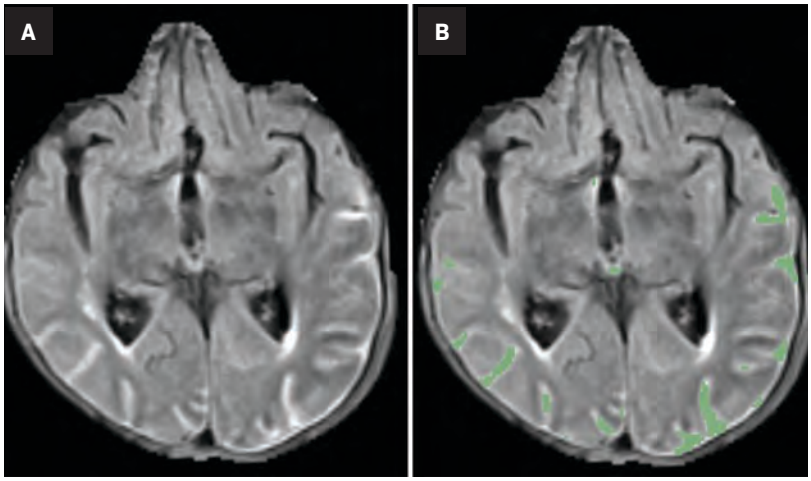

Guerbet
Digital Solutions

Got DACS?

Dose Archiving and Communications System

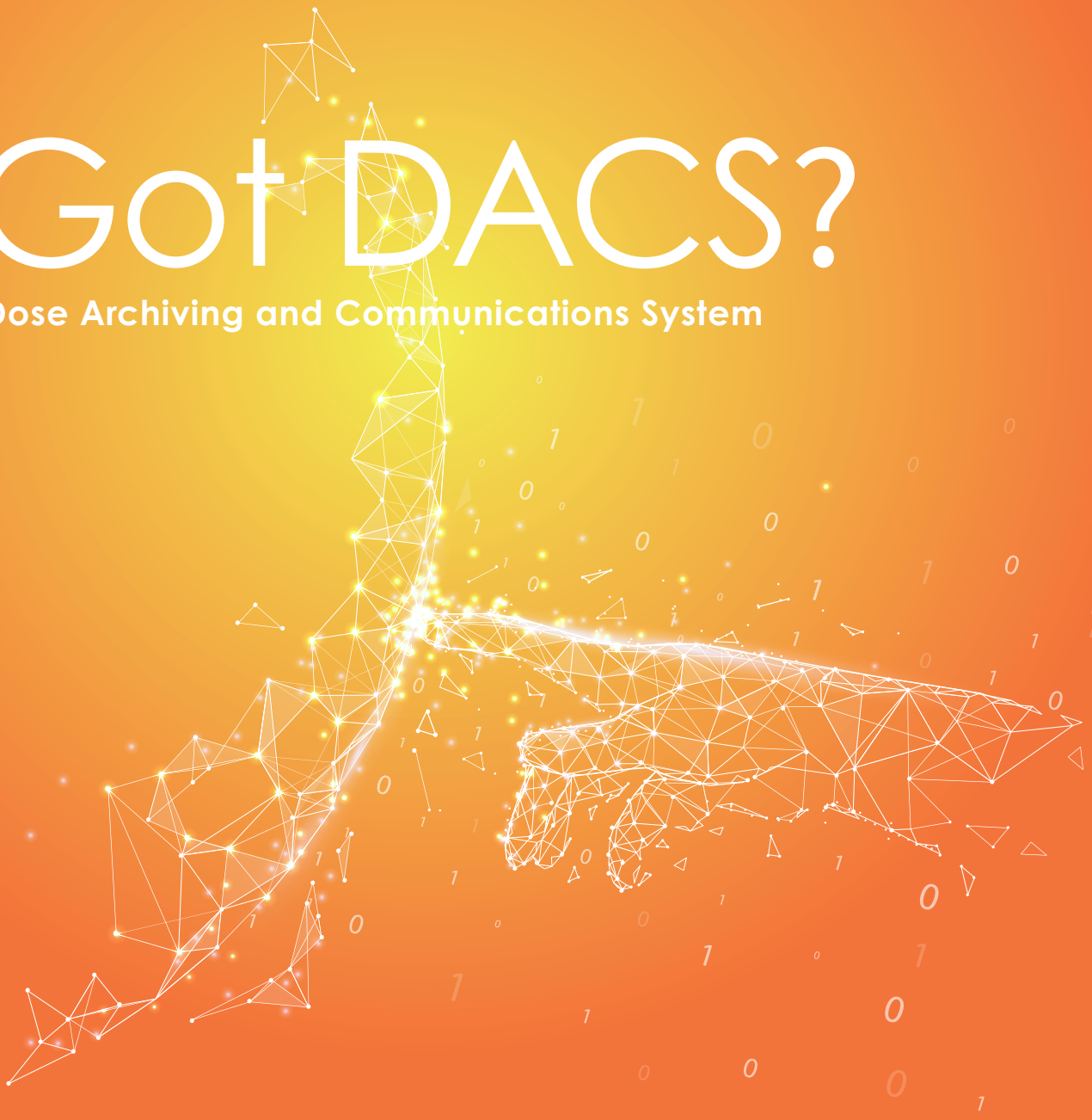

Dose&Care® is a state-of-the-art patient X-ray dose management solution to aid monitoring of patient radiation exposure. Contrast&Care® is an easy-to-use, injection data-management solution that integrates with existing medical platforms.

Both enable imaging centers to collect, archive and share information. Discover how Guerbet Digital Solutions can help you stay a step ahead.

Dose&Care® **Contrast**&Care®

©2021 Guerbet LLC
GU03210026

Proposed treatments must meet three critical requirements for eligibility in the FDA's Accelerated Approval Program (AAP):

1. **The therapy must treat a serious condition.**
2. **The therapy must fill an unmet medical need based on a surrogate endpoint thought to predict clinical benefit but is not itself a measure of clinical benefit.**
3. **The therapy's maker must conduct a Phase 4 trial to confirm the anticipated clinical benefit of the treatment.**

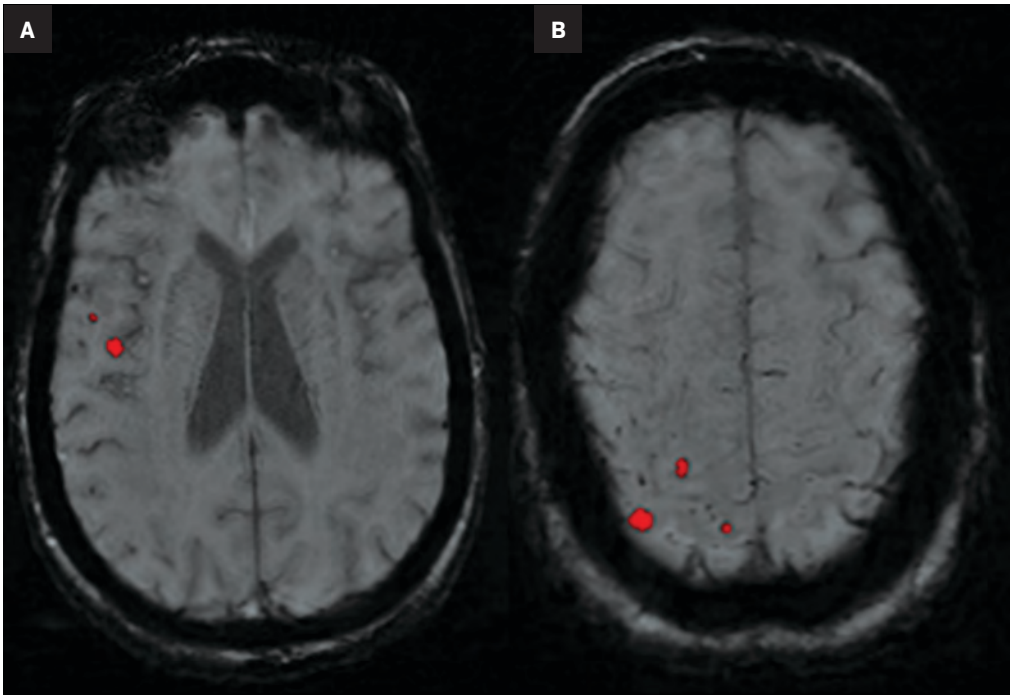

Figure 5. ARIA-H (parenchymal microhemorrhages) with quantitative MR segmentation in red with NeuroQuant™ on axial GRE in right operculum (A) and right parietal lobe (B).

puncture, amyloid PET (currently not reimbursed by CMS), or blood tests, such as Precivity AD.

A substantial uptick in the number of MRI studies for AD is expected. A minimum of three brain MRI exams are required for treatment (baseline, and prior to the seventh and tenth monthly infusions, respectively). However, many more brain MRIs will likely be ordered each year, particularly if patients develop any neurologic symptoms or signs during treatment (eg, headache, numbness, weakness) because 41 percent of treated patients will develop amyloid-related imaging abnormalities (ARIA) in the brain.

ARIA-E (edema or sulcal effusion) is usually self-limited, even in its severe form, and should not require a medication hold (Figures 3, 4). However, ARIA-H (micro-hemorrhages or superficial siderosis) will require a medication hold if severe (greater than 10 new microhemorrhages or two new superficial sideroses since the prior timepoint), but the hold is only required until follow-up MRI demonstrates stability (Figure 5).

ARIA risk factors include high-dose treatment, baseline cerebral amyloid angiopathy, and *APOE ε4* carriers. Fortunately, most (80-90 percent) of patients with ARIA will be asymptomatic. Since the interpreting radiologist is responsible for identifying findings that could result in a medication hold, a global educational initiative is required to educate the radiology community on the appearance of ARIA (Figures 6, 7). A good online resource can be found at *Alzimaging.com*.

Artificial intelligence has an important and growing role in screening for ARIA. Several QNI AI companies have developed dedicated ARIA functionality based on 3D

HARD DATA. HUMAN INSIGHTS.

A surface-level view of your patient isn't sufficient.

In today's healthcare world, you need to look deeper into the data – developing diagnosis based on the full picture.

With IBM Watson Imaging Patient Synopsis, our cloud-based solution – we're extracting all relevant EHR data into a single-view summary. So Radiologists can get the clinical context they need to make intelligently informed care decisions. All in a matter of seconds.

– Extract information from clinical reports
– Find the true "reason for exam" behind the imaging order
– Automatically load the patient summary in context
– Set up and receive automated reports

Guerbet Digital Solutions guerbet-us.com

©2021 Guerbet Group

GU12201247

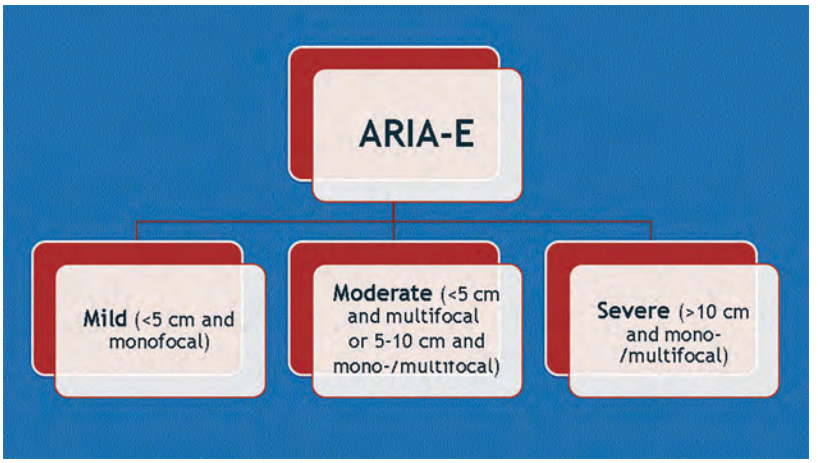

Figure 6. Grading the imaging severity of ARIA-E based on the extent of involvement.

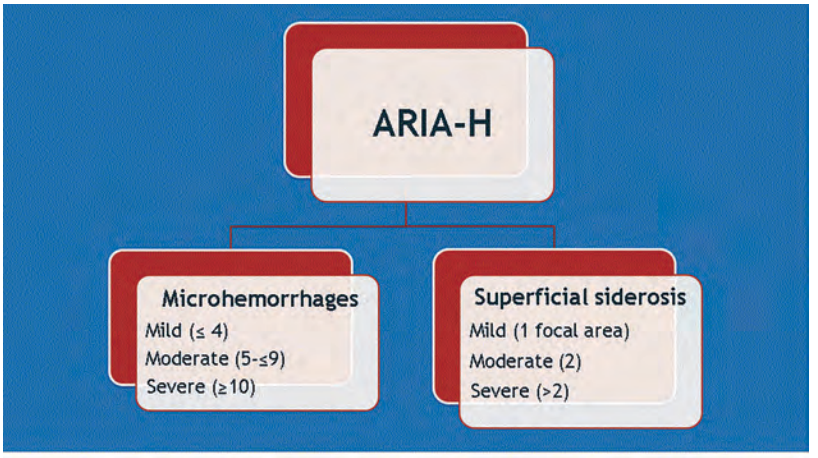

Figure 7. Grading the imaging severity of ARIA-H based on count.

T1, FLAIR, and blood/hemosiderin sensitive (gradient recalled echo and/or susceptibility weighted imaging) inputs. The reports typically have three components (See Figures 8-11 online). The first is a volumetric calculation of pertinent brain substructures (hippocampi and ventricles), which is compared to a normative database to establish a baseline and to help determine if patients demonstrate a hippocampal volume plateau while on treatment. The second consists of ARIA-E screening to assess the volume, count, location, and dynamic change of white matter disease, which is especially useful across longitudinal studies. Finally, the ARIA-H screening component provides the number and location of new microhemorrhages or superficial siderosis along with dynamic change data.

Pharmacology companies are aware of the benefits of AI-fueled QNI and it will be incorporated as subset analysis in Biogen's upcoming required Phase 4 confirmatory trial, which is expected to start in 2022.

Alzheimer disease is devastating. For the first time, potential disease-modifying therapies are on the horizon, and AI will play an important role in screening for ARIA, as well as in characterization and longitudinal evaluation of patients with dementia.

Coping with COVID: Resilience in Radiology

Kerri Reeves

Kerri Reeves is a freelance writer based in Ambler, PA.

Since the COVID-19 pandemic took hold of the US in the spring of 2020, radiology has been on a roller coaster ride. Patient volumes initially plummeted, only to rise again to accommodate case backlogs once medical imaging departments reopened for non-emergent and elective procedures.

As a result, an intense need to operationalize numerous changes quickly has arisen without the availability of the resources necessary to meet all of them, especially where staffing and patient care are concerned.

But medical imaging departments and private practices have shown remarkable resilience in the face of the uncertainties brought about by COVID-19, says Kris Giordano, BSMI, RT(R)(MR), director of imaging at Robert Wood Johnson (RWJ) Barnabas Health Ambulatory Care Center in Livingston, NJ.

"Medical imaging, as a whole, has just been unbelievable under the pressures of the unknown," Giordano said. "Radiology departments have shown tremendous confidence and value in meeting the needs of both patients and health systems during this time."

Indeed, Giordano and other radiology department leaders agree the pandemic has served as a much-needed spark for making improvements as they head into 2022 with greater confidence in their ability to handle other challenges sure to come their way.

Mounting a Quick Response

By the spring of 2020, much of the US population fell under stay-at-home orders for COVID-19 mitigation. As a result, imaging volumes across the country fell—particularly for outpatient-heavy procedures—and revenues plummeted in tandem.[1] Medical imaging providers were forced to temporarily eliminate non-essential procedures in order to comply with COVID-19 mandates.

"Obviously, radiology is still vital to the flow of health care," Giordano said. "MS [Multiple sclerosis] still flares up, strokes still occur, surgeries are still required. We really took a hard look at the prioritization of our volume to figure out how to optimize operations."

Some of the steps Giordano implemented included reducing exam hours and availability. While volume for many modalities dropped, cardiac magnetic resonance imaging grew exponentially, owed in large part to the impact of COVID-19 on cardiopulmonary function. Positron emission tomography (PET) volume, meanwhile, remained steady as oncologists continued to manage their patients reliant on PET results.

"In term of our usual operations, we had to pivot," explained Kernesha S Weatherly, DHA, MHA, CNMT, RT(CT), director of radiology at University of Alabama at Birmingham (UAB) Medicine, who manages both breast imaging and inpatient services.

"It was important [to be] extremely intentional in our efforts to identify the patients we really needed to get in and those we felt comfortable pushing back," she said. Screening mammograms were halted entirely, while it was business as usual for diagnostic breast exams and non-elective inpatient services.

Jeff McGough, MSHA, CRA, UAB's director of ambulatory radiology services, explained that pivoting—particularly during the first two months of the pandemic—meant redefining "essential imaging."

"We continued to serve our oncology population across all services, but restricted everything else to patients with infection, ischemia, or acute neurologic changes. This action saw a 70 percent reduction in ambulatory imaging."

Meanwhile, at the Moses H Cone Hospital Campus of Cone Health in Greensboro, NC, Sherry W Nance, RT-RN, CNMT, MHA, director of radiology and imaging services, said the health system transitioned a vacated women's hospital into a temporary COVID-19 care center in an effort to group these patient populations separately from routine hospital patients across several settings.

"Volume fluctuations, staffing challenges, employee health screenings, ever-changing procedures and protocols, and virtual experiences became 'the name of the game,'" Nance said.

"Overcoming the initial fear of the unknown presented great challenges," she added, noting that personal protective equipment (PPE) availability and maintaining appropriate disinfection protocols have been ongoing concerns.

Giordano agreed. "We had to implement new guidelines and protocols and validate that staff were indeed performing the infection control practices and cleaning the equipment after every patient encounter," he said, observing that the new protocols added significant time to most imaging procedures.

"We had to clean the equipment in front of the patient to help alleviate anxiety," he said, adding that ultraviolet (UV) cleaning machines and robots were used, and the institution's environmental services department regularly deep cleaned the department.

Like other imaging centers throughout the US, RWJ has had to execute detailed patient screenings both ahead of, and upon patient arrival for, their appointments. Providers have also had to modify their check-in and waiting areas to comply with six-feet social distancing mandates, and to provide staff and patients with PPE, including MRI-safe facemasks.

Through measures like these, however, many providers have been able to increase their hours and reschedule appointments to relieve backlogs resulting from the "essential services-only" phase of the pandemic, said McGough, who managed UAB's social distancing efforts from May to October 2020, whereupon the department returned to normal operations.

"Since October, we have been able to maintain pre-COVID templates, and since March of 2021, we have exceeded pre-COVID volumes across all modalities while maintaining health screens, social distancing, and pre-procedure testing," he reported. "Our biggest challenge now is keeping up with demand. Since March, we have set volume records four times."

Managing Staffing Issues

As many providers experience a rebound in imaging volumes, staffing issues remain top of mind. Early in the pandemic, outpatient imaging centers in particular slashed their hours and reallocated staff. Giordano said he had to reassign some technologists to infection control duties, such as health screenings. The RWJ call center staff, which handles scheduling and authorizations, also began working remotely, which was a "huge win" for employees hoping to both remain working and manage at-home responsibilities, he added.

At UAB, shifts have been adjusted to accommodate their employees' at-home needs and to limit the potential for COVID-19 exposure, Weatherly said, while McGough added that the institution also continued to support the salaries of staff whose responsibilities were temporarily suspended.

Nevertheless, McGough said staff recruitment has been a challenge across most modalities as the department returns to higher, pre-pandemic patient volume. "Refilling positions has taken two to three times longer compared to historical practice," he said.

"As a level-one facility, a lot of employees have said, 'I'm burnt out. I can't do this anymore,'" agreed Weatherly. She said many staff are either retiring or moving on to per diem agencies, where they can often make more money.

"Our pipeline was also disrupted because schools closed, and they weren't doing clinicals. It's been uncomfortable all the way around," she said.

Weatherly suggests organizations undergoing similar challenges evaluate and adjust their staffing and compensation models to attract and retain staff post-pandemic. It's especially

important to identify staff needs and how to meet them, she said.

"Many organizations haven't done a market review in an extended period of time due to the pandemic. People are leaving due to work intensity not corresponding with pay," she said. "As you navigate the 'new normal,' identify ways you can help your employees have a life outside of work—a real work/life balance. Because work is exhausting on a whole different level now."

Giordano says RJW has added per diem staff to meet the demands of the facility's nearly complete return to pre-pandemic patient volumes, while ensuring its ability to remain competitive with both compensation and job assurance. "We've really tried to provide as much security as we can in spite of everything going on around us."

Strategizing for 2022

Amid all the uncertainty, radiology decision-makers have found it challenging to develop strategic plans and allocate finances with confidence. "Budgetary plans were derailed while balancing routine business and community needs at the same time as juggling the impacts of the pandemic," said Nance. "Capital plans were negatively impacted. 'What once was' came to an immediate interruption."

McGough and Weatherly similarly said all capital projects at their facilities were put on hold for a year. They are now striving to play "catch up" with increasing construction pricing.

"We were looking to replace certain equipment, but what we're seeing across the board is that the cost of new construction is absolutely astronomical compared to what it was pre-pandemic," Weatherly said. "We're having those conversations now about whether this is the most appropriate time to move forward with these projects."

To forecast department needs for 2022, Giordano said he is comparing current referral patterns to those of 2019, since referrals of the past two years have been so far out of the norm. Heading into 2022, radiology leaders will likely leverage "lessons learned" from the pandemic for what ideally will be a more stable and secure year.

"Having gone through this experience, we will be in a much better position to react to unforeseen crises should another occur," said McGough.

For her part, Weatherly describes the pandemic as an opportunity to "eliminate the clutter" and identify "stress points" to improve workflows in radiology. She recommends that medical imaging leaders assess various areas for improvement.

"Ask yourself, 'How much time does it take from when an order is generated until the exam is complete?' How many of these steps could be cut out to make it a smoother, faster process? What can be streamlined, what should be revitalized, and what may be eliminated altogether?" she said.

"As an imaging leader, I can have the biggest impact on my staff by identifying ways to make processes easier and less complicated for them. Instead of avoiding pain points, leaders will address them."

Reference

1) Malhotra, A., Wu X., Fleishon, H., et. Al. (2020). *J Am Coll Radiol.* 17: 1525-31. Accessed via *https://www.jacr.org/article/S1546-1440(20)30809-7/pdf*

Training Radiologists for Global Service

Farouk Dako MD, MPH; Abass Noor, MD; Luis Goity, MD; Mary Scanlon, MD, FACR

Growing interest among US-based radiology trainees for a broader health experience has led many residency programs to add global health electives to their offerings.[1,2] The field's professional societies are also expanding their opportunities for involvement in worldwide health initiatives. These trends have led to a variety of options, particularly those relating to remote educational experiences.

Owing to the intricate incorporation of information technology into its workflows, radiology is in a unique position to benefit from the proliferation of internet access throughout the world. Fundamental components of education, such as didactic lectures, clinical case interpretation, and implementation projects can be performed remotely at a high level. Although remote interactions should not replace in-person visits, they can complement them and allow for continuous engagement with international partners, even during times of limited travel.

Global health education in radiology is still in the early stages of adoption, and it requires stakeholder collaboration and strong leadership to achieve a strong and sustained presence in residency programs.

Affiliations: Department of Radiology, Perelman School of Medicine, University of Pennsylvania, Philadelphia, Pennsylvania (Drs Dako, Scanlon); Center for Global Health, University of Pennsylvania Health System, Philadelphia, Pennsylvania (Drs Dako, Noor), Department of Radiology, University of Pennsylvania Health System, Philadelphia, Pennsylvania (Drs Noor, Goity).

Integration of International Rotations

The Accreditation Council for Graduate Medical Education (ACGME) provides guidelines for international elective rotations, recommending that they should be created by program directors in consultation with their graduate medical education committees and designated institutional officials.[3] RAD-AID International offers a guide for creating an international elective that includes important components, such as finding an international partner and creating a curriculum.[4]

Moreover, information regarding global health training is appearing more and more frequently on residency program websites and publications, revealing their training focus and types of international partnerships. International partnerships can be developed through personal connections, collaboration with other organizations, or by leveraging existing institutional partnerships. Their area and scope of focus is often determined by partner site needs, available resources, and trainee interests.

A global health elective may include time devoted to focusing on implementation projects; eg, PACS, tumor boards; creation and delivery of educational content, and/or participation in clinical care. Trainees should expect to participate in multiple program components and be prepared to adapt to unforeseen events—an essential aspect of global health education.

Creating a Radiology Global Health Track

The global health experience offered by radiology residency programs has evolved over time, ranging from participation in one- to two-week outreach trips to low- and middle-income countries (LMIC), to enrollment in longitudinal programs spanning several years of residency and culminating in spending weeks or even months on educational, clinical, and research activities in LMICs.[5]

As more of these opportunities become available, collaboration is needed among stakeholder organizations to establish core competency requirements, ethical considerations, and safety guidance. Part of this process is defining the components of education in global health and whether it should focus solely on LMICs or include all low-resource regions, including those in the US. A prerequisite to these efforts is defining global health radiology and outlining its scope; ie, whether it should be viewed as the spread of radiology

Figure 1. Dr Brian Currie (pictured) and Dr Vlasios Sotirchos presenting a lecture on Acute Abdomen to first-year medical students at the University of Botswana.

Figure 2. Dr Brian Currie and Dr Vlasios Sotirchos (kneeling, center) at the end of their rotation posing with other members of the radiology department at Princess Marina Hospital in Gaborone, Botswana.

Figure 3. Dr Vlasios Sotirchos and Dr Brian Currie enjoying their time off at a national park.

into low-resource regions and/or a developing subspecialty of radiology itself — similar to the evolution of imaging informatics. Creating a global health track requires envisioning job opportunities for graduate trainees and ensuring that our departments and profession reflect them.

Leveraging Institutional Partnerships

An example of a global health elective is one in the Department of Radiology at the University of Pennsylvania, which builds on the existing Botswana-UPenn Partnership (BUP) and allows radiology residents to complete a four- to six-week clinical rotation at Princess Marina Hospital in Gaborone, Botswana.[6]

The University of Pennsylvania's Perelman School of Medicine's involvement in Botswana began in 2001 at the request of the African Comprehensive HIV/AIDS Partnership, and it has evolved into a collaboration with Botswana's Ministry of Health and Wellness and the University of Botswana to improve clinical care, research, and medical education.[7] The BUP has residency programs in internal medicine, pediatrics, anesthesiology, emergency medicine, family medicine, and pathology.[8] Collaboration with these programs is an essential part of the Penn Radiology global health elective experience.

The BUP employs approximately 120 full-time staff in Botswana, including US-trained physicians.[9] The partnership provides a process for

Table. ACGME Objectives and Core Competencies

OBJECTIVE	ACGME CORE COMPETENCY
Increase and support radiology services in low- and middle-income countries through education, training, and research.	PC, MK, ICS, PBLI, P, SBP
Build medical and radiologic knowledge in the context of global health.	PC, MK, PBLI
Develop an appreciation for and understanding of radiology in health equity as an academic discipline and how it informs radiology practice.	PC, SBP, MK

Abbreviations: PC = Patient Care, MK = Medical Knowledge, PBLI = Practice-based Learning and Improvement, ICS = Interpersonal and Communication Skills, P = Professionalism, SBP = Systems-based Practice

Penn Radiology trainees to obtain a medical license in Botswana. In addition, flight expenses and in-country transportation and lodging are covered by BUP. Prior to travel, residents must complete a global health equities seminar offered through UPenn's department of internal medicine, and obtain a certificate of proficiency in global health radiology from RAD-AID to improve sociocultural competence. Residents are also given the option to return to Princess Marina Hospital as fellows for up to six more weeks of additional training.

Our global health radiology clinical rotation objectives are presented in the context of six core competencies endorsed by ACGME and the American Board of Medical Specialties (Table).[10]

Conclusion

A growing number of global health electives and longitudinal training opportunities are being offered by radiology residency programs. Experiences like these that build on strong institutional partnerships provide for robust educational experiences and sustainable training programs.

References

1) Haver HL, Rosen MP, DeBenedectis CM. Global radiology training prevalence among radiology residency programs. *Current Prob Diagn Radiol.* 2021;50(2):141-146.

2) England RW, Lugossy AM, Mollura DJ. Increasing opportunities for trainees to engage in global health radiology: radiology in training. *Radiology.* 2021; 210371.

3) "420_Guidelines_for_IntlRotations_in_DiagRad.pdf." n.d. https://www.acgme.org/globalassets/PFAssets/ProgramResources/420_Guidelines_for_Intl Rotations_in_DiagRad.pdf. Accessed October 28, 2021.

4) Escalon JG, Renjen P. A step-by-step guide to creating an elective rotation abroad for radiology residents. [cited 30 Oct 2021]. Available at: https://rad-aid.org/wp-content/uploads/Guide-to-Creating-an-Elective-Rotation-Abroad-for-Radiology-Residents.pdf

5) Pool KL, Culp MP, Mollura DJ, Suh R. A structured global health training program for radiology residents. *JACR J Am Coll Radiol.* 2018;15(2):334-339.

6) Health Equity Leadership Track. (n.d.). Retrieved October 30, 2021, from https://www.pennmedicine.org/departments-and-centers/department-of-radiology/education-and-training/residency-programs/special-resident-programs/health-equity-leadership

7) Cohn J, Friedman HM. Sustainable international partnership building for academic medical centers: experiences with the Botswana-UPenn Partnership. *Virtual Mentor.* 2010;12(3):179-183.

8) Home. (n.d.). Retrieved October 30, 2021, from https://www.med.upenn.edu/botswana/

9) Mokone GG, Kebaetse M, Wright J, et al. Establishing a new medical school: Botswana's experience. *Acad Med.* 2014;89(8 Suppl):S83-S87. doi:10.1097/ACM.0000000000000329.

10) The Milestone Guidebook. Accreditation Council for Graduate Medical Education. 2020. Available at: https://www.acgme.org/globalassets/milestonesguidebook.pdf. Accessed October 28, 2021.

Stress Fracture

Norman Holl, PhD; Kolja M Thierfelder, MD; Martin Ellenrieder, MD; Wolfram Mittelmeier, MD; Marc-André Weber, MD

Case Summary

A young adult presented with a three-month history of persistent pain in the right thigh after running a marathon. A seasoned amateur long-distance runner, the patient endorsed a rigorous training protocol. The patient's pain was increased during hip extension exercises. Physical examination revealed free range of motion (ROM) of both hips and knee joints. Nonspecific pain in the right thigh could be provoked by forced passive ROM testing of the hip. No localized tenderness or swelling were evident. Lumbar spine and sacroiliac joints were clinically normal.

Imaging Findings

Findings on radiographs were unremarkable. Magnetic resonance imaging (MRI) revealed intraosseus signal changes on T1 and T2-TIRM sequences in the proximal femoral diaphysis (Figure 1) representing bone marrow edema. Initial, conservative therapy consisted of six weeks of partial weight-bearing. Follow-up MRI six weeks post-treatment demonstrated persistent bone marrow edema, as did a third MRI examination eight weeks after initial imaging. A noncontrast computed tomography scan three months after presentation revealed a non-displaced fracture of the right femoral diaphysis extending from middle of the shaft up to the neck (Figure 2) with callus formation around the shaft

Affiliation: Rostock University Medical Center, Rostock, Germany

Diagnosis

Stress fracture

Discussion

Femoral fractures are among the most common sites of stress-related injuries. This is partially explained by the fact that the largest bending moments during movements occur at the proximal femur.[1] In locomotor tasks, such as running, the impact phase constitutes peak magnitudes of force. The characteristics of the loading stimulus (eg, frequency of loading, number of load repetitions) are essential for injury development.[2] An accumulation of structural damage could result in complete fracture. Kang, et al,[3] retrospectively reported on seven cases of femoral stress fractures in female athletes. Sudden and abrupt changes in the athletes' training regimen were identified as the main factors in the development of stress fractures. In contrast, in the case presented here, an abrupt change in training intensity could not be identified. A three- to four-month preparation period for a marathon is common among well-conditioned runners.

To avoid possible complications such as avascular necrosis, refracture, pseudarthrosis, and prolonged recovery time, early diagnosis of stress fractures is essential.[4] Kang, et al, further emphasized that the type of fracture is the most important factor influencing complication rate, with displaced fractures causing the highest rates. Consequently, proper imaging shortly after injury is crucial for detecting early signs of stress fracture.

As the development of stress fracture is considered a continuous process, they may vary in appearance.[5] In this regard, the importance of MRI evaluation is highlighted in the literature.[6] However, Seki, et al,[7] reported the case of a teenaged long-distance runner who suffered a stress fracture of the femoral neck that did not show typical signal changes on MRI. Nevertheless, compared with alternative imaging modalities (CT, radiography, bone scintigraphy), MRI seems the most sensitive and specific imaging approach.[8]

Adding to the notion that recovery times differ among types of stress

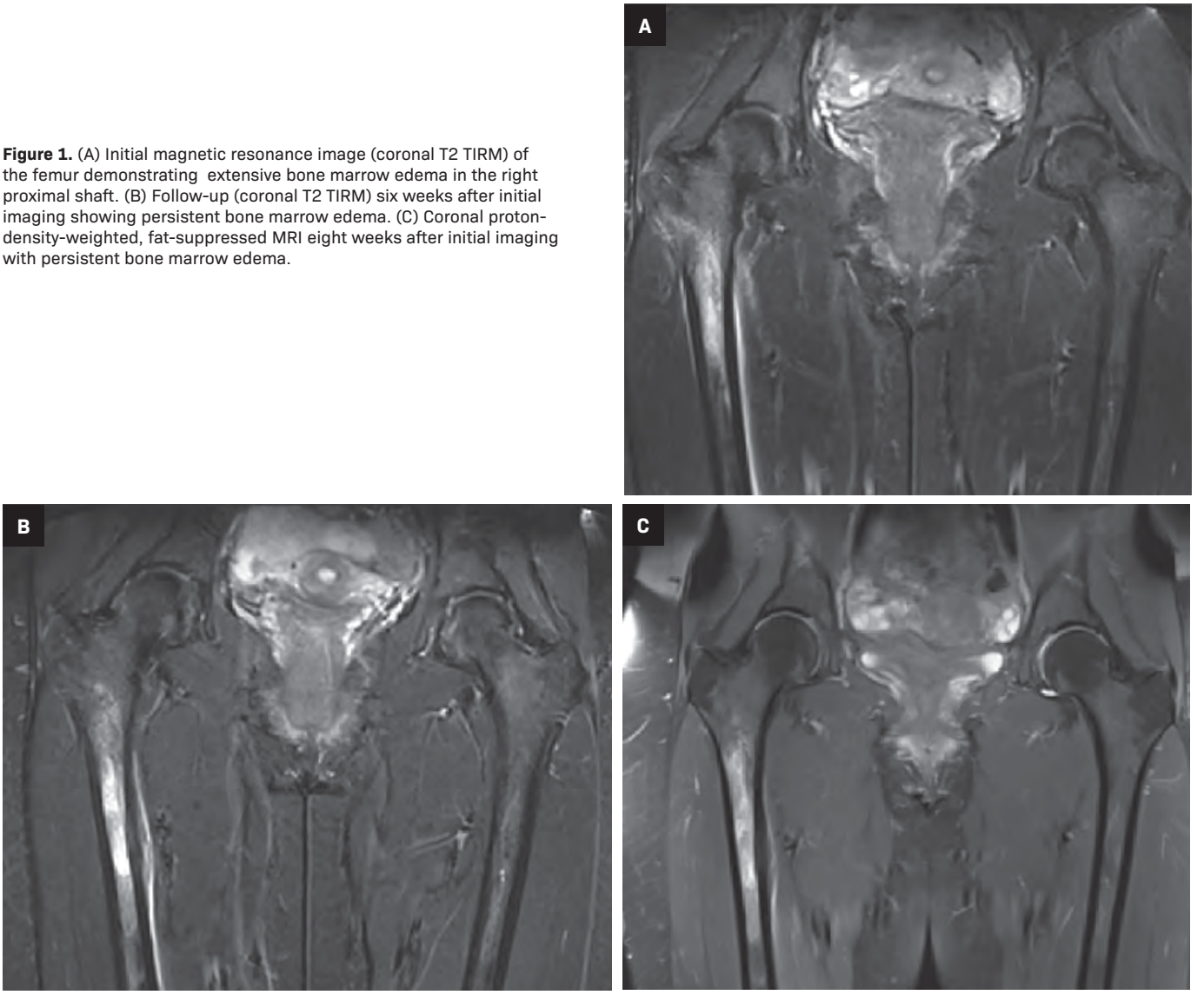

Figure 1. (A) Initial magnetic resonance image (coronal T2 TIRM) of the femur demonstrating extensive bone marrow edema in the right proximal shaft. (B) Follow-up (coronal T2 TIRM) six weeks after initial imaging showing persistent bone marrow edema. (C) Coronal proton-density-weighted, fat-suppressed MRI eight weeks after initial imaging with persistent bone marrow edema.

injuries, Nattiv, et al,[9] proposed a four-grade MRI grading scheme. These grades correlate with risk factors and time to return to sports. Involvement of trabecular structures and subsequent severe bone marrow edema on MRI evaluations (MRI grades 3 and 4), in particular, were associated with significantly prolonged time-to-return to activity.

Further, menstrual dysfunction, low energy availability, and decreased bone mineral density might affect MRI grading severity and are believed to contribute to bone stress injury.[9] After other diagnoses such as malignancy have been excluded, pathologic fracture or muscle strain must be considered.[10] Additionally, sports-related pubalgia (eg, resulting from secondary or superior cleft injuries) may mimic the pain characteristics of stress fracture but must be treated differently.

With respect to identifying other differential diagnoses, MRI is advantageous to alternative imaging modalities, as it allows a detailed assessment of surrounding tissues. Moreover, Datir, et al,[5] pointed out that imaging may help avoid biopsy in many cases. This is of special importance, as stress-fracture biopsies may contain immature cells and osteoid tissue and hence may be misleading.

Conclusion

Stress-related injury of the femur may lead to persistent changes in radiologic exams; rendering a complete clinical picture and correct diagnosis is essential for treatment. MRI evaluation is considered the most sensitive and specific imaging technique for diagnosing stress fracture.

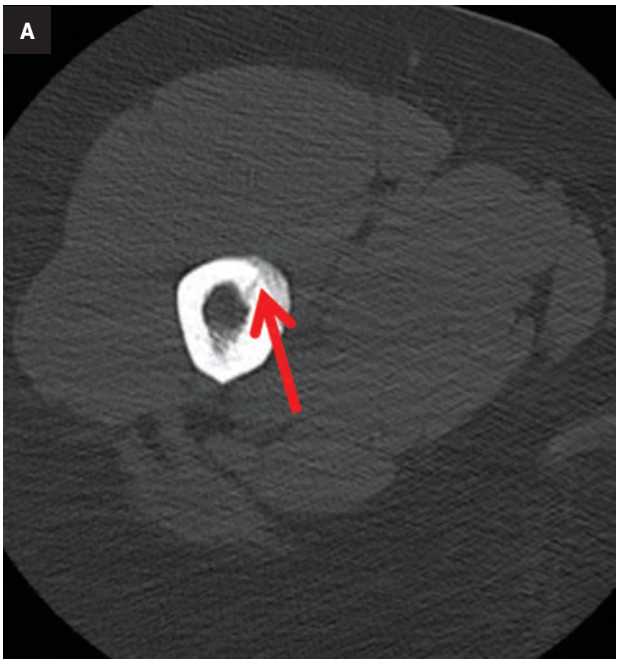

Figure 2. Computed tomography scan in (A) transverse and (B) coronal planes three months after presentation, revealing stress fracture with callus formation in the diaphysis (arrow).

As in the presented case, adding CT may provide a correct diagnosis. An early diagnosis of stress-related fracture is essential for proper treatment and to exclude other differential diagnoses. The presented case also shows that femoral stress fractures may occur in patients without clear risk factors.

References

1) Edwards WB, Gillette JC, Thomas JM & Derrick TR. Internal femoral forces and moments during running: implications for stress fracture development. *Clin. Biomech.* 2008; 23: 1269–1278.

2) Warden SJ, Burr DB, Brukner PD. Stress fractures: pathophysiology, epidemiology, and risk factors. *Curr Osteoporos Rep*. 2006;4(3):103–109.

3) Kang L, Belcher D, Hulstyn MJ: Stress fractures of the femoral shaft in women's college lacrosse: a report of seven cases and a review of the literature. *Br J Sports Med*. 2005, 39: 902-906.

4) Johansson C, Ekenman I, Tornkvist H, et al. Stress fractures of the femoral neck in athletes. The consequences of a delay in diagnosis. *Am J Sports Med.* 1990; 18:524–528.

5) Datir AP, Saini A, Connell A, Saifuddin A. Stress-related bone injuries with emphasis on MRI. *Clin Radiol* 2007; 62: 828– 836.

6) Wall J, Feller JF. Imaging of stress fractures in runners. *Clin Sports Med.* 2006;25(4):781–802.

7) Seki N, Nobutoshi N, Okuyama K, Kam K, Chiba M, Shimada Y. Negative magnetic resonance imaging in femoral neck stress fracture with joint effusion: a case report. *Skeletal radiology*. 2016. 45(6):843-846.

8) Niva MH, Kiuru MJ, Haataja R, Pihlajamaki HK. Fatigue injuries of the femur. *J Bone Joint Surg Br.* 2005; 87:1385–1390.

9) Nattiv A, Kennedy G, Barrack MT, et al. Correlation of MRI grading of bone stress injuries with clinical risk factors and return to play: a 5-year prospective study in collegiate track and field athletes. *Am J Sports Med*. 2013; 41(8):1930–1941.

10) Patel DS, Roth M, Kapil N. Stress fractures: diagnosis, treatment, and prevention. *Am Fam Physician*. 2011; 83: 39-46.

Mazabraud Syndrome

Aynur Turan, MD; Tuba Dilay Unal, MD; Azad Hekimoglu, MD; Meltem Ozdemir, MD; Huseyin Coşkun, MD; Guldem Sagra, MD

Case Summary

A middle-aged woman presented with a one-year history of a slow-growing and painless medial thigh mass. The patient had no history of trauma or primary malignancy. She had been on medication for hypertension for many years. There was no other medical history. A mobile mass in the middle of the leg was identified in the clinical examination.

Imaging Findings

Initial radiographs of the left femur and hip showed well-defined, ground-glass lesions with sclerotic rims and no periosteal reaction (Figure 1). MRI of the left hip and thigh revealed a 5.6 × 3.1 × 3.0 cm lesion in the intramedullary area of the left iliac bone, causing slight bone expansion. The lesion was hypointense on T1 images, intermediate signal intensity on T2 images, and minimally enhanced following contrast administration. There was another lesion with similar imaging features in the left proximal femur. These bone lesions were diagnosed as polyostotic fibrous dysplasia (Figure 2).

Figure 1. Radiography shows well-defined, ground-glass appearance lesions of the proximal femur and left iliac bone with sclerotic rim and no periosteal reaction.

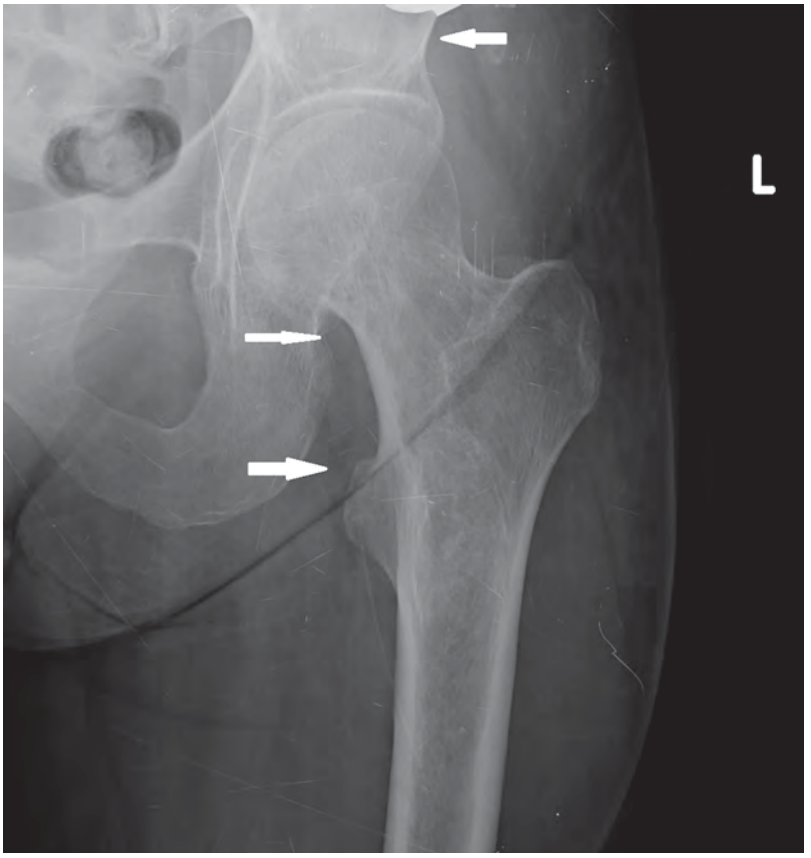

Ultrasonographic (US) findings of the clinically apparent soft tissue lesion showed a well-defined, mobile, heterogeneous, predominately hypoechoic mass. On MRI this measured 4.1 × 3.4 × 3.0 cm and was a well-defined, round, soft-tissue mass in the left vastus medialis muscle. The mass revealed prominent hypointense signal on T1 imaging, markedly hyperintense signal on

Affiliations: University of Health Sciences, Diskapi Yildirim Beyazit Health Application and Research Center, Radiology Dept., Ankara, Turkey (Drs Turan, Hekimoglu, Ozdemir, Koskun); University of Health Sciences, Kayseri Health Application and Research Center, Radiology Department, Kayseri, Turkey (Dr Unal); Ordu Medicalpark Hospital, Ordu, Turkey (Dr Sagra).

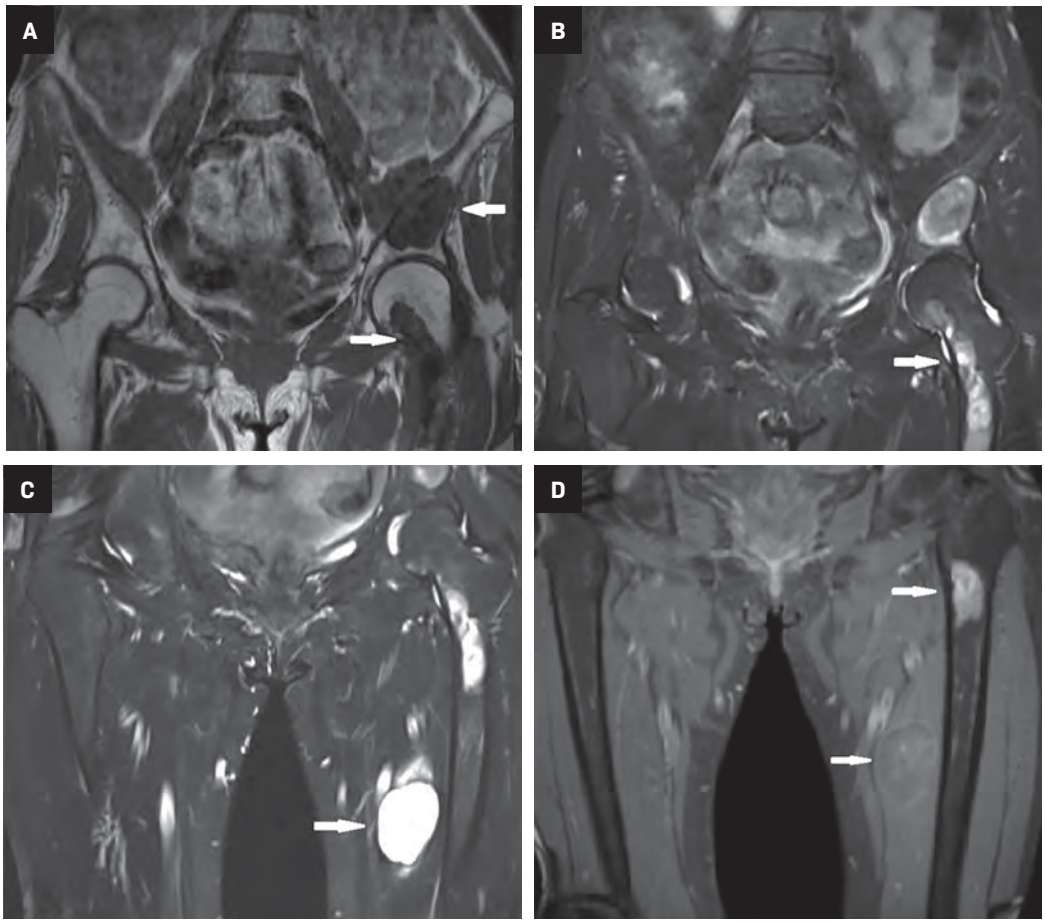

Figure 2. MRI of hip shows intramedullary lesions of the left proximal femur and iliac bone which are hypointense on coronal T1 image (A), hyperintense on T2 (B) and show mild enhancement on fat-saturated T1 images (D) after contrast administration. There is a solitary mass lesion in the vastus medialis muscle which is prominently hyperintense on T2 image (C) and shows slight enhancement on contrast-enhanced images (D).

T2 imaging compared to muscle, and minimal septal and peripheral enhancement following contrast administration (Figure 2). The MRI findings of the soft-tissue lesion led to myxoma as a diagnosis.

Surgical excision of the soft-tissue mass showed a well-circumscribed soft-tissue mass measuring 5 × 4.3 × 5 cm. Histologically, the lesion consisted of bland-appearing spindle cells within an abundant myxoid matrix. Hypocellular and hypovascular areas were surrounded by fine fibrocollagenous fibers. Atypical mitosis, nuclear pleomorphism, and necrosis were not observed (Figure 3). The lesion was histopathologically diagnosed as a myxoma.

Diagnosis

Mazabraud syndrome

Discussion

Mazabraud syndrome (MS) is a rare and complex disease that typically presents as the coexistence of fibrous dysplasia (FD) and intramuscular myxoma. This disease presents differently in children and adults.[1] There is no evidence of genetic transition and it most commonly affects middle-aged females.[2]

The molecular etiology of MS is not entirely clear, but some genetic studies suggest that a mutation of Gsα protein encoded by GNAS-1 exists, and that this protein alters the level of cyclic adenosine monophosphate.[3]

Fibrous dysplasia is a congenital lesion of the bones. This osteoblastic maturation defect appears as a fibrous stroma and immature bone mold instead of normal bone. The monostotic form is more common; however, the polyostotic form is more highly associated with MS. It tends to affect the long bones, ribs, and cranium. It may cause pain, bone deformities, and pathological fractures.[4]

On radiography, FD is defined as an intramedullary lesion with cortical thinning and a sclerotic rim. A ground-glass appearance is typical on radiography and CT.[1,4] On MRI, the lesions are iso-hypointense on T1 imaging, iso-hyperintense on T2, and show variable, heterogeneous contrast enhancement. It is reported that the sarcomatous transformation of FD is rare, occurring in less than 1% of cases.[4] In the differential diagnosis of FD, other intramedullary bone lesions such as enchondroma, simple bone cyst, and medullary bone infarct may be considered.[5]

Figure 3. A hypocellular-hypovascular lesion consisting of stellate cells embedded in an abundant myxoid stroma.

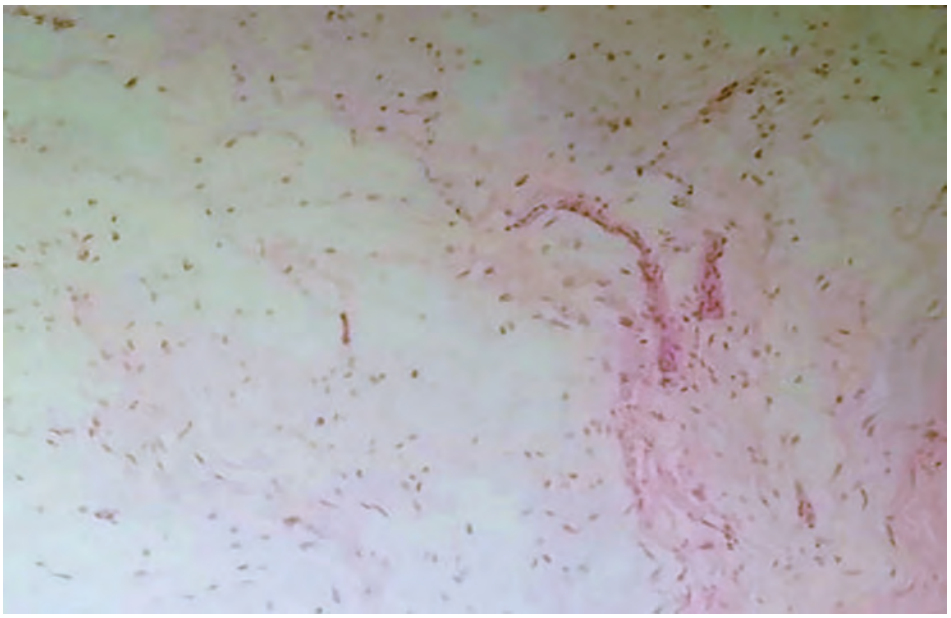

Myxoma presents as a slow-growing palpable mass which can be painful or painless. It is primarily located in the thigh, upper arm, calf, or buttock muscles. These are most often multiple in MS but sometimes can be solitary, as in our case.[6]

Myxoma is a primitive mesenchymal tumor that produces hyaluronic acid and immature collagen fibers. Because of the lack of mature collagen, it contains few stellate-shaped cells and rare vascular structures embedded in mucoid material. On US, it is seen as a hypo-anechoic mass with well-defined margins and can show a microcystic appearance or contain internal echoes. It is hypovascular on color Doppler US.[6]

MRI typically demonstrates high signal intensity on T2WI and low signal intensity on T1WI. Lesions are commonly homogeneous and well-circumscribed. A thin rim of fat can be seen around the mass secondary to atrophy.[1] In the perilesional region, fluid signal can be observed due to the leakage of myxoid material. There is a mild-moderate diffuse or peripheral-septal enhancement pattern.[6]

Myxoma should be differentiated from myxoid peripheral nerve sheath tumors, myxoid liposarcoma, and myxoid leiomyosarcoma. The perilesional fluid and thin rim of fat tissue around the myxoma are useful for differential diagnosis. Biopsy may not be required to establish the diagnosis of myxoma.[1,6]

Myxomas are always benign, and biopsy or surgical excision is generally not necessary.[7] Fibrous dysplasia commonly shows slow progression; therefore, a conservative approach is preferable.[2,5]

Conclusion

Radiologists must be aware of the rarely seen solitary or multiple soft tissue lesions which are associated with FD. Knowing that the accompanying soft tissue mass is a myxoma will prevent unnecessary biopsy and resection. Following FD can provide early diagnosis in rare cases of malignant transformation.

References

1) Case DB, Chapman CN Jr, Freeman JK, et al. Best cases from the AFIP: Atypical presentation of polyostotic fibrous dysplasia with myxoma (Mazabraud syndrome). *Radiographics.* 2010; 30(3):827-832.

2) Fu S, Tian Z, Zhang C, et al. Monosotic fibrous dysplasia and solitary intramuscular myxoma of the head and neck: A unique presentation of Mazabraud's syndrome and a literature review. *Oncol Lett.* 2015;10(5):3087-3094.

3) Okamoto S, Hisaoka M, Ushijima M, et al. Activating gs(alpha) mutation in intramuscular myxomas with and without fibrous dysplasia of bone. *Virchows Arch.* 2000;437:133–137.

4) Fitzpatrick KA, Taljanovic MS, Speer DP, et al. Imaging findings of fibrous dysplasia with histopathologic and intraoperative correlation. *AJR Am J Roentgenol.* 2004;182(6):1389-1398.

5) Singnurkar A, Phancao JP, Chatha DS, et al. The appearance of Mazabraud's syndrome on 18F-FDG PET/CT. *Skeletal Radiol.* 2007;36(11):1085-1089.

6) Petscavage-Thomas JM, Walker EA, Logie CI, et al. Soft-tissue myxomatous lesions: review of salient imaging features with pathologic comparison. *Radiographics.* 2014;34(4):964-980.

7) Munksgaard PS, Salkus G, Iyer VV, et al. Mazabraud's syndrome: case report and literature review. *Acta Radiol Short Rep.* 2013;2 (4):1-4.

Medulloblastoma

Jeff Wellard; John Sfondouris, MD; Scott A Jorgensen, MD; David Aria, MD, Carrie M Schaefer, MD, Richard B Towbin, MD, Alexander J Towbin, MD

Case Summary

A toddler was brought to the emergency room for vomiting and a bulging anterior fontanelle.

Imaging Findings

Noncontrast CT demonstrated a heterogeneous, hyperattenuating posterior fossa mass compressing the 4th ventricle anteriorly. This caused obstructive supratentorial hydrocephalus with interstitial flow of CSF (Figure 1).

Brain MRI subsequently demonstrated the mildly T2 hyperintense mass to be centered in the medial aspect of the right cerebellar hemisphere with local mass effect, including compression of the fourth ventricle and brainstem (Figure 2). The solid portions of the mass showed restricted diffusion (Figure 3). Marked lateral ventricular enlargement was present with increased signal intensity in the adjacent periventricular white matter corresponding to transependymal flow of CSF. The mass was heterogeneously enhancing following gadolinium administration (Figure 4).

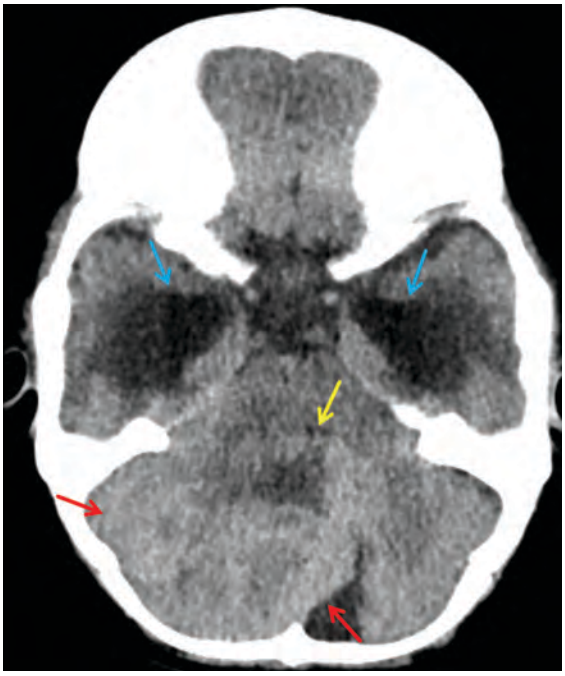

Figure 1. Noncontrast CT of the head demonstrates a heterogeneous, hyperattenuating posterior fossa mass (red arrows) compressing the fourth ventricle anteriorly (yellow arrow), and enlarged temporal horns of the lateral ventricles (blue arrows).

Diagnosis

Medulloblastoma. Differential diagnosis includes ependymoma, astrocytoma, and atypical teratoid rhabdoid tumor.

Discussion

Medulloblastomas (MB) are a subtype of CNS embryonal tumors that arise exclusively in the posterior fossa and are the most common malignancy in the pediatric population, especially males, with a peak incidence around the age of 8 years. A well-circumscribed, hyperintense, round mass arising in the area of the cerebellar vermis, hemispheres, and fourth ventricle with impairment of CSF flow in male pediatric patients, is typical of MB. The incidence of MB begins to fall after childhood and is rarely seen in patients over age 40.[1]

Historically, MBs have been defined histologically. This anatomic

Affiliations: University of Arizona College of Medicine –Phoenix (Mr Wellard); Barrow Neurological Institute, Phoenix, AZ. (Dr Sfondouris); Phoenix Children's Hospital, Phoenix, Arizona (Drs Jorgensen, Aria, Schaefer, R Towbin), and Children's Hospital Medical Center, Cincinnati, Ohio (Dr A Towbin).

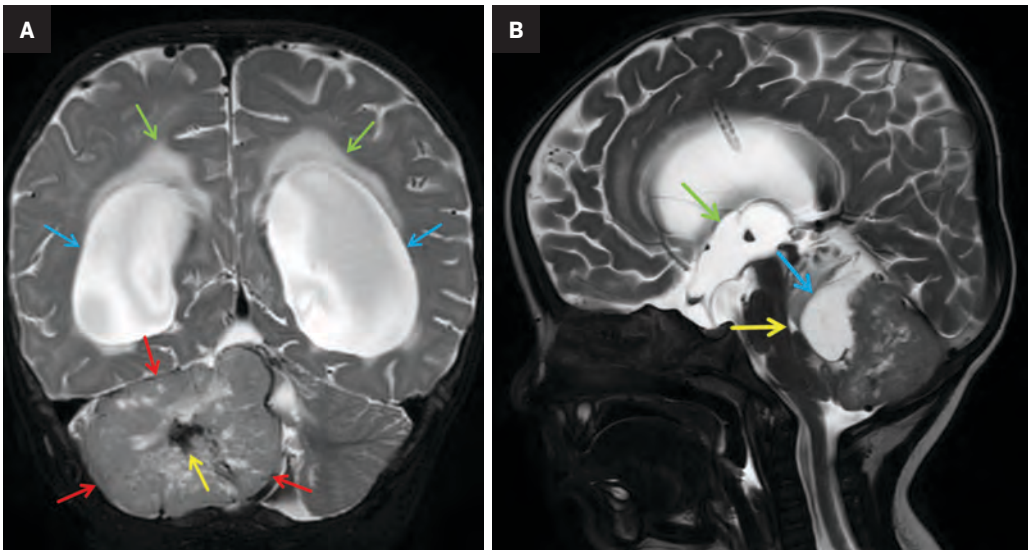

Figure 2. (A) Coronal T2 demonstrates mildly hyperintense mass (red arrows) with central hypointensity related to blood products (yellow arrow). Marked enlargement of the lateral ventricles (blue arrows) is present with increased signal intensity in the periventricular white matter which corresponds to transependymal flow of CSF (green arrows). (B) Sagittal T2 shows the mass within the cerebellum, compressing the fourth ventricle (yellow arrow) and compressing and displacing the brainstem anteriorly. A cystic component is seen within the anterosuperior aspect of the mass (blue arrow). Enlarged third ventricle (green arrow) and lateral ventricular catheter are also shown.

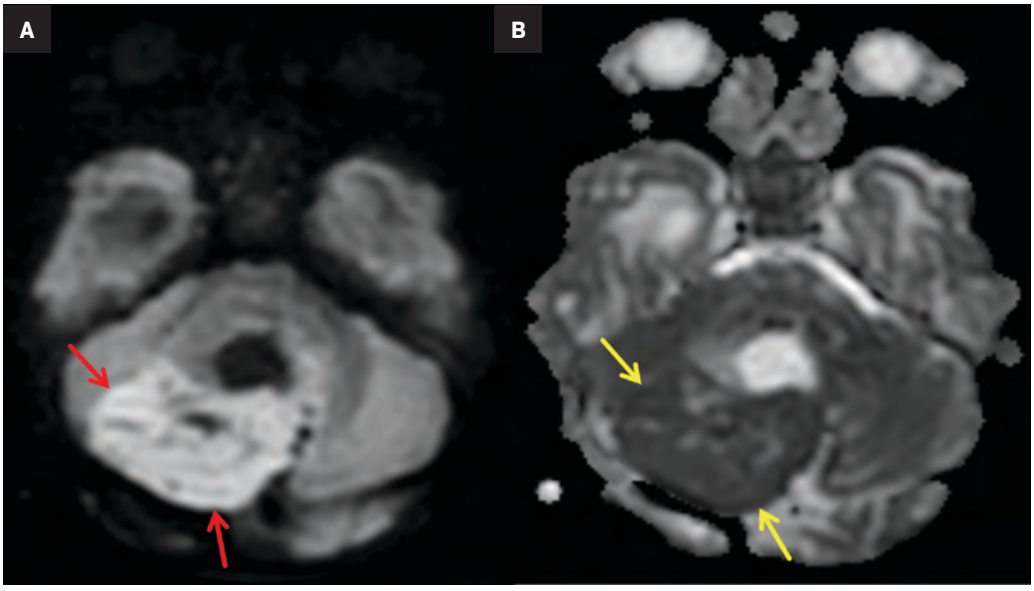

Figure 3. Trace diffusion weighted image (A) and apparent diffusion coefficient (B) images show restricted diffusion with increased signal on DWI (red arrows) and decreased signal on ADC (yellow arrows).

approach to classification does not, however, influence the approach to therapy. Recently, MBs have been characterized using molecular subtyping, which has led to the creation of four additional categories to consider: WNT activated (WNT), sonic hedgehog activated (SHH) — which can be *TP53*-wildtype or mutant — and Group 3 and 4 , which are tumors not related to WNT or SHH, also sometimes grouped as non-WNT/non-SHH tumors.[2]

Research into the molecular groupings of MBs demonstrate the heterogeneity of these tumors. SHH tumors have been linked to granular neuron precursor cells (GNP) of the cerebellar external granule cell layer. WNT tumors appear to arise from progenitor cells in the dorsal brainstem. Group 3 tumors may occur in GNPs but also in cerebellar ventricular zone cells or other progenitors, and Group 4 tumors, being the most heterogeneous of the groups, may arise from a variety of precursors.[3] Molecular subtyping has been linked to patient outcomes and has been used to stratify patients into risk categories.[2]

On computed tomography, MBs typically are hyperattenuating midline vermian masses with contrast enhancement that obstruct the fourth ventricle.[1] However, magnetic resonance imaging is the gold standard for evaluating pediatric MB. MRI should include T1, T2, and diffusion weighted imaging (DWI). The appearance of MB on T1 can range from hypo- to isointense, with masses on T2 ranging from hypo- to hyperintense.[5] DWI is an excellent tool for discriminating different posterior fossa masses, with MBs showing increased restriction and diffuse hyperintense signal.[5]

Evidence suggests MB molecular subtypes display specific features on MRI. One feature, tumor location, appears to have a high positive predictive value for determining molecular subgroups.[6] Perreault, et al, reported that WNT tumors often arise in the cerebellopontine angle cistern/cerebellar peduncle, SHH tumors (as is most likely in our case) most commonly arise in the cerebellar hemispheres, and Group 3 and 4 tumors arise within the vermis.[6]

Further investigation has expanded upon these findings by showing that, while all molecular subtypes may be extracerebellar, only SHH tumors can be completely intracerebellar.[7] In addition, WNT, Group 3, and Group 4 tumors almost always invade the fourth ventricle.[7] Currently, diagnosing MB molecular subtypes based on MRI is not always standard of care, but continued research, refinement of MRI protocols, and improved technology may create such a possibility.

Treatment is based on the presenting size, shape, and age of the patient, typically starting with surgical resection followed by combined radiation and chemotherapy. Imaging should include the entire neuroaxis to evaluate for leptomeningeal metastasis.

Post-treatment imaging vigilance, including diffusion weighed imaging must be maintained to assess for recurrent tumor[8] and delayed leptomeningeal spread of disease.

Conclusion

Medulloblastomas are the most common pediatric malignant tumor and should be considered in any patient presenting with signs and symptoms of cerebellar dysfunction or intracranial hypertension. These tumors can be divided into molecular subgroups that influence treatment and, while not currently the standard of care, MRI may be beneficial to differentiate them.

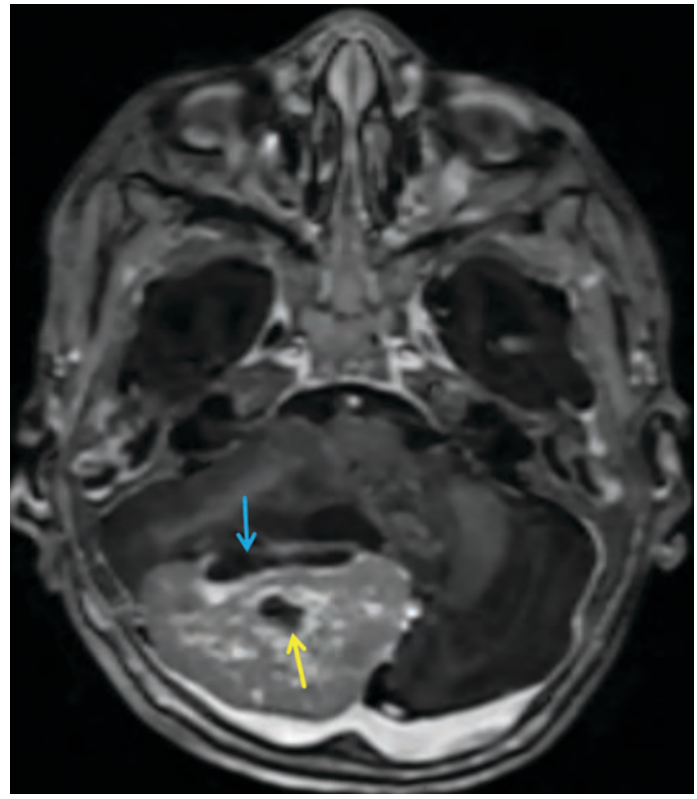

Figure 4. Postcontrast axial T1 shows the heterogeneously enhancing mass centered in the medial aspect of the right cerebellar hemisphere with central hypointensity (yellow arrow) which corresponds to hemorrhage, and anterior cystic components (blue arrow).

Standard treatment consists of surgical resection followed by radiation and chemotherapy.

References

1) Alli S, Isik S, Rutka JT. 11 - posterior fossa and brainstem tumors in children. *Principles of Neurological Surgery (Fourth Edition)*. 2018:183-203.e7. http://www.sciencedirect.com/science/article/pii/B9780323431408000111. doi: https://doi.org/10.1016/B978-0-323-43140-8.00011-1.

2) Khatua S, Song A, Citla Sridhar D, Mack SC. Childhood medulloblastoma: Current therapies, emerging molecular landscape and newer therapeutic insights. *Curr Neuropharmacol*. 2018;16(7):1045-1058. Accessed Mar 6, 2020. doi: 10.2174/1570159X15666171129111324.

3) Azzarelli R, Simons BD, Philpott A. The developmental origin of brain tumours: A cellular and molecular framework. *Development*. 2018;145(10):dev162693. http://dev.biologists.org/content/145/10/dev162693.abstract. doi: 10.1242/dev.162693.

4) Gur RE, Kaltman D, Melhem ER, et al. Incidental findings in youths volunteering for brain MRI research. *AJNR. Am J Neuroradiol.* 2013;34(10):2021-2025. https://www.ncbi.nlm.nih.gov/pubmed/23811972. doi: 10.3174/ajnr.A3525.

5) Eran A, Ozturk A, Aygun N, Izbudak I. Medulloblastoma: Atypical CT and MRI findings in children. *Pediatr Radiol*. 2010;40(7):1254-1262. Accessed Mar 6, 2020. doi: 10.1007/s00247-009-1429-9.

6) Perreault S, Ramaswamy V, Achrol AS, et al. MRI surrogates for molecular subgroups of medulloblastoma. *AJNR. Am J Neuroradiol*. 2014;35(7):1263-1269. https://www.ncbi.nlm.nih.gov/pubmed/24831600. doi: 10.3174/ajnr.A3990.

7) Colafati GS, Voicu IP, Carducci C, et al. MRI features as a helpful tool to predict the molecular subgroups of medulloblastoma: State of the art. *Ther Adv Neurol Disord*. 2018;11. https://www.ncbi.nlm.nih.gov/pmc/articles/PMC6024494/. Accessed Mar 6, 2020. doi: 10.1177/1756286418775375.

8) Morana G, Alves CA, Tortora D, et al. Added value of diffusion weighted imaging in pediatric central nervous system embryonal tumors surveillance. *Oncotarget*. 2017;8(36):60401–60413. Published 2017 Jul 25. doi:10.18632/oncotarget.19553.

Hydranencephaly

Thane H Rosette; Richard B Towbin, MD; Carrie M Schaefer, MD; Alexander J Towbin, MD; David J Aria, MD

Case Summary

A term newborn with an enlarged head and normal reflexes; brain anomaly was identified on prenatal ultrasound imaging.

Image Findings

A severe brain anomaly was diagnosed prenatally by ultrasound. Postnatal brain magnetic resonance imaging revealed near-complete absence of brain tissue above the tentorium, with only a small component of the right posterior parietal and bilateral occipital lobes present. The brainstem, cerebellum, and thalami were identified below the tentorium. A normal falx cerebri was noted.

Diagnosis

Hydranencephaly.

Differential diagnosis includes severe hydrocephalus (as can be seen in the setting of aqueductal stenosis) and holoprosencephaly.

The lack of a thin rim of normal brain tissue helps to exclude severe hydrocephalus while the lack of parenchymal fusion across the midline and presence of a normal falx excludes the diagnosis of holoprosencephaly.

Discussion

Neurodevelopmental disorders occur during the early phases of embryonic development. Hydranencephaly is one type of neurodevelopmental disorder that leads to the absence or near-total absence of the cerebral hemispheres.[1] Structures that typically remain intact include the cranial vault, meninges, thalami, midbrain, and cerebellum.[1] The basal ganglia may also be present.

Hydranencephaly is an *in utero* destructive lesion of previously normally formed brain.[2] Several hypotheses attempt to describe the etiology of this condition. They include: 1) bilateral internal carotid artery occlusion leading to infarction; 2) primary agenesis of the neural wall; and 3) intrauterine infection. It is also a component of Fowler syndrome (proliferative vasculopathy and hydranencephaly-hydrocephaly syndrome).[1,2] If the condition goes undiagnosed prenatally or at the time of birth, then presenting signs usually include seizures, respiratory failure, and poor posture while being in a vegetative state.

The hypothesis regarding internal carotid artery (ICA) occlusion is the most widely accepted explanation for hydranencephaly, as an intact blood supply is necessary for normal fetal brain growth and development. Early ICA occlusion can lead to blockage of the downstream arteries that supply the cerebral hemispheres, leading to infarction of the brain with subsequent reabsorption of the injured brain tissue as the infarcted brain is replaced by cerebrospinal fluid.

Hydranencephaly can be diagnosed using any imaging modality that can evaluate the fetal or newborn brain. Imaging findings include macrocephaly *in utero* and absence of the supratentorial brain, with a large, cerebrospinal fluid collection in the cranial vault. The brain structures primarily supplied by the posterior cerebral artery circulation (brainstem, midbrain, thalami, and portions of the basal ganglia) are preserved. Additionally, small portions of the parietal and occipital lobes may be preserved if they are supplied by small vessels outside of the ICA distribution. There is variable presence of the third ventricle. The falx cerebri may be incomplete; however, it is usually present and can help to distinguish hydranencephaly from alobar holoprosencephaly.[1] Prenatal diagnosis can be made with obstetrical ultrasound or fetal MRI during the second trimester.[6]

Affiliations University of Arizona College of Medicine, Phoenix, Arizona (Mr Rosette); Phoenix Children's Hospital, Phoenix, Arizona (Drs R Towbin, Schaefer, Aria); Cincinnati Children's Hospital, Cincinnatti, Ohio (Dr A Towbin).

Figure 1. (A) Sagittal T2 image of the brain shows a large cerebrospinal fluid filled space occupying much of the calvarium. There is almost complete absence of the supratentorial brain with only a minimal amount of brain parenchyma seen posteriorly. (B) Axial T2 images at the level of the thalami shows fully formed right and left thalami [T]. Lateral ventricles are largely indistinguishable from the CSF-filled supratentorial space. A small amount of layering blood [arrow] birth is present in the left lateral ventricle, commonly seen in neonates. (C) Axial T2 image in the more superior portion of the skull shows an absence of brain parenchyma but the presence of a normal appearing falx cerebri.

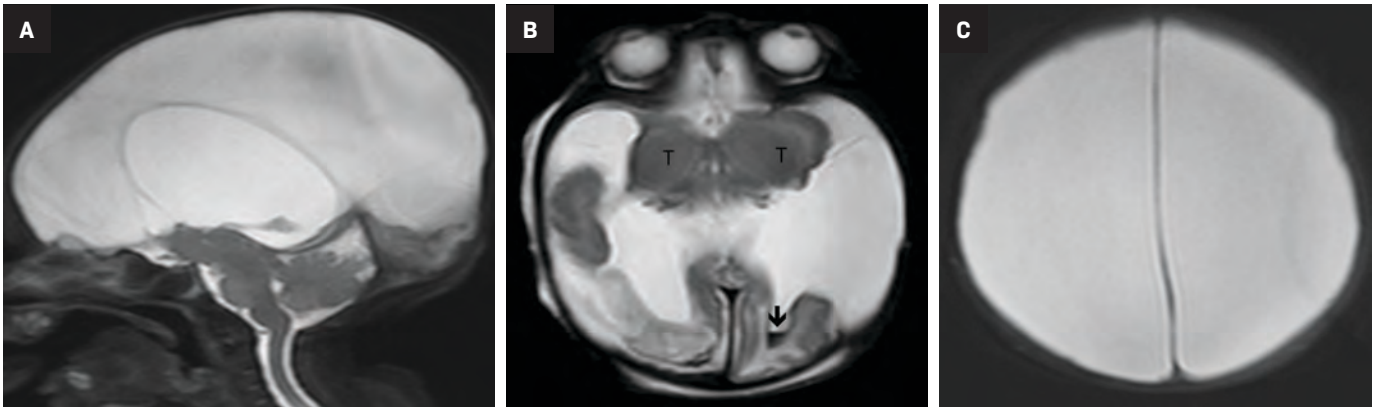

The prognosis for hydranencephaly is very poor. Most patients live for weeks to months after birth. However, there are case reports of patients living up to 22 years.[8,9] Disease severity may be indicated by degree of brain loss and associated anomalies. Treatments focus on managing symptoms, especially treating the hydrocephalus and seizures.

Conclusion

Hydranencephaly is a congenital neurodevelopmental anomaly in which there is an absence of the cerebral hemispheres and intact infratentorial structures. It is generally thought to occur as a result of bilateral occlusion of the ICAs. Diagnosis can be made prenatally or postnatally using ultrasound, CT, or MRI. Imaging findings include the presence of primitive brain structures, variable presence of the falx cerebri, and total or near-total absence of the cerebral hemispheres. There is no cure for hydranencephaly, and the prognosis is poor.

References

1) Pretorius, DH, et al. Diagnosis of brain neuropathology in utero. *Neuroradiolog.*, 1986; 28(5-6): 386-397.

2) Greene MF, Benacerraf B, Crawford JM. Hydranencephaly: US appearance during in utero evolution. *Radiology*. 1985; 156(3): 779-780.

3) Menshawi K, Mohr JP, Gutierrez J. A functional perspective on the embryology and anatomy of the cerebral blood supply. *J Stroke*. 2015; 17(2): 144-158.

4) Brismar J. *P*ersistent hypoglossal artery, diagnostic criteria. Report of a case. *Acta Radiol Diagn (Stockh).* 1976; 17(2): 160-166.

5) Padget, DH. The circle of Willis: Its embryology and anatomy. In: Dandy, W.E., Ed., *Intracranial Arterial Aneurysms,* Chapter III, Comstock Publishing, New York, 67-90..

6) Sepulveda W, et al. Prenatal sonography in hydranencephaly: findings during the early stages of disease. *J Ultrasound Med*. 2012; 31(5): 799-804.

7) Quek YW, et al. Hydranencephaly associated with interruption of bilateral internal carotid arteries. *Pediatr Neonatol.* 2008; 49(2): 43-47.

8) McAbee GN, Chan A, Erde EL. Prolonged survival with hydranencephaly: report of two patients and literature review. *Pediatr Neurol.* 2000. 23(1): 80-84.

9) Bae, JS, Jang MU, Park SS. Prolonged survival to adulthood of an individual with hydranencephaly. *Clin Neurol Neurosurg.* 2008; 110(3): 307-309.

"But as to myself, having been wearied out for many years with offering vain, idle, visionary thoughts, and at length utterly despairing of success, I fortunately fell upon this proposal, which, as it is wholly new, so it hath something solid and real."
—Jonathan Swift, "A Modest Proposal."

A Modest Proposal

C Douglas Phillips, MD, FACR

Well, old Jon had something else in his satirical mind to "propose" to his readers. One of the most original and thought-provoking pieces of literature ever. I have something entirely different to propose that may be a bit more easily applied (and less cringe-worthy).

My wife (A radiologist, as well. Have I told you this before? Pretty sure I have. We discuss this stuff all the time.) and I are well into the third or fourth round of what we both refer to as "niceness training." I'm sure you all have been ruthlessly bombarded with this material, as well. Diversity, social acceptance, cultural acceptance, religious acceptance, I-like-country-music acceptance. We must read and then be quizzed on being a respectful and caring human being. And I get it; there are people out there who just don't like people who aren't just like them. I have two observations to make on this and will, through this little discourse, subject you to them.

No.1. Except for the interventional group among us, we look at gray-scale images. I don't pay much attention to names (except for the rare potential misidentification from the medical record number) so I see my patients as shades of gray on the screen. Short, tall, green or purple, boy or girl---my screen shows your matter as shades of gray. We seem to have the perfect specialty to ignore all but the pathology. We just recently moved into color (and how I remember the excitement of those first few excuses to have color monitors!) and so far as I can tell, the only judgment about color in that movement seems to be that regardless of technique, we seem to have assigned red as bad. This may lead to a deluge of red-hating radiologists, but I think likely not. Too much opposing energy from red wine, apples, or cherries. Net result is balance.

No.2. Here's an easy one. Instead of using all these training models to teach us life's lessons, how about we just only accept residents/fellows/colleagues who don't ignore them to begin with? Four years of medical school are training for residency, so let's just take residents who were nice to people during medical school. Four years of residency are training for fellowship, so let's just take fellows who were accepting of all during residency. If you're not nice-nice to your companions, I don't want to have to educate you in a basic life skill. To select our trainees, how about less time with personal essays? Let's ask their colleagues (as a group) how they are as a ***human being***. This reminds me that all you need to know you learned in kindergarten.

Be nice. Clean up your mess. Share.
Class dismissed.

Keep doing that good work. Be nice. Mahalo.

Dr Phillips is a Professor of Radiology, Director of Head and Neck Imaging, at Weill Cornell Medical College, NewYork-Presbyterian Hospital, New York, NY. He is a member of the *Applied Radiology* Editorial Advisory Board.

FUJIFILM
Value from Innovation

Visionary Performance.

For the Radiologist, a quick, confident diagnosis means everything to your patient.

Persona CT delivers fast, sharp images to facilitate confident decision-making.

Be visionary.

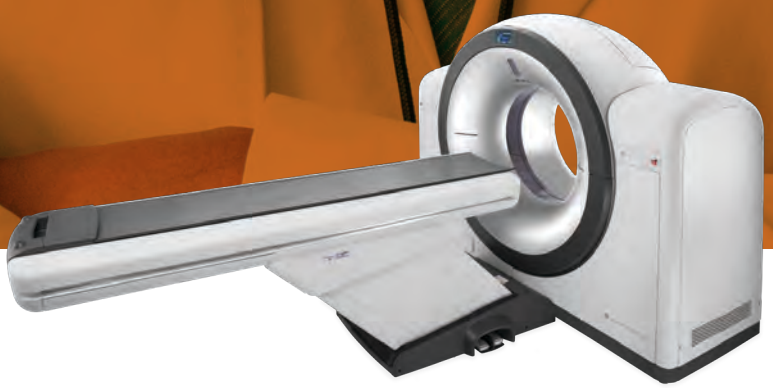

#VisionaryCT

Persona CT

Powerful, Protective, and a Great Communicator.

MEDRAD® Intego SMART Package* Automatic Integration to ec² Software Solutions® NMIS® / BioDose®

It's the Complete Package.

Saves time, steps, stress and exposure with smart workflow integration and powerful decision support.

1. Patient information is automatically added to MEDRAD® Intego and NMIS/BioDoes software from MWL Server.
2. The F-18 FDG bulk vial information is added to MEDRAD® Intego and NMIS/Biodose Software.
3. Once the patient is infused with MEDRAD® Intego, the NumaStatus™ interface automatically updates NMIS/Biodose with the accurate patient radiopharmaceutical dose information.
4. The NumaStatus interface exports the dose report as a DICOM secondary capture to PACS and other systems.
5. Optionally the EMR, dose management and radiopharmacy systems are updated with the patient dose information.

ec² Software Solutions
Numa

Note: The workflow above requires the site to have the MEDRAD® Intego SMART Package, NMIS/Biodose with HL7/ DICOM options and NumaStatus with Intego interface option.

Learn more about MEDRAD® Intego at radiologysolutions.bayer.com
Learn more about ec² and Numa products at ec2software.com

*ec² Software Solutions NMIS / BioDose is a separate product owned by a separate company that has a secondary capture capabilities via DiCOM. This software is not integrated into Intego's software.

ec² Software Solutions, NMIS, BioDose are trademarks owned and/or registered to ec² Software Solutions LLC and are used with permission. Numa, NumaStatus are trademarks owned and/or registered to Numa LLC and are used with permission.

Bayer, the Bayer Cross, MEDRAD, MEDRAD Intego, and Intego are trademarks owned by and/or registered to Bayer in the U.S. and/or other countries. © 2021 Bayer. This material may not be reproduced displayed, modified or distributed without the express prior written consent of Bayer. Only available in the US.
PP-M-INT-US-0103-1 April 2021

MEDRAD® Intego
PET Infusion System